REVISTA PORTUGUESA DE QUÍMICA

RPTQAT 16(3) 129-194 (1974)

Rev. Port. Quím., Vol. 16, N.º 3
Pp. 129/194 — Lisboa, 1974

REVISTA PORTUGUESA DE QUÍMICA

Propriedade e edição da
SOCIEDADE PORTUGUESA DE QUÍMICA
em continuação da
REVISTA DE QUÍMICA PURA E APLICADA
fundada em 1905 por
Ferreira da Silva.
Subsidiada pelo
INSTITUTO NACIONAL DE INVESTIGAÇÃO CIENTÍFICA

Director	A. HERCULANO DE CARVALHO
Editor	C. M. PULIDO
Comissão redactorial	F. CARVALHO BARREIRA JORGE C. G. CALADO RENATO DA SILVA LEAL J. SIMÕES REDINHA J. J. R. FRAÚSTO DA SILVA M. INÊS VALENTE SOARES VASCO TEIXEIRA CÉSAR A. N. VIANA
Subsidiada pelas seguintes empresas	PETROGAL ELECTRICIDADE DE PORTUGAL SAPEC INDÚSTRIAS LEVER PORTUGUESA, LDA. NITRATOS DE PORTUGAL SOCIEDADE PORTUGUESA DE PETROQUÍMICA SODA PÓVOA SIDERURGIA NACIONAL COMPANHIA INDUSTRIAL PRODUTORA DE ANTIBIÓTICOS INDÚSTRIA NACIONAL DE PRODUTOS QUÍMICOS, LDA. SOCIEDADE INDUSTRIAL FARMACÊUTICA

Os artigos publicados são de exclusiva responsabilidade dos seus autores.

Redacção e administração	Instituto Superior Técnico — Lisboa-1 (Tel. 56 29 13)
Gravuras, composição e impressão	Gráfica Brás Monteiro, Lda. — Lisboa
Capa e arranjo gráfico	Luís Filipe de Abreu

Publicação trimestral. Número avulso: 150$00. Assinatura (quatro números): Portugal, Brasil e Espanha: 500$00
outros países: U.S. $18.00

índice

J. E. SIMÃO

A. S. VEIGA

Laboratório Químico
Faculdade de Ciências e Tecnologia
Universidade de Coimbra — Portugal

INFLUÊNCIA DOS IÕES CLORETO SOBRE A REACÇÃO DE REDUÇÃO DO TELÚRIO(IV)

Estudou-se o comportamento polarográfico do telúrio (IV) em ácido clorídrico. No que se refere particularmente à reacção de redução do Te(IV) a Te(0), admite-se que esta se possa dar em dois passos sucessivos de dois electrões, com formação de $TeCl_2(s)$ como intermediário. A interpretação dos dados experimentais obtidos faz-se também em termos das espécies electroactivas presentes em solução.

1 — INTRODUÇÃO

Em artigo anterior [1] referimos as conclusões do estudo do comportamento polarográfico do telúrio em meios azótico e perclórico. É objecto deste trabalho o estudo do mesmo sistema em meio clorídrico, particularmente no que diz respeito ao processo electroquímico que tem lugar na zona de potenciais correspondente à primeira onda polarográfica. Fizeram-se medidas de polarografia convencional, de polarografia rápida e de polarografia rápida com tensão alterna sobreimposta. A explicação dos resultados experimentais dessas medidas polarográficas do Telúrio (IV) em função, simultaneamente, do pH da solução e da concentração dos cloretos é dada, por um lado, em termos das espécies electroactivas presentes nas diferentes soluções e, por outro, dos mecanismos da reacção de redução daquele elemento no eléctrodo de mercúrio gotejante.

2 — PARTE EXPERIMENTAL

A preparação das soluções e a aparelhagem utilizada foram já descritas noutro lugar [1]. Os polarogramas de tensão alterna sobreimposta foram obtidos com um Modulador CA E393, da firma METROHM, Herisau, Suíça, acoplado ao POLARECORD E 261 R, da mesma firma.

3 — RESULTADOS

3.1 — *POLAROGRAMAS RÁPIDOS* *(tempos de gotejamento < 1 segundo)*

Tal como em meio azótico ou perclórico, também em meio clorídrico os polarogramas dos iões Te (IV) apresentam duas ondas (fig. 1, curva 1). A primeira corresponde à redução do Te (IV) a Te (0), e a segunda à redução do Te (IV) a Te (– II). Esta segunda onda ocorre em meio clorídrico praticamente ao mesmo potencial que em meio azótico ou perclórico ($E_{1/2} = -0{,}90V$ vs. Ag/AgCl). Quanto à primeira onda, cujo $E_{1/2}$ em meio azótico anda à volta de $-0{,}30V$ vs. Ag/AgCl (depende do pH), ela aparece em meio clorídrico a potenciais mais positivos do que este, variando o seu potencial

de meia onda quer com a concentração do ião cloreto quer com o pH.

Assim, para valores do pH compreendidos entre 1,45 e 1,60, os valores de $E_{1/2}$ vão-se tornando mais positivos à medida que a concentração do ião cloreto cresce desde $2{,}7.10^{-4}$ M até 2,2 M. Por outro lado, mantendo a concentração do Cl^- constante, os potenciais $E_{1/2}$ deslocam-se para valores mais positivos à medida que o pH baixa de 2 até 0. Já o mesmo não sucede quando se faz aumentar a concentração hidroniónica de 1M até 10M por adição de HCl. Nesta zona $E_{1/2}$ torna-se gradualmente mais negativo. Observou-se idêntico comportamento em meio azótico [1].

3.2 — *POLAROGRAMAS CONVENCIONAIS (tempo de gotejamento ≃ 3 segundos)*

Uma vez que a técnica da polarografia convencional, em que o mercúrio goteja livremente, e a da polarografia rápida, em que a gota de mercúrio é batida mecanicamente a intervalos de tempo definidos,

Fig. 1
Polarograma convencional (curva 1) e de tensão alterna sobreimposta (curva 2) do Telúrio (IV) numa solução com a seguinte composição: | Te(IV) | = 6,2 . 10^{-4} M, | KCl | = 2,8M, pH = 1,35. Frequência da tensão aiterna = 30 mV/mseg

diferem apenas no tempo de gotejamento, os polarogramas rápidos e convencionais da mesma substância deverão apresentar as mesmas características gerais. É o que de facto acontece com a redução dos iões Te (IV), tanto em meio azótico como em meio clorídrico.

Todavia, no que respeita à primeira onda, há na polarografia convencional um pormenor que não ocorre na polarografia rápida: em meio clorídrico a primeira onda (fig. 2, A) vem precedida de uma pré-onda (fig. 2, B) cuja definição se inicia a partir de uma concentração do ião cloreto igual a 0,2 M e se acentua à medida que esta concentração cresce.

Verifica-se também que a altura da onda A é proporcional à concentração de Te (IV) em solução, sendo a constante de proporcionalidade dada pela equação de Ilkovic, ao passo que a altura da pré-onda B começa por ser igual a cerca de metade da da onda A (contadas ambas as alturas a partir da linha base), ficando, depois, praticamente constante, mesmo quando a onda A continua a crescer por aumento da concentração de Te (IV) na solução.

A observação das curvas i-t (corrente em função do tempo) na zona de potencial em que se desenvolve a pré-onda B sugere que se forma sobre o eléctrodo uma camada protectora, que se mantém durante a vida da gota, mas desaparece logo que se atinge o potencial correspondente ao início da onda A.

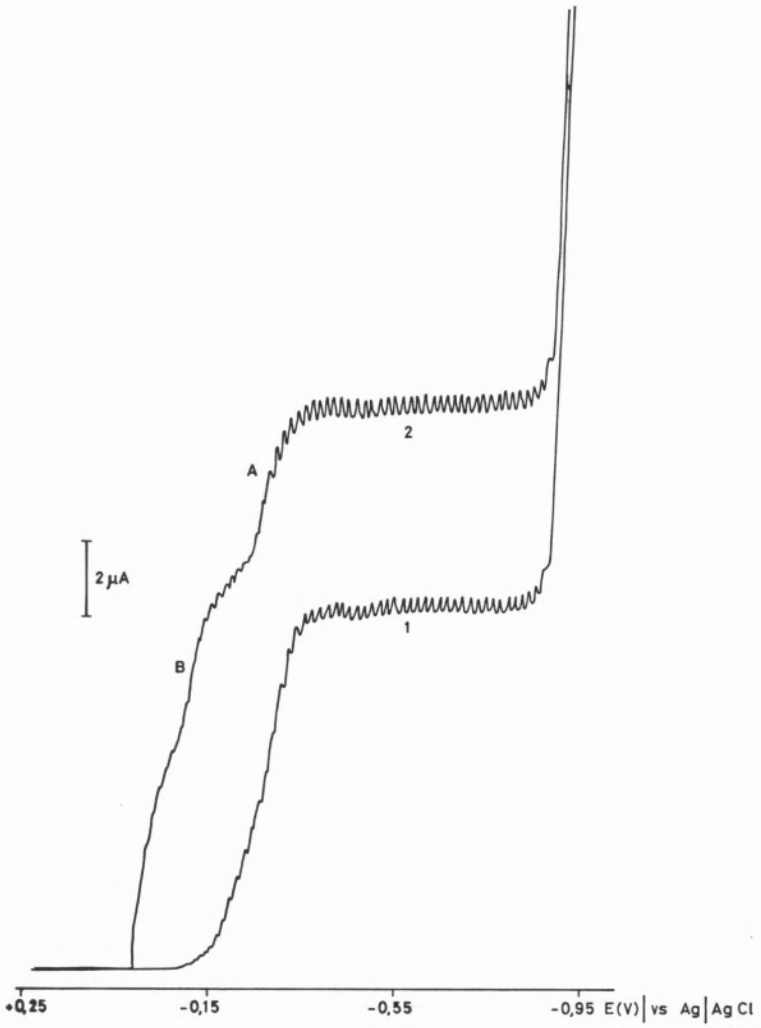

Fig. 2

Primeira onda polarográfica do Telúrio (IV): a) *na ausência de cloretos (curva 1) e* b) *na presença de cloretos (curva 2). Composição das soluções:*
a) $|Te(IV)| = 6{,}2 \cdot 10^{-4}$ M, $|HNO_3 + KNO_3| = 1$M, $pH = 1{,}3$;
b) $|Te(IV)| = 7{,}4 \cdot 10^{-4}$ M, $|KCl| = 1{,}2$M, $pH = 1{,}3$

3.3 — *POLAROGRAMAS DE TENSÃO ALTERNA SOBREIMPOSTA*

Neste tipo de curvas, obtidas com a imposição de uma tensão alterna de amplitude constante sobre a rampa do potencial aplicado numa polarografia rápida, observam-se dois picos (fig. 1, curva 2). O primeiro, cujo potencial E_p é, em meio azótico, igual a $-0{,}316$ V vs. Ag/AgCl, corresponde à primeira onda polarográfica (onda A) atrás referida. O segundo pico ($E_{p_2} = -0{,}90$ V vs. Ag/AgCl) diz respeito à onda polarográfica de redução do Te (IV) a Te (– II). Não aparece o pico correspondente à pré-onda B, o que é indício do carácter de irreversibilidade do processo nela envolvido. Uma vez que o presente estudo se refere ao processo relacionado com a primeira onda polarográfica em meio clorídrico, trataremos exclusivamente do primeiro pico, que lhe corresponde.

Observou-se que a corrente de pico, i_p, cresce com a concentração do Te (IV) em solução de acordo com a equação [9]

$$i_p = knFD^{1/2}m^{2/3}t^{2/3}\omega^{1/2}C\ nFE_o/2RT$$

onde C é a concentração da espécie electroactiva, E_o é a amplitude da tensão alterna sobreimposta, ω é a frequência e as outras letras têm o significado habitual.

A variação do potencial de pico, E_p, com a concentração hidroniónica da solução dá-se no mesmo sentido da variação de $E_{1/2}$ com o pH, atrás descrita.

Partindo de soluções de Te (IV) em ácido azótico sem cloretos, para as quais $E_p = -0{,}316$ V vs. Ag/AgCl, e juntando gradualmente cloretos à solução, a pH constante, verifica-se que E_p se desvia ligeiramente para valores mais positivos, acabando por se manter praticamente estacionário para $|\ Cl^-\ | \geqslant 2$ M.

4 — DISCUSSÃO DOS RESULTADOS

Ao procurar interpretar os resultados experimentais obtidos, põem-se, logo de início, duas questões. A primeira, é a de saber quais as espécies de telúrio presentes nas soluções de Te (IV) que contêm cloretos. A segunda, diz respeito aos mecanismos das reacções de eléctrodo envolvidas.

Quanto à primeira questão, vários são já os trabalhos, descritos na literatura da especialidade, que se referem às espécies de Te (IV) em meio clorídrico. Assim, MIZUMACHI [2], por estudos de troca iónica a partir de soluções mistas de LiCl-HCl, admitiu a existência de clorocomplexos aniónicos do telúrio em soluções de força iónica total igual a 10 M. Para uma força iónica mais baixa (2,0 a 4,0 M) as soluções conteriam hidroxocomplexos.

SHITAREVA e NAZARENKO [3], estudando coficientes de distribuição entre soluções aquosas de HCl-LiCl de força iónica constante e uma mistura de n-hexanol e benzeno 3 : 7, concluíram que, para $|\ H^+\ | > 2{,}79$ M, o clorocomplexo formado seria da forma $TeCl_5(H_2O)^-$ e não haveria hidrólise nas condições da experiência.

Por seu lado, SHIKHEEVA [4], fazendo estudos espectrofotométricos, admite a existência do equilíbrio

$$H_2O + TeCl_6^{2-} \leftrightarrows TeCl_5(H_2O)^- + Cl^-$$

para concentrações de HCl compreendidas entre 8,5 M e 10 M. Para valores da concentração de HCl compreendidos no intervalo 7,8-8,0 M ter-se-ia o equilíbrio

$$H_2O + TeCl_5(H_2O)^- \rightleftarrows TeCl_4(H_2O)_2 + Cl^-$$

e, no intervalo $2{,}0 < |\ HCl\ | < 5{,}0$ M, os equilíbrios a considerar seriam

$$TeCl_4(H_2O)_2 \leftrightarrows TeOCl_4^{2-} + 2H^+ + H_2O$$

e

$$H_2O + TeOCl_4^{2-} \leftrightarrows TeO(OH)Cl_3^{2-} + Cl^- + H^+$$

Este autor verificou também que os hidroxocomplexos do telúrio (IV) são extremamente instáveis e libertam facilmente água convertendo-se nos correspondentes oxocomplexos.

Os trabalhos de NABIVANETS e KAPANTSYAN [5] descrevem um estudo do telúrio (IV) em soluções de HCl e de HCl + LiCl pelos métodos da solubilidade, espectrofotométricos e de cromatografia de troca iónica. Tendo verificado que a solubilidade de $TeO(OH)_2$ em água é proporcional à primeira potência da concentração do ião hidrogénio, deduzem para constante do equilíbrio de solubilização

$$TeO(OH)_2 + H^+ \leftrightarrows TeO(OH)^+ + H_2O$$

o valor de $(2{,}1 \pm 0{,}7) \times 10^{-2}$. O efeito da concen-

tração de H^+ sobre a solubilidade de $TeO(OH)_2$ em soluções de HCl, nas quais a concentração de Cl^- era constante, mostrou-se também linear, sendo a solubilidade maior do que em ácido perclórico. Nestas condições a solubilização pode ser representada pela equação

$$TeO(OH)_2 + H^+ + Cl^- \rightleftarrows TeO(OH)Cl + H_2O$$

cuja constante é igual a $(6{,}4 \pm 0{,}9) \times 10^{-3}$. Combinando este equilíbtio com o anterior deduz-se

$$K_{inst} = \frac{|\,TeO(OH)^+\,|\;|\,Cl^-\,|}{|\,TeO(OH)Cl\,|} = (3{,}1 \pm 0{,}8) \times 10^{-1} \qquad (1)$$

Com o aumento da concentração de Cl^- de 1 N até 5 N formam-se sucessivamente os seguintes complexos.

$$TeO(OH)Cl + Cl^- + H^+ \rightleftarrows TeOCl_2 + H_2O$$

$$K_1 = \frac{|\,TeO(OH)Cl\,|\;|\,Cl^-\,|\;|\,H^+\,|}{|\,TeOCl_2\,|} = 0{,}59$$

$$TeOCl_2 + Cl^- \rightleftarrows TeOCl_3^- \;;\; K_2 = 2{,}74$$

$$TeOCl_3^- + Cl^- \rightleftarrows TeOCl_4^{2-} \;;\; K_3 = 5{,}90$$

Um aumento subsequente de $|\,Cl^-\,|$ de 6 N até 9 N promove a ligação de mais dois iões cloreto ao complexo do telúrio, formando um composto em que a relação Cl^- : Te (IV) é de 6 : 1. Cálculos adicionais mostraram que, à medida que $|\,H^+\,|$ aumenta, a zona em que predominam os clorocomplexos sobre os oxoclorocomplexos é deslocada para menores concentrações de cloretos.

A variação do $E_{1/2}$ da onda A com o pH e o pCl, por nós observada experimentalmente e já atrás referida, poderá ser explicada admitindo a formação de vários complexos de telúrio.

De acordo com resultados descritos em trabalho anterior [1], em meio não complexante (meio azótico ou perclórico), as formas predominantes do Te (IV), presentes nas soluções de diferentes valores do pH, são as seguintes: $TeO(OH)^+$ para 0,01 M $< |\,H^+\,| <$ < 4 M e Te^{4+} (aq) para $|\,H^+\,| > 4$ M.

Admitindo aqui também a mesma influência do pH, pode-se analogamente supor que, por junção gradual de cloretos às soluções de Te (IV) em que 0,01 M $< |\,H^+\,| < 4$ M, se formarão consecutivamente os complexos TeO(OH)Cl, $TeOCl_2$, $TeOCl_3^-$ e $TeOCl_4^{2-}$; tratando-se de soluções em que $|\,H^+\,| > 4$ M, formar-se-ão vários complexos de fórmula genérica $TeCl_x^{(4-x)+}$.

Ora, existindo clorocomplexos em solução, a espécie electroactiva será, não directamente $TeO(OH)^+$, como em meio azótico, mas um clorocomplexo:

$$TeO(OH)Cl + 3H^+ + 4e^- \rightleftarrows Te + H_2O + 2Cl^-$$

ou, de uma maneira geral,

$$TeOCl_x^{(2-x)+} + 2H^+ + 4e^- \rightleftarrows Te + H_2O + xCl^- \qquad (2)$$

pois os clorocomplexos são mais facilmente redutíveis do que os correspondentes hidroxocomplexos. Além disso, a equação (2) mostra que, enquanto os clorocomplexos contiverem oxigénio, a sua redução será sempre favorecida por um aumento da concentração hidroniónica. Isto explica o deslocamento do potencial $E_{1/2}$ para valores mais positivos à medida que o pH baixa até pH = 0. Mas quando, por subsequente adição de HCl à solução, $|\,H^+\,| >$ > 1 M, a acção conjunta da concentração hidroniónica e da concentração do ião cloreto apenas permite a existência de clorocomplexos do tipo $TeCl_x^{(4-x)+}$. Então a reacção de redução

$$TeCl_x^{(4-x)+} + 4e^- \rightleftarrows Te + xCl^-$$

deixa de depender do pH da solução, o que também está de acordo com o que foi observado experimentalmente. O facto de $E_{1/2}$ se deslocar para valores mais negativos (redução dificultada) quando a concentração de ácido clorídrico vai de 1 M até 10 M, deixa supor que os clorocomplexos do Te (IV) sem oxigénio são mais dificilmente redutíveis do que os correspondentes cloro-oxocomplexos.

4.1 — *A PRÉ-ONDA B*

Dissemos já que a observação das curvas i-t na zona da pré-onda B sugere que, para esses potenciais, se forma sobre o eléctrodo uma camada sólida impeditiva da reacção, camada que se não desfaz du-

rante a vida da gota, mas começa a ser redissolvida logo que o potencial atinge o valor correspondente ao início da onda A. Qual a natureza desta camada sólida? Como resposta diríamos que ela poderia ser de $TeCl_2$(s), de TeO (s), de $Te(OH)_2$ (s) ou de Te(0) (s).

Dado que a pré-onda B apenas se evidencia em meio clorídrico, excluímos a forma TeO (s), pois, de contrário, ela deveria ocorrer igualmente em meio azótico, o que não se verifica. Por sua vez, a forma $Te(OH)_2$ (s) é pouco provável, quanto mais não seja em virtude das condições de pH do meio. A forma Te(0), como resultado de uma reacção de 4 electrões, não sendo impeditiva da transição de electrões, não seria, portanto, a causa do bloqueamento da superfície do eléctrodo. Resta-nos, assim, encarar como possível a formação de $TeCl_2$ (s) como passo intermediário na redução do Te (IV) no eléctrodo de mercúrio em meio clorídrico.

Referimos já que a pré-onda B se começa a individualizar quando $|\,Cl^-\,| > 0,2$ M. Ora de acordo com a expressão (1), a uma concentração de ião cloreto igual a 0,2 M corresponde $|\,TeO(OH)Cl\,| = {}^2/_3|\,TeO(OH)^+\,|$. Isto significa que a pré-onda B só aparece quando começa a ser significativa a concentração de clorocomplexos na solução.

A reacção de redução responsável pela pré-onda B será, nestas circunstâncias,

$$TeO(OH)Cl + 3H^+ + Cl^- + 2e^- \rightleftarrows TeCl_2\ (s) + 2H_2O$$

Esta reacção é efectivamente favorecida por um aumento tanto da concentração hidroniónica como da concentração do ião cloreto. Por crescimento ulterior desta concentração o clorocomplexo passa a ter sucessivamente um número maior de cloretos. Já com dois cloretos, $TeOCl_2$, a reacção de redução a $TeCl_2$ é independente da concentração dos cloretos e, com mais do que os dois, aquela reacção é impedida, deixando a pré-onda B de se individualizar.

A ulterior redução do $TeCl_2$ (s) a Te (0) ocorre ao mesmo potencial da onda A:

$$TeCl_2\ (s) + 2e^- \rightleftarrows Te\ (0) + 2Cl^-$$

Uma tal redução escalonada de 2 + 2 electrões explica o facto, atrás referido, de as alturas da pré-onda B e da onda A, crescendo ambas proporcionalmente à concentração do Te (IV) em solução, se manterem iguais até ocorrer a cobertura completa do eléctrodo pelo $TeCl_2$ (s). Por ulterior aumento da concentração do Te (IV) a altura da onda A continua a crescer, mas a da pré-onda B não.

A existência da espécie $TeCl_2$, admitida por RABENAU e RAU [7] como estável na fase gasosa e como metaestável em fases condensadas, foi também suposta por KOMANDENKO [8] como intermediário na redução do Te (IV) no eléctrodo de telúrio em ácido clorídrico.

BIBLIOGRAFIA

[1] SIMÃO, J. E. J. e VEIGA, A. S., *Rev. Port. Quím.*, **14**, *137 (1972)*.

[2] MIZUMACHI, K., *Nippon Kagaku Zasshi*, **83**, *73 (1962) in* SHIKHEEVA, L. V., *Russ. J. Inorg. Chem.*, **13**, *1528 (1968)*.

[3] SHITAREVA, G. G. e NAZARENKO, V. A., *Russ. J. Inorg. Chem.*, **13 (3)**, *941 (1968)*.

[4] SHIKHEEVA, L. V., *Russ. J. Inorg. Chem.*, **13 (11)**, *1528 (1968)*.

[5] NABIVANETS, B. I. e KAPANTSYAN, E. E., *Russ. J. Inorg. Chem.*, **13 (7)**, *946 (1968)*.

[6] POURBAIX, M., «Atlas of Electrochemical Equilibria in Aqueous Solutions», Pergamon Press, London, 1966.

[7] RABENAU, A. e RAU, H., *Z. Anorg. Allgem. Chem.*, **395**, *273 (1973)*.

[8] KOMANDENKO, V. M., *J. Appl. Chem. USSR*, **44**, *530 (1971)*.

[9] MATSUDA, H., *Z. Elektrochem.*, **62**, *977 (1958)*.

Recebido 17 Jan. 1975.

ABSTRACT

The polarographic behaviour of Te(IV) ions in HCl solutions was studied. Concerning the Te(IV)-Te(0) reaction, it is supposed that this reduction proceeds in two consequent two electrons steps with $TeCl_2$(s) as an intermediate. The experimental data are also discussed in terms of the electroactive species of Tellurium (IV) present in solution.

J. DE D. R. S. PINHEIRO

T. R. BOTT

Department of Chemical Engineering
The University of Birmingham
Edgbaston, Birmingham B15 2TT
U. K.

CONCENTRATION OF DILUTE MIXTURES IN ROTARY THERMAL DIFFUSION COLUMNS: THE THEORY

A phenomenological theory for the concentration of dilute solutions by a rotary thermal diffusion column is presented, based on the development of a simplified (2-dimensional) model for the rotary column and subsequent application of Ramser's derivation for the «moving-walls» column. The application of the idealised theory to practical apparatus is discussed and an «equivalent annulus width» for the rotary column defined in identical basis as for the static column. The separation equations thus obtained indicate that the performance of the rotary column is strongly dependent on the constancy (perfection) of the annulus width. For perfect apparatus the separation is independent of the speed of rotation and is greater than static separation. For imperfect columns, however, the separation decreases as the speed of rotation increases, and, ultimately, the rotary performance gets poorer than the conventional static apparatus. The limited experimental results available are discussed in terms of the present theory.

1 — INTRODUCTION

The separation of liquid mixtures by thermal diffusion has been the focus of several work since in 1938 CLUSIUS and DICKELL [1] presented the so-called thermogravitational column. The investigation has been mainly concerned with the establishment of a phenomenological theory for the column separation and with the improvement in the column performance (through some modifications in the basic design of the apparatus), both aims running almost concurrently.

Phenomenological theories have been proposed by several authors but the most successful and original are those of FURRY *et al.* [2] and DEBYE [3] which arrive at the same basic «transport equation» although the derivations and range of application are different. Modified theories have been sucessfully applied to modified column-designs with the exception of the rotary column, a prototype apparatus that, due to its promising characteristics has recently attracted the interest of investigators in thermal diffusion.

The reason why no adequate theory for the rotary column exists lies in the fact that the hydrodynamic pattern inside the annulus of such apparatus is unique; while the other types of columns have only one direction of convection (either natural or forced), in a rotary column the natural convection (axial flow) is normal to the forced convection (tangential flow). As a result, the particles streamlines are three-dimensional rather than two-dimensional, the shape of these streamlines being similar to a helically wrapped coil around the column (the angle of inclination, radius of the xy-position and distance between consecutive vertical points being dependent on the x-coordinate, i. e. the flow is not even symmetrical with respect to x (fig. 1).

2 — THE REDUCTION OF THE PROBLEM TO TWO-DIMENSIONS

The non-linear partial differential equation that arises from the application of the continuity equation in the absence of chemical reaction [4] to the 3-dimensional flow pattern in a rotary column is of such complexity that the analytical integration «qua tal» is virtually excluded. The difficulty has already been pointed out by ROMERO [5] who

suggested the reduction of the problem dimensions and a subsequent application of the mathematical derivation of the 2-dimensional conventional column. In doing so, the separation equations would be formally identical in both rotary and static columns and the design methods devised for the static apparatus could be «translated» to the rotary column.

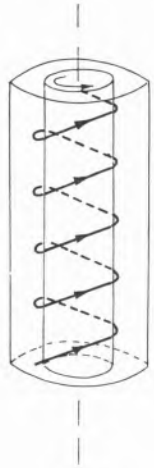

Fig. 1
Particle streamline in the «hot region» of a rotary thermal diffusion column with the inner cylinder rotating

In his pioneering work, in attempting to correlate his own experimental data, ROMERO [5] derived what he called «an elementary theory» which, in fact, involves a reduction of the problem dimensions. The basic assumption introduced was that the rotary column was physically equivalent to a parallel plate column whose walls move in opposite directions with equal absolute velocities and having the same rate of shear across the annulus as the rotary column. In other words, if the inner cylinder rotates with a tangential velocity V, the equivalent «moving walls» column would have wall velocities of $+ V/2$ and $- V/2$. Afterwards, Romero follows a derivation pattern similar to that of FURRY, JONES and ONSAGER [2] for the static column, obtaining a «transport equation» formally identical to the static case but with different transport coefficients. Somewhat surprisingly, though, that author used for the length of the «moving-walls» column the vertical height of the column which is in apparent contradiction with the physical analysis outlined by ROMERO [5] in which it is stated that the length of the particles streamlines (the effective length for cascading) is increased by rotation without, however, changing the residence-time of the particles. As a consequence, the theoretical predictions regarding the steady-state separation are far below the experimental results reported by Romero, but, on the contrary, the theory is in qualitative agreement with the experiment in what concerns the phenomenological parameters that do not depend on the column length.

It may therefore be concluded that the approach of Romero to reduce the problem dimensions, i.e., the physical analysis that led to the assimilation of the rotary column to a moving-walls column is a suitable basis upon which the present theory is to be derived.

Like the conventional theories, the range of validity of the theory presented here is limited by the simplifying assumptions introduced throughout the derivation. Hence, besides the usual limitations [8] it is necessary to consider those involved in the analogy with the «moving-walls» column (related to the speed of rotation) and the range of concentrations under examination (dilute mixtures).

3 — THE VELOCITY PROFILE

For the system of fig. 2, the Navier-Stokes equations for the viscous flow of an incompressible newtonian fluid at steady-state hydrodynamic conditions, at speed below the critical Taylor Number, $(N_{Ta})_c$, are [4]

$$\frac{\partial}{\partial z}\,\rho v_z = 0 \tag{1}$$

$$\frac{\partial p}{\partial x} = 0 \tag{2}$$

$$\eta\,\frac{\partial^2 v_y}{\partial x^2} = 0 \tag{3}$$

$$\eta\,\frac{\partial^2 v_z}{\partial x^2} = \frac{\partial p}{\partial z} + \rho g \tag{4}$$

with the following boundary conditions valid for a reservoirless column operated batchwise

$$v_y = V\,, \qquad v_z = 0 \quad \text{at} \quad x = +\omega \tag{5}$$

$$v_y = 0\ , \qquad v_z = 0 \quad \text{at} \quad x = -\omega \tag{6}$$

$$\int_{-\omega}^{+\omega} v_z dx = 0 \tag{7}$$

The integration of equations (3) and (4) subjected to the above boundary conditions yields

$$v_y = \frac{V}{2}\left(\frac{x}{\omega} + 1\right) \tag{8}$$

$$v_z = \frac{\beta g(\Delta T)\omega^2}{12\eta}\left\{\frac{x}{\omega}\left[1 - \left(\frac{x}{\omega}\right)^2\right]\right\} \tag{9}$$

where it was assumed that $\partial T/\partial x = \Delta T/2\omega$ which is generally valid [7].

The resultant velocity, $\vec{v}_R(x)$, has, thus, a magnitude of

$$\left|\vec{v}_R\right| = \sqrt{v_y^2 + v_z^2} \tag{10}$$

and its deflection angle from the horizontal, $\psi(x)$, is defined through

$$\tan \psi = \frac{y_z}{v_y} \tag{11}$$

It may be easily seen that the angle ψ is at a maximum at $x = +\omega/2$ and that the lowest value of ψ in the interval $[+\omega, -\omega]$ is at $x = -\omega$, respectively:

$$\tan \psi \Big|_{x = \frac{\omega}{2}} = \frac{1}{24}\ \frac{\beta g(\Delta T)\omega^2}{\eta V} \tag{12}$$

$$\tan \psi \Big|_{x = -\omega} = -\frac{1}{3}\ \frac{\beta g(\Delta T)\omega^2}{\eta V} \tag{13}$$

For speeds of notation above a certain value [7] — the lower limit of velocity — the extreme values referred to in equations (12) and (13) are sufficiently close for the following assumption to be acceptable:

$$\tan \psi \simeq (\tan \psi)_{av} = -\frac{1}{18}\ \frac{\beta g(\Delta T)\omega^2}{\eta V} \tag{14}$$

In this case, also

$$\left|\vec{v}_R\right| \simeq \left|v_y\right| \tag{15}$$

It is convenient, for simplicity, to express the velocity profile of equation (8) in the symmetrical form

$$v_y = \frac{V}{2}\ \frac{x}{\omega} \tag{16}$$

i.e., to assume that both walls are moving in opposite directions with velocities $+V/2$ and $-V/2$ [5]. The substitution of equation (8) by equation (16) does not interfere with the validity of the model since what is important in terms of the remixing-cascading effects within the annulus are the relative velocities of the particles and not the absolute velocity of the fluid (providing the flow remains below the critical Taylor Number and above the lower limit of velocity).

If, now a new coordinate system, xy′z′, is introduced, obtained from the xyz-system of fig. 2 by rotating it around the x-axis by an angle ψ_{av} given by equation (14), the velocity profile $v_R(x)$ in the new system is simply defined by

$$v_R = v_{y'} = \frac{V}{2}\ \frac{x}{\omega} \tag{17}$$

and the inclination from the xy′ plan is zero.

The length of contact between the upwards and

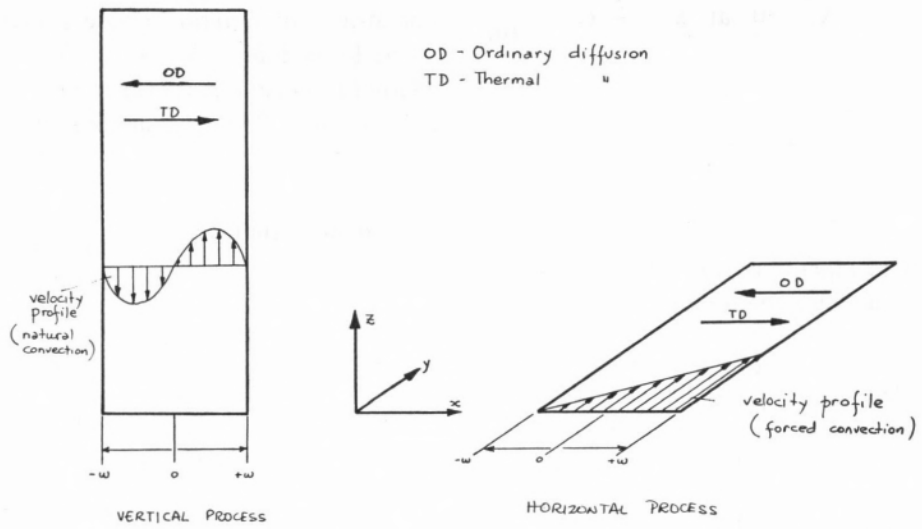

Fig. 2
Model of the rotary thermal diffusion column

downwards streams (the length of a particle streamline) for a column of vertical height L is, thus, on average

$$L^* = \frac{L}{|(\tan \psi)_{av}|} \tag{18}$$

or, using equation (14),

$$L^* = \frac{L}{|(\tan \psi)_{av}|} = \frac{18\eta V}{\beta g(\Delta T)\omega^2} \tag{19}$$

4 — THE MASS FLUXES

In the new coordinate system, xy′z′, the mass fluxes existing inside the rotary column, are ($v_x = v_{z'} = 0$)

$$J_x = -\rho D \frac{\partial c}{\partial x} + \frac{\alpha \rho D}{T_{av}} \frac{\partial T}{\partial x} c(1 - c) \tag{20}$$

$$J_{y'} = -\rho D \frac{\partial c}{\partial y'} + v_{y'} c\rho \tag{21}$$

$$J_{z'} = -\rho D \frac{\partial c}{\partial z'} \tag{22}$$

Since the angle ψ_{av} is assumed to be small,

$$\frac{\partial c}{\partial z} \simeq \frac{\partial c}{\partial z'} \tag{23}$$

and, noting that the flow pattern is such that

$$\frac{\partial c}{\partial z} = \frac{L^*}{L} \frac{\partial c}{\partial y'} \tag{24}$$

it is possible taking equations (23) and (24) together to write

$$\frac{\partial c}{\partial z'} = \frac{L^*}{L} \frac{\partial c}{\partial y'} \tag{25}$$

and, also

$$\frac{\partial \rho}{\partial z'} = \frac{L^*}{L} \frac{\partial \rho}{\partial y'} \tag{26}$$

The flux $J_{z'}$ becomes, then

$$J_{z'} = -\rho D \frac{L^*}{L} \frac{\partial c}{\partial y'} \tag{27}$$

and the corresponding term in the continuity equation [4],

$$\frac{\partial(c\rho)}{\partial t} = - \operatorname{div} \vec{J} \tag{28}$$

is, therefore

$$- \frac{\partial J_{z'}}{\partial z'} = \frac{\partial}{\partial y'} \left[\rho D \left(\frac{L^*}{L} \right)^2 \frac{\partial c}{\partial y'} \right] \tag{29}$$

The overall equation is thus

$$\frac{\partial(c\rho)}{\partial t} = - \frac{\partial J_{x'}}{\partial x'} + \\ + \frac{\partial}{\partial y'} \left\{ \left[\rho D \left(\frac{L^*}{L} \right)^2 + \rho D \right] \frac{\partial c}{\partial y'} \right\} - v_{y'} \frac{\partial(c\rho)}{\partial y'} \tag{30}$$

or, since $L^*/L \gg 1$.

$$\frac{\partial(c\rho)}{\partial t} = - \frac{\partial J_{z'}}{\partial x'} + \\ + \frac{\partial}{\partial y'} \left\{ \left[\rho D \left(\frac{L^*}{L} \right)^2 \frac{\partial c}{\partial y'} \right\} - v_{y'} \frac{\partial(c\rho)}{\partial y'} \right. \tag{31}$$

Equation (31) is formally identical to that of the more conventional columns for which the treatment of DEBYE [3] or of FURRY *et al.* [2] apply.

5 — BATCH SEPARATION EQUATIONS

The reduction of the problem to two dimensions presented in the preceding sections is equivalent to «substituting» the rotary column by a «moving-walls» column whose walls move in opposite directions with velocities $+ V/2$ and $- V/2$ and whose length of contact between upwards and downwards streams, L^*, is given by equation (19). In this case it is possible to use the results of RAMSER [6] for thermal diffusion under linear fluid shear.

Besides the usual simplifying assumptions associated with the derivation of the «fundamental equation» upon which the phenomenological theories for thermal diffusion columns are based, fully discussed by ROMERO [8], the treatment of RAMSER [6] for the «moving-walls» column has the following extra-limitations:

1) $c(1 - c) \simeq c$ (i.e. dilute solutions) (32)

2) $T_{av} \gg \alpha (\Delta T)$ (i.e. moderate temperature gradients) (33)

3) $V \gg \frac{11\ D}{2\omega}$ (i.e. forced convection $\gg$ natural convection) (34)

Under the above conditions the mathematical treatment of Ramser arrives at the following solution for the concentration profile in the direction of shear, which converges for large values of the time variable, t:

$$c = c_o \left\{ 1 + \frac{40\ \Omega}{120 + \Omega^2} \frac{qh}{\pi^2 (2\omega)} \sum_{n=0}^{\infty} (-1)^n \cdot \right. \\ \left. \cdot \frac{\sin \left[(2n+1) \frac{2\omega}{h} \xi \right]}{(2n+2)} \left[1 - e^{-(2n+1)^2 \cdot t/\theta} \right] \right\} \tag{35}$$

where

$$\Omega = \frac{(2\omega)\ V}{D} \tag{36}$$

$$q = \frac{\alpha (\Delta T)}{T_{av}} \tag{37}$$

$$\theta = \frac{h^2}{\pi^2 D} \frac{1}{1 + \Omega^2/96} \tag{38}$$

$$\xi = \frac{y - h}{2\omega} \tag{39}$$

h = length of a particle streamline (40)

The degree of separation, Δ, defined as the difference between the top and bottom concentrations, respectively, c_T and c_B, involves the difference between the two infinite series obtained from equation (35) by substituting ξ by

$$\frac{h}{2\omega}$$

and zero, respectively. However, after a time $t \geq 0.3\, t_r$ the terms of the series beyond the first can be neglected with an error less than 1 % and, after rearranging the following expression is obtained

$$\Delta = \Delta_\infty \left(1 - k_3\, e^{-t/t_r}\right) \tag{41}$$

with

$$\Delta_\infty = \frac{10 c_o \alpha D (\Delta T) h}{T_{av} (2\omega) 2V} \tag{42}$$

$$t_r = \frac{96 D h^2}{\pi^2 (2\omega)^2 V^2} \tag{43}$$

$$k_3 = \frac{8}{\pi^2} \tag{44}$$

Introducing the dimensionless length, λ, defined by

$$\lambda = \frac{504 \alpha D \eta L}{\beta g T_{av} (2\omega)^4} \tag{45}$$

and substituting h which in this case is equivalent to L* by its value given in equation (19) the following equations are obtained

$$\Delta_\infty = 1.43 \lambda c_o \tag{46}$$

$$t_r = 3.44 \cdot 10^5 \frac{D \eta^2 L^2}{\pi^2 \beta^2 g^2 (\Delta T)^2 (\omega)^6} \tag{47}$$

It is interesting to note that the steady-state separation, Δ_∞, and the relaxation time, t_r, of the rotary column defined by equations (46) and (47) may be expressed in terms of the corresponding static parameters, $(\Delta_\infty)_{st}$ and $(t_r)_{st}$, as

$$\Delta_\infty = 1.43 (\Delta_\infty)_{st} \tag{48}$$

$$t_r = 1.37 (t_r)_{st} \tag{49}$$

where

$$(\Delta_\infty)_{st} = \lambda c_o \tag{50}$$

$$(t_r)_{st} = \frac{9! D \eta^2 L^2}{\pi^2 \beta^2 g^2 (\Delta T)^2 (2\omega)^6} \tag{51}$$

The identical functional dependence of the separation of the rotary and static columns emphasised by equations (48) and (49) is somewhat surprising since it is believed, according to experimental reports, that separation and relaxation-time are affected by rotation. Another interesting observation is that equation (48) predicts that rotation increases the steady-state separation attainable, which has not been always observed in the non-dilute concentration range [5].

It is anticipated that the above conclusions, based on a model derived for an «ideal» situation which may be widely different from the «real» conditions encountered in practice [12], are strongly affected by non-ideal conditions.

6 — APPLICATION OF THE «IDEAL» THEORY TO «REAL» COLUMNS

The principal factor affecting the agreement between predicted and experimental results in the conventional static columns has been the non-constancy of the annulus width, due mainly to the eccentricity (either local or along the entire column length). The problem has been the focus of study of several workers [9-11] and, ultimately, BOTT and ROMERO [12] introduced the concept of «equivalent annulus width» based on the physical interpretation of the role played by the eccentricity in altering the fluxes

within the column. Briefly, it can be said that the eccentricity of the annulus of a static column promotes and extra-remixing that decreases the separation as if the column had a larger annulus width. The concept was used recently [14] to correlate the experimental results obtained in a commercial column and proved to account for the irregularities in the annular space over the entire separation range.

The effect of eccentricity when the column rotates is qualitatively the same — increase in remixing — but the «equivalent annulus width» must, in principle, be different from the static one since the flow pattern is also different. In fact, in a static column, the particles streamlines are practically parallel to the column walls, whereas for a rotary column (at speeds above the «lower limit») the angle between the particles streamlines and the vertical direction is almost 90 degrees. As a result, the existence of an eccentricity will induce a somewhat «pulsating» remixing effect similar to that of the static column but repeated (L*/L) times. Thus, the equivalent annulus width for a rotary column will be different from that of the static column and, in principle, greater. Also, it is expectable that the speed of rotation will affect strongly the value of the equivalent annulus width of the rotary apparatus since the angle between the particles streamlines and the walls depends on the speed of rotation (and, thus, depends the «pulsating» effect).

If, then (2ω) in the previous equations is considered the static equivalent annulus width as defined by BOTT and ROMERO [12], the «rotary equivalent annulus width», $(2\omega^*)$, must be

$$2\omega^* = \frac{2\omega}{\gamma} \tag{52}$$

$$\text{with } \gamma \leq 1 \tag{53}$$

Taking equation (52) into account, the «real» expressions for the steady-state separation, Δ_∞, and relaxation-time, t_r, to use in equation (41) become

$$\Delta_\infty = 1.43\gamma^4\lambda c_o \tag{54}$$

or

$$\Delta_\infty = 1.43\gamma^4 \cdot (\Delta_\infty)_{st} \tag{55}$$

and

$$t_r = 3.44 \cdot 10^5\gamma^6 \frac{D\eta^2L^2}{\pi^2\beta^2g^2(\Delta T)^2(2\omega)^6} \tag{56}$$

or

$$t_r = 1.37\gamma^6 \cdot (t_r)_{st} \tag{57}$$

With equations (55) and (57) it is now seen that the improvement or decrease in separation relatively to the static column will depend essentially on the actual value of γ, that is, on the constancy of the annulus width and speed of rotation.

A means of testing the validity of the theory and the adequacy of the parameter γ just introduced is to determine the steady-state separation and relaxation-time experimentally and compare the values of γ evaluated through equations (55) and (57) that carry distinct functional dependences on γ.

7 — PUBLISHED EXPERIMENTAL WORK AND THE THEORY

Although the concentration of dilute solutions by conventional thermal diffusion has been often referred in the literature, the use of a rotary column in this range of concentration has only been reported by BOTT [13] who worked with a dilute aqueous solution of glycerol (5 % mole per. glycerol).

Bott studied the influence of the speed of rotation on separation but restricted it to the first phase of the transient period of separation where $\partial\Delta/\partial t$ is larger (this phase has the greater potential interest for large-scale application). The results of BOTT [13] are, therefore, of limited value to a complete test of the theory. Notwithstanding, the experimental separation curves obtained, shown in fig. 3, allow some inferences:

(1) The separation is increased by rotation which,

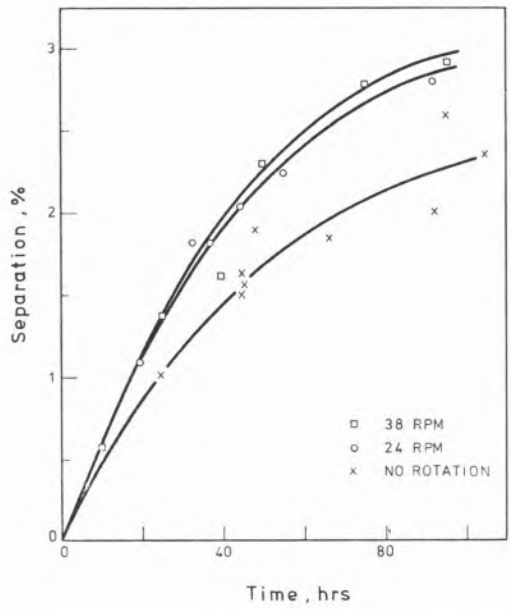

Fig. 3
Separation as a function of time for 5 % glycerol-water system [12]

in terms of the theory means that γ is close to unity or, at least, $(1.43\ \gamma^4) > 1$.

(2) The separation curves for the two speeds of rotation, 24 and 38 RPM, are not significantly deviated which again is an indication that the column is not much imperfect, i.e. that γ is close to unity.

As far as the equilibrium-separations and relaxation-times involved are concerned, it is necessary to extrapolate the results of fig. 3 to greater times. This extrapolation may involve a large error and is therefore severely limited in terms of confirming or rejecting the theory. Nevertheless it is worthwhile to estimate, though roughly, the orders of magnitude of the extrapolated and calculated parameters since it provides an example of the type of determinations involved.
By a least squares method it is possible to define the parameters Δ_∞ and t_r that give the best fit between equation (41) and the experimental points:

$$(\Delta_\infty)_{st} = 0.028$$

$$(\Delta_\infty)_{24} \simeq (\Delta_\infty)_{38} \simeq 0.033$$

$$(t_r)_{st} \simeq 60 \text{ hrs}$$

$$(t_r)_{24} \simeq (t_r)_{38} \simeq 55 \text{ hrs}$$

The value of γ may now be evaluated through either equation (55) or (57) aud if the theory is correct those values — referred to as γ_Δ and γ_t — should be equal

$$\gamma_\Delta = \left[\frac{0.033}{(1.43)(0.028)}\right]^{\frac{1}{4}} = 0.95$$

$$\gamma_t = \left[\frac{55}{(t.37)(60)}\right]^{\frac{1}{6}} = 0.94$$

If the extrapolated values of Δ_∞ and t_r are assumed to be valid, the above results indicate that the column is almost perfect ($\gamma \sim 1$) and the test of the theory, positive ($\gamma_\Delta \simeq \gamma_t$).

8 — CONCLUSIONS

By comparing the rotary column to a «moving-walls» column with an equal rate of shear across the annulus and defining an «effective length of cascading», it is possible to use the general derivation pattern of the «moving-walls» theory to study the rotary column. The principal results thus obtained may be summarised as follows:

1) Apart numerical factors the separation equations of a rotary column for the concentration of dilute mixtures (c (1 — c) $\simeq$ c) are identical to the corresponding static equations when the column is geometrically perfect.

2) For a rotary column not geometrically perfect it is necessary to define an equivalent annulus width by $2\omega^* = 2\omega/\gamma$, in which (2ω) is the static equivalent annulus width as defined by BOTT and ROMERO [12] and γ is a correction factor less than unity that may be evaluated experimentally.

3) The separation and relaxation-time are more favourable in the rotary column (better performance), providing that the value of γ is close to unity, i.e. that the column is near perfect.

ACKNOWLEDGEMENT

J. de D. R. S. Pinheiro wishes to express his gratitude to the Calouste Gulbenkian Foundation for the provision of a scholarship which made possible this work.

LIST OF SYMBOLS

c — molar fraction of specified component
c_o — initial feed composition
c_T — composition at the top of the column
c_B — composition at the bottom of the column
D — mutual diffusion coefficient
D' — thermal diffusion coefficient
g — gravity acceleration
h — length of column (for cascading)
$\vec{J}$ — molar flux
k_3 — dimensionless parameter defined by eq. (44)
k — thermal conductivity
L — column length (height)
N_{Ta} — Taylor number, $N_{Ta} = 2\rho^2(2\omega)^3V^2/r_m\eta^2$
$(N_{Ta})_c$ — critical Taylor number $= 3.39 \times 10^3$
p — hydrostatic pressure
q — dimensionless parameter defined by eq. (37)
r — cylinder radius
T — absolute temperature
t — time
t_r — relaxation-time
V — tangential velocity (velocity of the moving wall)
v — velocity
v_R — resultant velocity of the combined natural and forced convection
x, x', y, y', z, z' — coordinate directions

GREEK LETTERS

α — thermal diffusion constant
β — temperature coefficient of density
γ — correction factor defined by eq. (52)
Δ — degree of separation ($\Delta = |c_T - c_B|$)
ΔT — temperature difference between hot and cold walls
ξ — dimensionless vertical coordinate defined by eq. (39)
λ — dimensionless length defined by eq. (45)
η — viscosity coefficient
θ — dimensionless time defined by eq. (38)
π — 3.141592...
ρ — density of the mixture
ψ — deflection angle of the particles streamlines from horizontal
Ω — dimensionless parameter defined by eq. (36)
2ω — annulus width (equivalent annulus width) of static column
$2\omega^*$ — equivalent annulus width of rotary column

SUBSCRIPTS

av — average value
st — static
∞ — steady-state
x, y, z — component identification

REFERENCES

[1] CLUSIUS, K. and DICKELL, G., *Naturwissenschaften*, **26**, *546 (1938)*.
[2] FURRY, W. H., JONES, R. C. and ONSAGER, L., *Phys. Rev.*, **55**, *1063 (1939)*.
[3] DEBYE, P. J., *Ann. Physik*, **36**, *284 (1939)*.
[4] BIRD, R. B., STEWART, W. E. and LIGHTFOOT, E. N., «Transport Phenomena», Jokn Wiley & Sons, London, 1960.
[5] ROMERO, J. J. B., *Dechema Monograph.*, **65**, *337 (1971)*.
[6] BOTT, T. R. and PINHEIRO, J. D. R. S., To be published.
[7] RAMSER, J. H., *Ind. Eng. Chem,,* **49**, *155 (1957)*.
[8] ROMERO, J. J. B., *Rev. Fis. Quim. Eng., (ULM)*, **2**, *Sér. A, 1 (1970)*.
[9] HOFFMAN, D. and EMERY, A. H., *A. I. Ch. E. (Am. Inst. Chem. Engrs.) J.*, **9**, *653 (1963)*.
[10] KORCHINSKY, W. J. and EMERY, A. H., *A. I. Ch. E. (Am. Inst. Chem. Engrs.) J.*, **13**, *224 (1967)*.
[11] POWERS, J. E., «Thermal Diffusion», in «New Chemical Engineering Separation Techniques», ed. Schoen, Interscience Publishers, London, 1962.
[12] BOTT, T. R. and ROMERO, J. J. B., *Trans. Inst. Chem. Engrs. (London)*, **47**, *T166 (1969)*.
[13] BOTT, T. R., «Chemeca-70» (Australia), Butterworths, London, 1970.
[14] ROMERO, J. J. B. and PINHEIRO, J. D. R. S., To be published.

Recebido 6. Maio. 1975.

RESUMO

Apresenta-se uma teoria fenomenológica aproximada para descrever a concentração de soluções diluídas numa coluna de difusão térmica rotativa. A teoria baseia-se na construção de um modelo bidimensional simplificado e subsequente aproveitamento da metodologia de Ramser no tratamento de colunas «de paredes móveis». Discute-se a aplicação do modelo teórico a colunas reais, definindo-se, por analogia com a coluna termogravitacional, uma «espessura equivalente» de coluna rotativa. As equações de separação assim obtidas mostram que o rendimento da coluna rotativa depende apreciavelmente da constância (perfeição geométrica) do espaço anular. Para colunas perfeitas o grau de separação é praticamente independente da velocidade de rotação, sendo superior ao grau de separação que se obtém em idênticas condições na coluna estática. Para colunas não perfeitas, contudo, o grau de separação diminui à medida que a velocidade de rotação aumenta, tornando-se, acima de determinada velocidade, inferior ao da coluna estática. Os (poucos) resultados experimentais existentes são discutidos em termos da presente teoria.

C. McDERMOTT

N. ASHTON

Department of Chemical Engineering
University of Birmingham
Birmingham — B15 2TT — U. K.

THE CONVERGENCE OF PLATE TO PLATE DISTILLATION CALCULATIONS (1)

A calculation method for multicomponent distillation is proposed which is based on the Lewis and Mathieson method for the plate to plate calculations. The convergence method used is based on the θ-method but involves only a single θ irrespective of the number of sidestreams involved. The method is applicable in the case of multiple feeds, non-ideal mixtures and non-constant molal overflow and has been found converge satisfactorily on a variety of problems.

I — INTRODUCTION

During recent years the application of computers to multicomponent distillation problems has tended to use one of three basic approaches. The first could be viewed as the automation of the methods previously existing and generally employing the approach of progressing plate by plate through the column. The difficulty here is to start the calculation at one end with compositions or flowrates which, after completing the plate to plate calculations, provide compositions for the remaining external streams which satisfy the overall material balance. This leads to the procedure of estimating product composition or compositions and then improving these estimates by various «convergence» methods.

The second approach to the problem is to solve the basic equations throughout the column for one component at a time. This method was used by AMUNDSEN and PONTINEN [1] who set up a system of equations from the mass balance and equilibrium relationships for a particular component. The matrix of such a system is of tri-diagonal form and is easily solved using standard procedures available on most machines. The problem with this method is to ensure that, when compositions have been calculated for each component, they will sum to unity on each plate. A simple approach is to normalise the compositions, carry out bubble point calculations to re-estimate the equilibrium K-values and repeat possibly using a relaxation factor to aid convergence. Variations on this technique with improved convergence properties have been suggested by SARGENT [7] and BOYNTON [2].

---

(1) Presented at CHEMPOR' 75 held in Lisbon, 7-12 September 1975 at the Calouste Gulbenkian Foundation Center.
Papers presented at this International Chemical Engineering Conference can be purchased directly from Revista Portuguesa de Química (Instituto Superior Técnico, Lisboa 1, Portugal) at the following prices per volume sent by surface mail, postage included (in Portuguese Escudos):

Whole set	500
Transport processes	200
Reaction engineering	150
Environmental engineering	150
Management studies	150

This paper was presented at the Transport processes section.

Finally there exists a group of methods which make use of modern techniques for solving systems of non-linear algebraic equations. Particularly popular here are the «quasi-Newton» methods developed by BROYDEN [3]. Such methods in effect produce, at each stage of the calculation, an estimate of the Jacobian matrix of the system of equations and then use this in a Newton type of step to improve the current estimates of the values of the unknown variables. TOMICH [9] among others, has claimed sucess in applying this method to distillation, but indepentent trials by STROUD [8] at Birminghan have shown the time required for such methods to be large. This may be because these methods fail to exploit the existing knowledge of the structures of distillation problems and so waste a great deal of time making numerical experiments in regions which are not profitable.

The present study is an example of a method belonging to the first group using the Lewis Mathieson method for the plate to plate calculations. That is the mass balance and equilibrium relationships are satisfied simultaneously for a particular plate rather than as in the Thiele and Geddes method, determining equilibrium temperatures throughout the column as a separate step. HOLLAND [5] has described the θ-method for complex columns using the Thiele-Geddes calculation method and HIROSE [4] and SAITO [6] have considered its use with the Lewis-Mathieson method. In the above applications a separate θ was used to correspond to each side stream and a system of non-linear equations solved at each iteration so that the overall balance and sidestream flowrates are more closely satisfied at the next iteration. The following is a method which achieves a similar result using only a single θ even in the presence of sidestreams.

2 — PROPOSED METHOD

2.1 — *BASIC EQUATIONS*

Consider a column consisting of N plates, a condenser and a reboiler which is to separate a mixture of M components. The feed enters on a plate in the column at which we will choose to match the liquid or vapour plate compositions calculated from assumed distillate and bottoms component flowrates. Suppose we denote the assumed distillate flowrates by d_i ($i = 1, \ldots, M$) and the bottoms flowrates by b_i ($i = 1, \ldots, M$) and further that, by carrying out a plate to plate calculation from the reboiler to the matching plates, we obtain matching plate liquid flowrates C B_i and from the condenser down to the matching plate we obtain C T_i for the same variables. We require a set of values of d_i and b_i such that

$$\sum_{i=1}^{M} D_i = D \tag{1}$$

$$\sum_{i=1}^{M} b_i = B \tag{2}$$

and

$$CB_i = CT_i \, (i = 1, \ldots, M) \tag{3}$$

where D and B are the specified distillate and bottoms flowrates respectively. Finally we may include the effect of the side streams in each section by denoting the total flowrate from the bottom or stripping section of the column by SB_i and the corresponding flow from the top of the column by ST_i.

The argument for the use of the θ-method is that an increase in one of the bottoms flows, b_j, say will produce a corresponding increase in each of the plate flowrates (liquid or vapour) in the stripping section of the column. In particular the corresponding CB_j will increase as well as the flowrate of component j in each sidestream in that part of the column. The assumption following from this is that the ratio of the plate flowrate (or composition) to the bottoms rate will remain constant from one iteration to the next. Preserving this ratio for the sidestreams, however, will mean that a change in the bottoms composition will violate the sidestream flowrate. This problem is overcome in the θ-method by multiplying the ratios for a particular sidestream by θ and then choosing θ so that the flowrate for that stream is preserved. It is the view of the present authors that this device can be shown to be unnecessary by the way the sidestream component flows are calculated. Suppose that a liquid

stream is taken from a particular plate, then from the stage calculations from the plate below, a plate liquid composition is determined for the plate in question without any reference to the sidestream. In particular the mass balance envelope would include feeds and sidestreams for plates below, the vapour leaving the plate immediately below and the liquid leaving the plate in question. From this a liquid composition is determined which is then multiplied by the specified sidestream total flowrate to obtain the required component flowrate. There is thus no necessity to take steps to choose bottoms flows to produce the required sidestream flowrate. The only difficulty which arises is that the overall component balance may be violated so the only assumption which is necessary is that say the ratio of SB_i to b_i is preserved from one iteration to the next but this ratio may be modified by multiplication by some θ to preserve the specified bottoms flowrate.

Suppose then that the total feed rate for component i is F_i thus, for the corrected b_i and d_i which will be denoted by b_i^c and d_i^c, we require

$$ST_i + SB_i = F_i \tag{4}$$

or

$$d_i^c \frac{ST_i}{d_i} + b_i^c \frac{SB_i}{b_i} = F_i \tag{5}$$

where the ST_i and SB_i in (5) refer to values calculated using the assumed values d_i and b_i.

In order to relate d_i^c to b_i^c we appeal to equation (3) which assuming the ratio preservation gives

$$b_i^c \frac{CB_i}{b_i} = d_i^c \frac{CT_i}{d_i} \tag{6}$$

or

$$b_i^c = d_i^c \frac{CT_i b_i}{CB_i d_i} \tag{7}$$

Substituting equation (7) into equation (5) we have

$$d_i^c \left\{ \frac{ST_i}{d_i} + \frac{CT_i b_i}{CB_i d_i} \frac{SB_i}{b_i} \right\} = F_i \tag{8}$$

or

$$d_i^c = \frac{F_i d_i CB_i}{ST_i GB_i + SB_i CT_i} \tag{9}$$

Equation (9) forms the basis of the method for the recalculation of the distillate flowrates for the next iteration. Using the same method as that used to obtain equation (9) from equation (6), it is straightforward to develop the corresponding formula for the bottoms flowrate viz.

$$b_i^c = \frac{F_i b_i CT_i}{ST_i CB_i + SB_i CT_i} \tag{10}$$

2.2 — *CONVERGENCE METHOD*

Clearly there is no guarantee that the flowrates calculated using equations (9) or (10) will satisfy the appropriate equation (1) or (2). Various choices are now open to us for the precise values to be used in the next iteration. One could use the values calculated from equations (9) and (10) directly thus in general, violating the specified distillate and other bottoms flowrates. There would be no reason in this case for equations (1) and (2) to be satisfied even when the matching plate flowrates agree. Alternatively the calculated rate could be normalised to satisfy (1) and (2) which corresponds to the method of simple iteration and in this case, if convergence results, the basic defining equations will all be satisfied.

In this work the method used by HOLLAND [5] for simple columns (i.e. single feed, no sidestreams) was used. This involves modifying the coefficient of d_i^c in equation (7) by a multiple, θ, that is equation (7) becomes

$$b_i^c = d_i^c \frac{CT_i b_i}{CB_i d_i} \theta \tag{11}$$

After following through this modification, we obtain revised forms of equations (10) and (11), that is

$$d_i^c = \frac{F_i d_i CB_i}{ST_i CB_i + \theta SB_i CT_i} \tag{12}$$

and

$$b_i^c = \frac{\theta F_i b_i CT_i}{ST_i CB_i + \theta SB_i CT_i} \qquad (13)$$

Note that equation (13) may also be written

$$b_i^c = \frac{F_i b_i CT_i}{\theta^{-1} ST_i CB_i + SB_i CT_i} \qquad (14)$$

which is in a form more closely related to equation (9) and which may be simply derived from (6) in the same way as (12) but with a multiple of θ^{-1} for the coefficient of b_i^c in the equation corresponding to (7).

We may now choose θ by either substituting equation (12) into equation (1) and solving the resulting equations for θ, or substituting equation (13) [or (14)] into equation (2) and solving for θ. It must be realised that unless convergence has already been obtained, two different values of θ will result so that it is not possible by this method to satisfy both of equations (1) and (2) at every stage of the calculation. However as the iterations progress the values of θ tend towards unity. The effect of this is to ensure that, as the iterations progress towards convergence, whichever of equations (1) or (2) has been sacrificed, will finally be satisfied. This can also be seen to be forced by the satisfaction of the overall component balances.

In the present work it was decided to use equations (12) and (1) and thus produce bottoms flows at each stage needing normalisation before being used in the plate to plate calculations.

From equations (12) and (1) then, we have

$$\sum_{i=1}^{M} \frac{F_i d_i CB_i}{ST_i CB_i + \theta SB_i CT_i} - D = 0 \qquad (15)$$

which, for convenience we may write as

$$f(\theta) = 0 \qquad (16)$$

The question now arised whether this equation has a solution for a positive value of θ. For a zero of θ, the left hand side of equation (15) takes the form

$$\sum_{i=1}^{M} \frac{F_i d_i}{ST_i} - D \qquad (17)$$

and it is shown in the Appendix that the first term in this expression must always exceed the second. Further, if θ is then allowed to increase without limit then, provided the coefficient of θ in equation (15) is positive, the first term in equation (15) will tend to zero making the left hand side negative. Thus for zero or small θ $f(\theta)$ is positive and for large θ $f(\theta)$ becomes negative and, as equations (15) is continuous in θ, there must be a value of θ for which $f(\theta)$ vanishes.

The method adopted for the solution of equation (16) was that of Newton which was chosen because the derivative of $f(\theta)$ is easily calculated and the convergence is rapid. Fig. 1 shows a typical form of the function $f(\theta)$ vs. θ and the progress of the Newton formula

$$\theta_{n+1} = \theta_n - \frac{f(\theta_n)}{f'(\theta_n)} \qquad (18)$$

towards the solution. From the shape of the curve it is evident that any starting guess for θ which is between zero and the solution will converge rapidly to the solution. However a value which is much too large can produce a corrected value from equation (18) for which θ is negative. A simple way to ensure convergence is to replace the recalculated negative value by one half of the

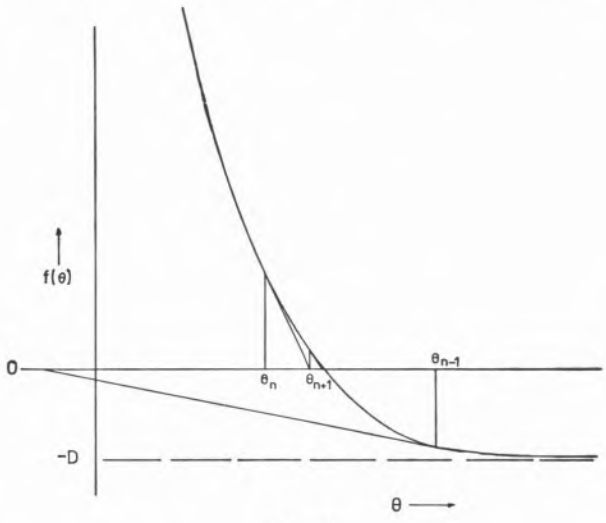

Fig 1
Typical plot of $f(\theta)$ vs. θ

Table 1

Physical property data

Component	Antoine constants			Entalphy constants			
	A	B	C	k_i	k_2	H_i	H_2
$i - C_4$	6.4786	763.416	230.0	6074.6	69.4	15132.0	45.0
C_4	6.5742	816.405	230.0	6633.8	69.6	16015.0	46.6
$i - C_5$	6.7204	972.162	230.0	7200.7	86.2	18849.0	57.0
C_5	6.8122	1024.920	230.0	7584.2	85.4	19986.0	55.4

previous value. If this again produces a negative value the halving is repeated until a value is obtained for which convergence results. The above modification has sucessfully located the solution in all cases.

3 — RESULTS

The method has been applied successfully to a range of examples. Fairly typical are the following, based upon the work of VAN WINKLE [10]. The physical property data for the componentes, presented by Van Winkle, is in a different form to that required in the program and so it was necessary to fit the data to the correlating equations used by the program. First the K-values needed to be expressed in the form of the Antoine equation for vapour pressure:

$$\log_{10} p_i = \log_{10} (K_i \pi) = A_i - \frac{B_i}{T + C_i} \quad (19)$$

where p_i is the vapour pressure of pure component i, π is the total pressure, K_i the K-value for component i and A_i, B_i and C_i are the Antoine constants. Secondly the enthalpy data given for specific temperatures was represented by

$$h = h_1 + h_2 T \quad (20)$$

for the liquid and similarly

$$H = H_1 + H_2 T \quad (21)$$

for the vapour. The results of these operations for the four components used in the examples are given in Table 1.

3.1 — *EXAMPLE I*

The details of the column specification are given in Table 2. The physical property data is as given in Table 1 but the calculation was carried out assuming constant molal overflow and the results obtained by this method are compared with those obtained by Van Winkle in Table 3. The results were obtained after 11 iterations of the method from an arbitrary first guess to an agreement of less than 10^{-4} in the calculated matching plate compositions. The differences between the solution given here and that of Van Winkle is explained by the discrepancies in the representation of physical properties. The top and bottoms temperatures calculated by Van Winkle were 58.05 and 99.39 °C respectively and for this work the results were 55.94 and 97.2 °C.

Table 2

Column specification

Number of components	4	Distillate rate	24.31
Number of plates	17	Bottoms rate	75.69
Operating pressure	5170 mm Hg	Recycle ratio	3.7
Pressure drop per plate	6.08 mm Hg	Feed to plate	6
Total condenser		Feed condition	liquid at 80 °C

Table 3

Comparison of results for example I

Component	Distillate composition			Bottoms composition	
	Feed	This work	Van Winkle	This work	Van Winkle
i — C_4	0.06	0.2463	0.2461	0.0002	0.0002
C_4	0.17	0.6746	0.6677	0.0079	0.0101
i — C_5	0.32	0.0551	0.0607	0.4051	0.4035
C_5	0.45	0.0240	0.0260	0.5868	0.5862

3.2 — *EXAMPLE II*

The column specification and physical property data for example II were identical to those used in example I except that the number of plates was increased to 18, the reflux ratio was 10 and extra feeds and sidestreams were introduced to test the proposed method on a complex column. The extra feed was 100 moles of liquid with mole fraction 0.25 for each component introduced onto plate 12 at 85 °C. The sidestreams were 50 moles of vapour withdrawn from plate 9 and 50 moles of liquid from plate 12.

In this example the enthalpy data given in Table 1 was used to recalculate the liquid and vapour rates throughout the column after each iteration.

The solution was reached in this case again from an arbitrary first guess in 30 iterations. This is rather more than is to be expected and is probably due to a damping factor which slowed the convergence rate to 1/4 of its natural value and which was included inadvertently. As no comparison is available computer output for the final iteration is given in Table IV.

4 — CONCLUSIONS

The above examples indicate that the method proposed is able to deal satisfactorily with distillation problems of both simple and complex nature. The convergence is rapid in most cases and is particularly good when the column approximates to the situation in which the θ-method is capable of providing the exact solution in a single step. This situation is of course, for a column operating with components of constant relative volatility at total reflux. Problems have been encountered near minimum reflux and work is continuing in this area. Of particular interest is example II where two sidestreams are taken. From this output it is evident that the final iteration gives a total bottoms rate equal to that specified and simultaneously satisfies the component overall balances and the other specified flowrates in the problem. This is of course in spite of the fact tha θ-method iterations are only aimed at meeting the specified distillate flowrates.

The proposed convergence method may of course be used in conjunction with the calculation method of Thiele and Geddes and is in no way limited to the Lewis Mathieson method adopted here. There are occasions when the Lewis Mathieson method is not able to represent adequately certain systems. That is systems involving completely separated components for which the Lewis Mathieson method would require non-zero distillate or bottoms flowrates smaller than the machine capacity. In such cases it would be advantageous to adopt the Thiele-Geddes calculation method.

NOMENCLATURE

A,B,C — Antoine constants
b — component flowrate in bottoms
B — total specified bottoms flowrate
CB — matching plate flowrate calculated from the bottom up
CT — matching plate flowrate calculated from the top down
d — component flowrate in distillate
D — total specified distillate flowrate
F — feed rate
f — function defined by equation (16)
h — liquid molar enthalpy
h_1 h_2 — constants in liquid entalphy correlation
H — vapour molar enthalpy
H_1 H_2 — constants in vapour enthalpy correlation
K — equilibrium K value
M — number of components
N — number of plates
p — vapour pressure

Table 4

```
                SOLUTION ACHIEVED AFTER  3  ITERATIONS

ITERATION NUMBER 50

                TOP PRODUCT
TEMP=   0.60369      0.39431      0.14944E-02 0.50632E-03
        60.48
                REFLUX
        0.60369      0.39431      0.14944E-02 0.50632E-03

                PLATE COMPOSITIONS AND FLOWRATES

                PLATE NUMBER  1
LIQUID  0.5339   0.4601   0.0042   0.0018
VAPOUR  0.6037   0.3943   0.0015   0.0005
TEMP=   50.5       LIQ. RATE=  242.357      VAP. RATE=  267.410

                PLATE NUMBER  2
LIQUID  0.4668   0.5167   0.0108   0.0057
VAPOUR  0.5403   0.4541   0.0040   0.0017
TEMP=   51.6       LIQ. RATE=  240.847      VAP. RATE=  266.667

                PLATE NUMBER  3
LIQUID  0.4012   0.5559   0.0261   0.0169
VAPOUR  0.4764   0.5055   0.0099   0.0052
TEMP=   53.1       LIQ. RATE=  237.724      VAP. RATE=  265.207

                PLATE NUMBER  4
LIQUID  0.3333   0.5619   0.0582   0.0466
VAPOUR  0.4106   0.5409   0.0238   0.0154
TEMP=   55.6       LIQ. RATE=  231.417      VAP. RATE=  262.038

                PLATE NUMBER  5
LIQUID  0.2564   0.5131   0.1148   0.1128
VAPOUR  0.3590   0.5460   0.0528   0.0422
TEMP=   60.0       LIQ. RATE=  221.794      VAP. RATE=  255.727

                PLATE NUMBER  6
LIQUID  0.1836   0.4047   0.1874   0.2241
VAPOUR  0.2934   0.5016   0.1035   0.1016
TEMP=   67.1       LIQ. RATE=  211.758      VAP. RATE=  246.107

                PLATE NUMBER  7
LIQUID  0.1404   0.3942   0.2019   0.2644
VAPOUR  0.2764   0.4997   0.1145   0.1093
TEMP=   68.2       LIQ. RATE=  210.415      VAP. RATE=  244.049

                PLATE NUMBER  8
LIQUID  0.1534   0.3706   0.2251   0.2508
VAPOUR  0.2582   0.4864   0.1331   0.1222
TEMP=   69.6       LIQ. RATE=  208.459      VAP. RATE=  242.725

                PLATE NUMBER  9
LIQUID  0.1347   0.3105   0.2597   0.2951
VAPOUR  0.2376   0.4563   0.1632   0.1429
TEMP=   72.4       LIQ. RATE=  204.037      VAP. RATE=  240.769

                PLATE NUMBER 10
LIQUID  0.1171   0.2829   0.2940   0.3020
VAPOUR  0.2174   0.4133   0.2003   0.1690
TEMP=   75.2       LIQ. RATE=  312.065      VAP. RATE=  288.347

                PLATE NUMBER 11
LIQUID  0.1016   0.2340   0.3357   0.3287
VAPOUR  0.1944   0.3619   0.2416   0.1920
TEMP=   78.1       LIQ. RATE=  310.837      VAP. RATE=  286.375

                PLATE NUMBER 12
LIQUID  0.0888   0.1897   0.3690   0.3526
VAPOUR  0.1828   0.3090   0.2825   0.2257
TEMP=   80.3       LIQ. RATE=  346.647      VAP. RATE=  285.147

                PLATE NUMBER 13
LIQUID  0.0505   0.1352   0.4200   0.3944
VAPOUR  0.1135   0.2421   0.3600   0.2843
TEMP=   85.0       LIQ. RATE=  347.963      VAP. RATE=  270.959

                PLATE NUMBER 14
LIQUID  0.0268   0.0895   0.4553   0.4283
VAPOUR  0.0644   0.1725   0.4253   0.3380
TEMP=   89.8       LIQ. RATE=  350.022      VAP. RATE=  272.273

                PLATE NUMBER 15
LIQUID  0.0134   0.0561   0.4751   0.4550
VAPOUR  0.0341   0.1137   0.4704   0.3818
TEMP=   92.5       LIQ. RATE=  351.880      VAP. RATE=  274.332

                PLATE NUMBER 16
LIQUID  0.0066   0.0342   0.4823   0.4769
VAPOUR  0.0179   0.0712   0.4955   0.4161
TEMP=   94.3       LIQ. RATE=  353.201      VAP. RATE=  276.199

                PLATE NUMBER 17
LIQUID  0.0032   0.0202   0.4799   0.4966
VAPOUR  0.0084   0.0430   0.5045   0.4441
TEMP=   95.4       LIQ. RATE=  353.973      VAP. RATE=  277.511

                PLATE NUMBER 18
LIQUID  0.0015   0.0117   0.4700   0.5168
VAPOUR  0.0040   0.0252   0.5014   0.4693
TEMP=   96.2       LIQ. RATE=  354.332      VAP. RATE=  278.283

                PLATE NUMBER 19
LIQUID  0.0007   0.0066   0.4535   0.5392
VAPOUR  0.0019   0.0144   0.4887   0.4950
TEMP=   96.7       LIQ. RATE=  354.396      VAP. RATE=  278.643

                PLATE NUMBER 20
LIQUID  0.0003   0.0036   0.4306   0.5655
VAPOUR  0.0008   0.0079   0.4677   0.5235
TEMP=   97.2       LIQ. RATE=  354.240      VAP. RATE=  278.708

                REBOILER
LIQUID  0.0001   0.0019   0.4009   0.5971
VAPOUR  0.0004   0.0041   0.4386   0.5569
TEMP=   97.6       LIQ. RATE=  75.690       VAP. RATE=  278.556

                SIDE STREAM MOLAR FLOWRATES

                PLATE NUMBER  9
LIQUID  0.0000   0.0000   0.0000   0.0000
VAPOUR 11.8816  22.8134   8.1598   7.1452

                PLATE NUMBER 12
LIQUID  6.4382   9.4830  18.4488  17.6209
VAPOUR  0.0000   0.0000   0.0000   0.0000
```

SB — flowrate from column below matching plate (including bottoms)

ST — flowrate from column above matching plate (including distillate)

SUBSCRIPTS

i — component

n — value at n^{th} iteration

GREEK LETTERS

θ — multiplied to modify coefficient of d in equation (7) in order to satisfy specified distillate rate

π — system total pressure

APPENDIX

To show that

$$\sum_{i=1}^{M} \frac{F_i d_i}{ST_i} - D > 0 \tag{A1}$$

where

$$\sum_{i=1}^{M} F_i - F = 0 \tag{A2}$$

and

$$\sum_{i=1}^{M} ST_i - S = 0 \tag{A3}$$

we first minimise the first term on the left of (A1) subject to the constraints (A2) and (A3). Do this by forming the Lagrangian, L, of the problem

$$L = \sum_{i=1}^{M} \frac{F_i d_i}{ST_i} + \lambda_s \left(\sum_{i=1}^{M} ST_i - S \right) + \lambda_F \left(\sum_{i=1}^{M} F_i - F \right) \tag{A4}$$

and finding its stationary points.

$$\frac{DL}{DF_i} = \frac{d_i}{ST_i} + \lambda_F = 0 \tag{A5}$$

$$\frac{DL}{DST_i} = -\frac{F_i d_i}{ST_i^2} + \lambda_s = 0 \tag{A6}$$

Now from (A5)

$$ST_i = -\frac{d_i}{\lambda_F} \qquad (A7)$$

thus using (A3) we have

$$-\frac{1}{\lambda_F}\sum_{i=1}^{M} d_i = S$$

or

$$\lambda_F = -\frac{D}{S} \qquad (A8)$$

and

$$ST_i = \frac{S}{D} d_i \qquad (A9)$$

From (A6) we get

$$F_i = \frac{\lambda_s ST_i^2}{d_i}$$

$$= \lambda_s \left(\frac{S}{D}\right)^2 d_i$$

so A2 gives

$$\lambda_s \left(\frac{S}{D}\right)^2 D = F$$

or

$$\lambda_s = \frac{FD}{S^2}$$

and

$$F_i = \frac{FD}{S^2} \frac{S^2}{D^2} d_i$$

$$= \frac{F}{D} d_i \qquad (A10)$$

From (A9) and (A10) we get

$$\frac{F_i}{ST_i} = \frac{F/D}{S/D} = \frac{F}{S}$$

from which we see that the first term in (A2) takes a minimum value of FD/S which, as $F > S$ (offtake from any part of column cannot exceed total feed) ensures that the first term is always greater than the second so that the result is positive. That this stationary value is indeed a minimum can be seen by considering that term in the summation corresponding to the smallest ST_i. If this value of ST_i is allowed to tend to zero, while compensating to preserve the specified sum using one of the other ST_i, the result can be made arbitrarily large. The above argument only applies for positive values of F_i which of course, is the case in any distillation calculation.

REFERENCES

[1] AMUNDSEN, N. R. and PONTINEN, A. J., *Ind. Eng. Chem.*, **50**, *730 (1958)*.

[2] BOYNTON, G. W., *Hydrocarbon Process.*, **19**, *153 (1970)*.

[3] BROYDEN, C. B., *Math. Comput.*, **19**, *577 (1965)*.

[4] HIROSE, Y., *Kagaku Kogaku*, **32**, *998 (1968)*.

[5] HOLLAND, C. D., «Multicomponent Distillation», Prentice-Hall, Englewood Cliffs, New Jersey, 1963.

[6] SAITO, H., YAMADA, I. and SUGIE, H., *Kagaku Kogaku*, **34**, *478 (1970)*.

[7] SARGENT, R. W. H. and MURTAGH, B. E., *Trans. Inst. Chem. Engrs. (London)*, **47**, *T85 (1969)*.

[8] STROUD, S. E., «Ph. D. Thesis», University of Birmingham, 1976.

[9] TOMICH, J. F., *A. I. Ch. E. (Am. Inst. Chem. Engrs.) J.*, **16**, *229 (1970)*.

[10] VAN WINKLE, M., «Distillation», McGraw-Hill, New York, 1967.

RESUMO

Propõe-se um método de cálculo para a destilação multicomponente baseado no método de Lewis e Mathieson para os cálculos de prato a prato. O método de convergência usado baseia-se no método θ envolvendo porém apenas um único θ independentemente do número de correntes laterais existentes. O método é aplicável aos casos de alimentações múltiplas, misturas não ideais e sobrecaudal molai não constante, tendo-se obtido uma convergência satisfatória em problemas diversos.

D. A. LIHOU

Department of Chemical Engineering
University of Aston in Birmingham
England — B4 7ET

THE JETUBE REACTOR (1)

The Jetube is an oval shaped tubular reactor. Momentum exchange with the feed causes recirculation of the reactants, c times say, where c is typically 2 to 5. The Jetube is thus a PFR with recycle and the product is a mixture of material of ages which are multiples p of τ/c where τ is the mean residence time. By operating at the appropriate values of τ and c, the yield pattern from consecutive or parallel reactions can be adjusted. Also with c times the mass throughput recirculating, convective heat transfer from the walls is enhanced. A single Jetube reactor was tested extensively as a steam cracker with gasoil as feedstock. The tube was 117.5 mm internal diameter and the oval length was 3.96 m, with 0.044 m^3 reactor space. The performance of the Jetube is analysed theoretically and the predicted product spectra and temperature agree quite well with measured data.

1 — INTRODUCTION

In 1966 a joint development programme was agreed between Wellman Incandescent Co. Ltd. and Esso Research Ltd., to investigate the performance of a Jetube as an oil gasification reactor. There was interest amongst olefin manufacturers to move from light virgin naphtha which was becoming scarce and expensive, to heavier feedstocks for steam cracking. Thus it was decided to feed gasoil and steam to a single Jetube (fig. 1) in a cabin furnace. Previous experiments with the Jetube were conducted by EDMONDSON [1] in 1959, consisting of four tests with kerosine, all of which ended after a few hours due either to equipment failure or blockage by soot and tar. Nevertheless the gas yield and calorific value were sufficiently encouraging for a provisional British Patent to be filed. Between 1959 and 1966 a number of new gasification processes were perfected and in particular DENT [2] patented a jet recirculated reactor in which olefins are saturated in the vapour phase by hydrogen rich gas.

The pilot plant work in 1966 was carried out by KOWSZUN [3] and the data shown in Table 1 were quoted in the U.S. Patent [4] granted in 1970. Kowszun found that a 2.4 mm diameter feed pipe for oil plus superheated steam avoided the blockage suffered by a pressure atomising nozzle. The objective of his tests was to produce a suitable fuel gas from gasoil, economically; he recommended burning the liquid product and tar in the surrounding furnace.

In 1967 the pilot plant and furnace were shipped to America and tested from 1968 to 1970 by Esso

(1) Presented at CHEMPOR' 75 held in Lisbon, 7-12 September 1975 at the Calouste Gulbenkian Foundation Center.

Papers presented at this International Chemical Engineering Conference can be purchased directly from Revista Portuguesa de Química (Instituto Superior Técnico, Lisboa 1, Portugal) at the following prices per volume sent by surface mail, postage included (in Portuguese Escudos):

Whole set	500
Transport processes	200
Reaction engineering	150
Environmental engineering	150
Management studies	150

This paper was presented at the Reaction engineering section.

Research and Engineering Company at Baton Rouge. The objectives of these tests were to analyse the liquid fraction of the product and develop the Jetube for olefins manufacture. Quantitative data from the American experiments are not available but the following qualitative conclusions are relevant to this paper which presents a theoretical analysis of the Jetube:

«Two factors contribute to the Jetube yield pattern. One is temperature. Because of its low surface to volume ratio, the Jetube must be fired to a higher tube metal temperature to produce useful conversions. Cracking at these high temperatures favours destruction of reactive intermediates such as propylene and pyrolysis gasoline to give added yield of ethylene. Some additional ethylene also comes from increased cracking of the propane and ethane by-products.

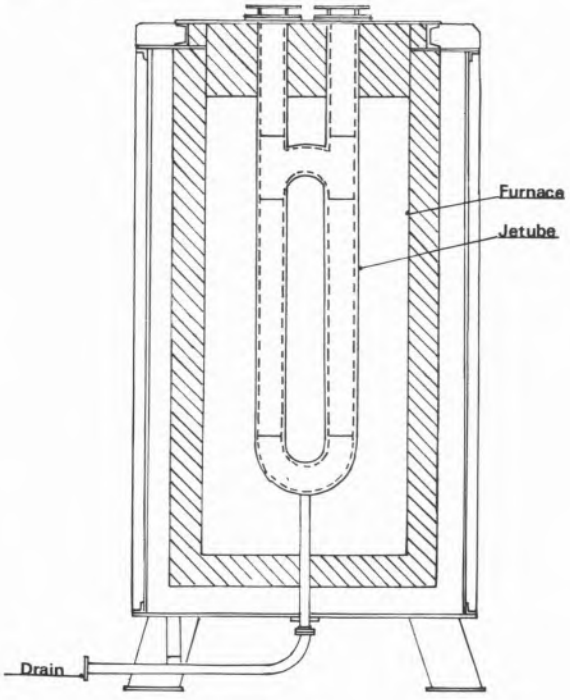

Fig. 1
Pilot plant Jetube and furnace

The second factor contributing to the Jetube yield pattern is the internal mixing provided by recycle or by the vortex induced by the atomising nozzle when the recycle loop is blocked. This mixing causes the reactor to behave more like a continuous stirred tank reactor (CSTR) than a plug flow reactor (PFR).

CSTR reactors favour the production of those products whose instantaneous selectivities increase with conversion. These include H_2, CH_4, coke, tar, and usually ethylene. On the other hand, plug flow reactors are best for producing products whose instantaneous selectivities decrease with conversion. These include propylene, butenes, butadiene and pyrolysis gasoline. These relationships can be demonstrated mathematically if one knows the rate constants for formation and destruction of each of the reactants, products, and intermediates. They are also consistent with our observations.

Our overall conclusions, therefore is that the Jetube is not the best type of reactor for producing the type of product yield that is most attractive in the present economical situation (1970).»

2 — RESIDENCE TIME DISTRIBUTION

The discussion by Esso Research and Engineering Co. regarding the relative merits of PFR and CSTR reactors for unimolecular consecutive reactions as shown in equation (1) is correct. The fractional yield of intermediate R is higher with a PFR than a CSTR for all ratios of the rate constants (k_1/k_2); see LEVENSPIEL [5] chapter 7, fig. 10.

$$A \xrightarrow{k_1} R \xrightarrow{k_1} S \qquad (1)$$

But the Jetube is a PFR with recycle; it is only when c is very large that it *approximates* to a CSTR.

2.1 — *MEAN RESIDENCE TIME*

This is usually the reactor volume (V) divided by volumetric flow rate. However, with cracking reactions the volumetric flow rate of products (v_2) is much more than the feed rate (v_1) due primarily to the increase in moles as the reaction proceeds but also to temperature changes along the reactor. The actual mean residence time is related by means of density, to the ratio V/v_2. Since the mean density (ρ) and product density (ρ_2) become

undistinguishable for $c > 2$, this report assumes that mean residence time is given by equation (2).

$$\tau = V/v_2 \qquad (2)$$

2.2 — *MINIMUM RESIDENCE TIME*

Because c is defined as a mass ratio, the volumetric flow rate in the reactor is cv_2, again assuming $\rho = \rho_2$. Thus the time τ/c defines a minimum residence time, being the time taken for the gases to flow from the injection point to the product outlet. The mean age of material in the product stream is τ but *the majority of the product has only the minimum age.*

2.3 — *AGE DISTRIBUTION IN PRODUCT*

The age distribution is a step function, defined by equation (3), where X_p is the proportion of material in the product with age $p\ \tau/c$; i.e. that which has flowed p times around the reactor.

$$X_p = \frac{1}{c}\left(1 - \frac{1}{c}\right)^{p-1} \qquad (3)$$

Equation (3) is plotted by LEVENSPIEL [5] page 291 in which is $(k + 1) = c$ and $a = (c - 1)/c$. For any recirculation ratio the proportion (X_c) of material residing for the mean residence time can be calculated by putting $p = c$ in equation (3); for example $X_c = 0.25$ for $c = 2$.

Esso investigated the yield pattern also with a blank in the 180° bend between the feed and product pipes. The Jetube then approximates to a CSTR followed by a PFR. BEÉR and LEE [6] have shown that this type of reactor is well suited to adiabatic combustion of pulverised anthracite. The same conclusion would be reached for any exothermic reaction carried out adiabatically. They show that the size of the reactor can be minimized (complete conversion $X = 1$ for shorter τ) if the transition from the CSTR zone to the PFR zone occurs at the conversion (X) at which the slope ($dX/d\tau$) for either total CSTR or total PFR are identical. A non-circulating Jetube is not a suitable combustor. It was developed as a radiant tube heater for heat treatment furnaces having controlled atmospheres. In this conventional application it relies on the entrainment of cool combustion products to moderate the flame temperature, without large amounts of excess air.

3 — MOMENTUM EXCHANGE

FRANCIS [7] has shown that equating pressure recovery from the feed to pressure loss in the Jetube gives an expression for velocity heads lost, which in the present case where the recycle contributes some momentum can be written:

$$1 + \frac{S}{2} = \frac{1}{c^2}\ \frac{M}{M_1}\ \frac{T_1}{T}\ \frac{A}{A_1} + \left(\frac{c-1}{c}\right)^2\ \frac{M}{M_2}\ \frac{T_2}{T} \qquad (4)$$

The major pressure loss occurs at the return bends which typically have an r/D ratio of 2.5. At each bend about 0.8 velocity heads are lost. The loss in the straight pipes is equivalent to about 0.1 velocity heads. One velocity head was allowed for one bend and one straight pipe plus incidental losses. Each velocity head is in terms of the velocity in the pipe immediately upstream. Therefore the value of S to be used in equation (4) is approximately

$$S = 1 + \left(\frac{c-1}{c}\right)^2\ \frac{M}{M_2}\ \frac{T_2}{T} \qquad (5)$$

Eliminating S between equation (4) and (5) leads to an expression whereby the area ratio of Jetube pipe to feed nozzle can be calculated, having selected a value of c. The subscripts 1 and 2 refer to feed and product values, while unsubscripted variables are mean values, at the bottom return bend for example.

$$\frac{A}{A_1} = \frac{3c^2}{2}\ \frac{M_1}{M}\ \frac{T}{T_1} - \frac{(c-1)^2}{2}\ \frac{M_1}{M_2}\ \frac{T_2}{T_1} \qquad (6)$$

Table 1

Results of gasoil cracking [3, 4]

Example No.	1	2	3	4	5	6	7	8	9	10
Furnace temperature (°C)	950	960	1,000	1,000	970	1,060	1,070	1,140	1,130	1,200
Steam temperature (°C)	820	795	800	800	715	825	790	810	805	830
Product temperature (°C)	635	638	650	670	640	700	655	750	835	845
Oil feed (lb/hr)	147	105	75.7	67	97	39	150	101	50	48
Steam feed (lb/hr)	100	100	95	95	102	101	150	98	58	57
C_4 — gas analysis:										
H_2 percent by vol	1.5	1.8	2.6	3.5	3.2	27.1	14.3	12.4	49.1	51.2
CO			0.1	0.1	0.2	6.4	0.6	1.7	3.4	11.6
CO_2			0.1	0.1	0.2	5.1		1.3	6.2	4.7
CH_4	22.9	23.2	25.6	27.2	22.4	28.5	20.2	31.8	26.4	20.6
C_2H_4	39.9	40.5	43.3	47.7	41.9	29.5	36.6	39.7	11.4	8.0
C_2H_6	5.1	4.2	3.2	2.3	6.0	0.5	3.3	2.0	3.5	3.9
C_3H_6	18.6	19.6	14.8	7.3	16.6	2.4	14.6	6.9		
C_3H_8					0.8			0.9		
C_4H_8	12.0	10.7	10.3	11.8	8.2	0.5	10.4	3.3		
C_4H_{10}					0.5					

4 — STEAM CRACKING

4.1 — *MECHANISM*

Steam in the feed may take part in the reactions to a limited extent. Fine soot particles and reactions catalysed by the wall can lead to CO and CO_2 in the product. It is assumed that the high severity cracking conditions which produced significant amounts of CO and CO_2 in examples 6, 9 and 10 in Table 1 (low feed rate and/or high temperature) would not be necessary to maximise ethylene yield from a Jetube. FREY and HEPP [8] found that cracking of pentane and larger normal paraffins takes place via the free radical intermediates predicted by RICE *et al.* [9]. The yield from distillate feedstocks cannot be predicted exactly by Rice's consecutive free-radical mechanism owing to polymerisation. In a series of 20 articles, ZDONIK, GREEN and HALLEE [10] dealt with all aspects of olefins manufacture. They correlated empirically the yield spectra from commercial PFR crackers in terms of «kinetic severity function» (KSF) where

$$\mathrm{KSF} = \int_0^\tau k_5 \, dt \qquad (7)$$

and k_5 is the rate constant for the first order cracking of n-pentane. For the purpose of analysing the Jetube cracker, Rice's mechanism was accepted. It can be represented by the following series of first order reactions starting with n-pentadecane P_{15} and yielding a mixture of normal paraffins, P_n and normal olefins U_n with n carbon molecules. Note that when a molecule cracks, each of the bonds has an equal chance of splitting and a paraffin produces one paraffin and one olefin whilst an olefin produces two smaller olefins.

$$P_N \rightarrow \frac{1}{N-1}\left(\sum_{n=2}^{N-2} P_n + \sum_{n=2}^{N-2} U_n + 2P_1 + 2U_{N-1}\right); \qquad 16 > N > 3 \qquad (8)$$

$$U_N \rightarrow \frac{2}{N-3}\left(\sum_{n=2}^{N-2} U_n\right); \qquad 15 > N > 3 \qquad (9)$$

Note from equation (8) that tetradecane P_{14} cannot be produced from pentadecane P_{15}.

Cracking of propane yields hydrogen P_0, propylene, methane and ethylene in equal quantities, so that equation (8) becomes

$$P_3 \rightarrow \frac{1}{2}(P_0 + P_1 + U_2 + U_3) \tag{10}$$

Cracking of pure ethane yields primarily ethylene but in the presence of propylene the ethylene formation rate is greatly reduced and is about equal to that of methane when there is 0.24 moles propylene per mole ethane [11]. Thus equation (11) is assumed to represent the cracking of ethane in propylene.

$$P_2 \rightarrow \frac{1}{2}(P_1 + 2P_0 + U_2 + C) \tag{11}$$

Methane cracking occurs to a limited extent but was neglected because the rate constant [12] is about 10^{-5} times that of ethane at 900 °K.
Pyrolysis of propylene produces heavy aromatics as well as methane, ethylene and hydrogen. At 873 °K the maximum yield of condensable product occurs after 10 minutes [13], whereas at 1090 °K the yield of aromatics remained constant at about 0.16 moles per mole propylene fed, for residence times of 0.4 to 10 s and then declined; also at this temperature 80 % of the propylene had reacted after 1 s [14]. Thus it is assumed that the product spectrum after 1 s at 1090 °K is typical for propylene.

$$U_3 \rightarrow 0.4U_2 + 0.6P_1 + 0.2P_0 + 0.16C_{10}H_{10} \tag{12}$$

At temperatures below 1073 °K ethylene polymerises by a second order mechanism [15] but at higher temperature these products crack almost immediately to coke, hydrogen and methane. Butadiene is an intermediate in the polymerisation [14, 16] and even at 1090 °K the yeld of butadiene [14] after 0.6 s is 5 moles per 100 moles ethylene used, which falls to zero in 6 s. At 896 °K the disappearance of ethylene is exactly second order and 30 % of the carbon is in the gas phase [15]. This is consistent with the following stoichiometric equation in which D_4 represents butadiene and MCH is methyl cyclohexane.

$$2U_2 \rightarrow 0.3D_4 + 0.3P_0 + 0.4MCH \tag{13}$$

Ethylene is very refractory due to the central double bond [17]. Nevertheless, at about 970 °K decomposition by first order reaction is detectable after 60 s and around 980 °K decomposition and polymerisation occur at the same rate [15].
Below about 1170 °K no acetylene is detected in the products from ethylene pyrolysis [18] and the gaseous products are primarily methane and hydrogen in the molar ratio 2 : 1. This ratio tends to unity after 10 % of the ethylene is used [15]. At temperatures above 1180 °K a significant amount of acetylene is formed and the reaction is via acetylene to hydrogen and coke or polymer with a high C : H ratio [16]. For ethylene cracking

$$U_2 \rightarrow \frac{1}{2}(P_1 + P_0 + C_3H_2) \tag{14}$$

The polymer product, methyl cyclohexane from equation (13) will crack to an alpha olefin which then cracks by equation (9).

$$MCH \rightarrow U_7 \tag{15}$$

Although its central bond should be relatively refractory, being in the α position to two double bonds [17], 1,3-butadiene could hydrogenate to butenes which then crack by equation (9) to ethylene. This is a cyclic reaction mechanism with butadiene as an intermediate. It was assumed that butadiene disappears by cracking to methane and tar with a rate equal to that of ethylene cracking.

$$D_4 \rightarrow P_1 + C_3H_2 \tag{16}$$

The «aromatics» $C_{10}H_{10}$ formed from propylene were assumed to be stable enough to emerge with the tars.

Table 2

Constants for equation 17

n — Paraffins			α — Olefins			ethylene	polymerisation
n	B	C (K)	n	B	C (K)	B	C (K)
2	14.6737	15807	2	13.2553	16619	12.7225	12430
3	12.6160	13069	3	13.8334	14694		
4	12.2545	12311					
5	12.2479	12117					

Data for ethylene from TOWELL and MARTIN [11]; remainder from ZDONIK, GREEN and HALLEE [10] part 5.

4.2 — *KINETICS*

The rate constants were conveniently expressed as logarithms to base 10 as follows

$$\log k = B - C/T \tag{17}$$

where the units of k is s^{-1} for all reactions except ethylene polymerisation, equation (13), for which the dimensions of k are time^{-1} (molar concentration)$^{-1}$ and the units used were m^3 k mole$^{-1}s^{-1}$. The constant B is dimensionless and C has the units of absolute temperature K.

The following empirical correlations of reaction rate constants were taken from ZDONIK, GREEN and HALLEE [10] part 6.

For normal paraffins with n carbon atoms the rate constant k_n is related to that of n-pentane k_5 by equation (18).

$$\log (k_n/k_5) = 1.5 \log n - 1.0485; \quad n \geq 5 \tag{18}$$

The rate constants for alpha olefins with n carbon atoms k_n' were assumed equal to that of the normal paraffin with two more carbon atoms; that is

$$k_n' = k_{n+2}; \quad n > 3 \tag{19}$$

For methyl cyclohexane it was assumed that its rate constant is the same as for n-pentane; $k_m = k_5$. The rate constant for butadiene was assumed to be the same for ethylene cracking; $k_4'' = k_2'$.

4.3 — *RATE EQUATIONS*

For the typical reaction shown by equation (1), which is assumed to be first order with respect to A, the rate of disappearance of A is related to its molar concentration C_A

$$-r_A = \frac{-1}{V}\frac{dN_A}{dt} = k_1 C_A \tag{20}$$

If there are N_T moles in the system at pressure P and absolute temperature T the concentration $C_A = N_A P/N_T RT$. Similarly the volume of the system $V = N_T\ RT/P$. Write the mole fraction of A as $(A) = N_A/N_T$ whereupon RT/P can be cancelled from equation (20). The dimension of k_1 remains time^{-1}.

$$\frac{1}{N_T}\frac{dN_A}{dt} = -k_1(A)$$

For a second order reaction such as the polymerisation of ethylene, equation (13), the rate of ethylene disappearance per unit volume is related to the square of molar concentration. Writing k_2'' as the rate constant with the units m^3 k mol$^{-1}s^{-1}$.

$$-r_{U_2} = \frac{-P}{N_T RT}\frac{d}{dt} N_{U_2} = k_2'' \left(\frac{N_{U_2} P}{N_T RT}\right)^2 \tag{21}$$

Again writing (U_2) as the mole fraction of ethylene transforms equation (21) to

$$\frac{1}{N_T}\ \frac{d}{dt}\ N_{U_2} = -\ \frac{k_2''}{v_m}\ (U_2)^2 \qquad (22)$$

In equation (22), v_m is the volume of 1 kmol of the gas mixture in the reactor.

$$v_m = RT/P = 22.41 \times \frac{T}{273.15} \times$$

$$\times\ \frac{1.013 \times 10^5}{P}\ m^3\ kmol^{-1} = 8311\ T/P\ m^3\ kmol^{-1}$$

Here T is the absolute temperature in the reactor which is at a pressure of P Nm^{-2}. Let (P_N) represent the mole fraction of paraffin C_NH_{2N+2} in the mixture containing N_T moles *per mole penadecane fed.* Let P_N be the fractional yield of P_N from each mole of P_{15} fed. A material balance on P_N over a small time interval can be written.

Rate of increase in moles of P_N = Rate of formation from larger paraffins $(N+2$ to $15)$ − Rate of reaction of P_N. Thus from equation (8):

$$\frac{1}{N_T}\ \frac{d}{dt}\ P_N = \sum_{n=N+2}^{15}\ \frac{k_n}{n-1}\ (P_n) - k_N(P_N)\ ;$$

$$14 > N > 1 \qquad (23)$$

For P_{15} equation (23) is simply

$$\frac{1}{N_T}\ \frac{d}{dt}\ P_{15} = -\ k_{15}(P_{15}) \qquad (24)$$

In these equations k_n is the first order rate constant for cracking the normal paraffin P_n. Similarly if k_n' and $k_4''(=k_2')$ are the rate constants for the olefin U_n and butadiene, respectively, a material balance for methane comes from equations (8, 10, 11, 12, 14 and 16) as follows:

$$\frac{1}{N_T}\ \frac{d}{dt}\ P_1 = 2 \sum_{N=4}^{15}\ \frac{k_n}{n-1}\ (P_n) + \frac{k_3}{2}\ (P_3) +$$

$$+\ \frac{k_2}{2}\ (P_2) + 0.6\ k_3'\ (U_3) + \frac{k_2'}{2}\ (U_2) + k_2'(D_4) \qquad (25)$$

Similarly for hydrogen, equations (10, 11, 12, 13 and 14) give equation (26) in which k_2'' is the rate constant for polymerisation of ethylene.

$$\frac{1}{N_T}\ \frac{d}{dt}\ P_0 = \frac{k_3}{2}\ (P_3) + k_2(P_2) +$$

$$+\ 0.2\ k_3'(U_3) + \frac{0.15}{v_m}\ k_2''(U_2)^2 + \frac{k_2'}{2}\ (U_2) \qquad (26)$$

The general material balance for olefins larger than propylene is obtained from equations (8 and 9) as follows:

$$\frac{1}{N_T}\ \frac{d}{dt}\ U_N = -\ k_N'(U_N) +$$

$$+ \sum_{n=N+2}^{15}\ \frac{k_n}{n-1}\ (P_n) + \frac{2}{N}\ k_{N+1}(P_{N+1}) +$$

$$+\ 2 \sum_{n=N+2}^{14}\ \frac{k_n'}{n-3}\ (U_n)\ ;\ 15 > N > 7 > N > 3 \qquad (27)$$

For heptene U_7 there is another term on the right, k_5 (MCH) due to equation (15). For propylene equations (8, 9 and 10) give:

$$\frac{1}{N_T}\ \frac{d}{dt}\ U_3 = -\ k_3'(U_3) +$$

$$+ \sum_{n=5}^{15}\ \frac{k_n}{n-1}\ (P_n) + \frac{2}{3}\ k_4(P_4) + \frac{k_3}{2}\ (P_3) +$$

$$+ \sum_{n=5}^{14}\ \frac{k_n'}{n-3}\ (U_n) \qquad (28)$$

For ethylene, equations (8, 9, 10, 11, 12, 13 and 14) apply thus:

$$\frac{1}{N_T}\ \frac{d}{dt}\ U_2 = -\ k_2'(U_2) - \frac{k_2''}{v_m}\ (U_2)^2 +$$

$$+ \sum_{n=4}^{15}\ \frac{k_n}{n-1}\ (P_n) + \frac{k_3}{2}\ (P_3) + \frac{k_2}{2}\ (P_2) +$$

$$+\ 2 \sum_{n=4}^{14}\ \frac{k_n'}{n-3}\ (U_n) + 0.4\ k_3'(U_3) \qquad (29)$$

Equations (13) and (16) give the following butadiene material balance

$$\frac{1}{N_T}\ \frac{d}{dt}\ D_4 = -\ k_2'(D_4) + \frac{0.15\ k_2''}{v_m}\ (U_2)^2 \qquad (30)$$

The material balance for methyl cyclohexane is from equations (13) and (15).

$$\frac{1}{N_T}\ \frac{d}{dt}\ MCH = \frac{0.2\ k_2''}{v_m}\ (U_2)^2 - k_5(MCH) \qquad (31)$$

If s moles of steam are introduced with each mole of pentadecane fed and the steam is inert, the total moles at any time is

$$N_T = s + \sum_{n=0}^{15} P_n + \sum_{n=2}^{14} U_n + D_4 + MCH \qquad (32)$$

The fractional yield of tar was found by overall carbon and hydrogen balances.

Residual carbon

$$R_c = 15 - \sum_{n=1}^{15} nP_n - \sum_{n=2}^{14} n\ U_n - 4D_4 + 7MCH \qquad (33)$$

Residual hydrogen

$$R_h = 32 - \sum_{n=0}^{15} (2n + 2)P_n - \sum_{n=2}^{14} 2n\ U_n - \\ - 6D_4 - 14MCH \qquad (34)$$

5 — HEAT TRANSFER

The convective heat transfer coefficient was calculated using the Dittus Boelter equation in which the Prandtl number was assumed to be 0.9 for the gas mixture. Thus, the rate of convection from the wall along length L of the reactor tube is

$$Q_c = 0.07\ LK(T_w - U)Re^{0.8} \qquad \text{watts} \qquad (35)$$

There will be some radiation absorbed by the gaseous reactants which were assumed to be grey with absorptivity and emissivity equal to 0.13; this corresponds to steam at 1000 °K (1800 °F) with partial pressure of 101.3 kNm^{-2} (1 atm) and a beam length of 0.107 m (0.35 ft). The emissivity of the steel wall was assumed to be 0.8 and the view factor is unity. The overall interchange factor F is then given by

$$\frac{1}{F} = \left(\frac{1}{0.8} - 1\right) + \left(\frac{1}{0.13} - 1\right) + 1 = 7.95$$

whence F = 0.126 and the radiative heat transfer over length L of the reactor tube of internal diamater D is given by

$$Q_r = 22450\ LD\ \{(T_w/1000)^4 - (T/1000)^4\} \qquad \text{watts} \qquad (36)$$

5.1 — *HEAT OF REACTION*

From tables of thermodynamic data published by the American Petroleum Institute the following generalised equations were determined for the heat of formation (kJ $gmol^{-1}$) of paraffins, olefins and 1,3 butadiene with N carbon atoms at T_2K. Thus for P_N,

$$\Delta H_N = -\ 42.33 - 22.89\ N - 0.01273\ T_2 - \\ - 0.002315\ NT_2\ ;\ N \neq O \qquad (37)$$

$$\Delta H_N' = 84.41 - 22.89\ N - 0.01047\ T_2 - \\ - 0.002315\ N\ T_2 \qquad (38)$$

$$\Delta H_N'' = 121.30 - 0.0452\ T_2 + 1.92 \times 10^{-5}\ T_2^2 \qquad (39)$$

Equations (37 to 39) include the sensible heat in the hydrocarbon so that the overall heat of reaction was found by subtracting the heat in steam and gasoil at the feed temperature T_1 from the total heat of steam and products at T_2. This difference multiplied by the molar flow of gasoil gave the

required heat transfer rate ($Q_c + Q_r$) which from equations (35) and (36) enabled the wall temperature to be calculated. The mean temperature T was usually assumed to be equal to the product temperature T_2.

6 — RESULTS

The mathematical model of the Jetube was used to predict its performance as a steam cracker for a wide range of operating conditions, represented by

Table 3

Fractional yield from a Jetube fed with pentadecane
($T = 973$ °K, $\tau = 0.55$ s, $c = 5$)

DRY GASEOUS PRODUCT

Component	Molar yield	Mass yield	Mole %	Kowszun [3] %
C_4H_{10}	0.0060	0.0016	0.25	0.0
C_3H_8	0.0206	0.0043	0.87	0.4
C_2H_6	0.0478	0.0068	2.02	2.2
CH_4	0.8845	0.0668	37.18	30.1
H_2	0.3794	0.0036	16.00	24.8
C_4H_8	0.0547	0.0144	2.31	1.9
C_3H_6	0.0997	0.0198	4.21	4.7
C_2H_4	0.8800	0.1162	37.20	34.9
C_4H_6	0.0015	0.0004	0.06	0.0
Total	2.3742	0.2339	100	99

DISTILLATE			OILY TAR		
Component	Molar yield	Mass yield	Component	Molar yield	Mass yield
$C_{10}H_{22}$	0.0256	0.0171	$C_{15}H_{32}$	0.3371	0.3371
C_9H_{20}	0.0263	0.0159	$C_{13}H_{28}$	0.0220	0.0191
C_8H_{18}	0.0275	0.0148	$C_{12}H_{26}$	0.0220	0.0176
C_7H_{16}	0.0294	0.0139	$C_{11}H_{24}$	0.0236	0.0174
C_6H_{14}	0.0316	0.0128	$C_{14}H_{28}$	0.0256	0.0237
C_5H_{12}	0.0610	0.0207	$C_{13}H_{26}$	0.0149	0.0128
$C_{10}H_{20}$	0.0248	0.0164	$C_{12}H_{24}$	0.0174	0.0138
C_9H_{18}	0.0299	0.0178	$C_{11}H_{22}$	0.0207	0.0150
C_8H_{16}	0.0371	0.0196	R_c	1.4681	0.0831
C_7H_{14}	0.0477	0.0221	R_h	1.0504	0.0050
C_6H_{12}	0.0605	0.0240			
C_5H_{10}	0.0807	0.0266	Total	2.9869	0.5445
Total	0.4821	0.2217	Mass balance: 0.2339 + 0.2217 + 0.5445 = 1.0001		

Kowszun [3]:

Molar yield of gaseous product = 6.59; Mass yield of oily tar = 0.46; Fraction of feed uncracked = 0

Table 1. From these experimental data KOWSZUN [3] compiled a set of design data for the Jetube and these are compared below with data from the mathematical model. KOWSZUN [3] recommended a product temperature of 710 °C, oil flow rate of 79 lb h^{-1}, steam at 102 lb h^{-1} and a furnace temperature of 1200 °C. From his product spectrum and the feed rate, the mean residence time would be 0.58 s and the recirculation ratio would be 6.5. Table 3 shows the predicted fractional yield of products under similar conditions ($T = 973$ °K, $\tau = 0.55$ s, $c = 5$). For these conditions and for those of KOWSZUN [3] the function $k_5\tau/c$ are identical. Kowszun's data are given for comparison in Tables 3 and 4.

The predicted gaseous composition differs from Kowszun's data by having less hydrogen but more methane and ethylene; also Kowszun found 0.9 % $CO + CO_2$ and 0.1 % C_3H_4. For his design conditions KOWSZUN [3] assumed complete conversion of the gasoil feed and predicted a gaseous product yield equivalent to 6.59 mole per mole of feed.

Table 4 is a comparison of predicted thermal data with Kowszun's feed and temperature data. His recommended furnace temperature of 1473 °K is about 250 °K higher than was calculated and indeed it is equal to the highest furnace temperature reported in Table 1.

In Table 3 the fractional yield of «aromatics» from equation (12) and residue C_3H_2 from equations (14) and (16) are included in the residual carbon and hydrogen, R_c and R_h. Similarly, methyl cyclohexane is included in heptene C_7H_{14}.

Table 4

Heat load and predicted temperatures for typical conditions

	Predicted	KOWSZUN [3]
Oil feed rate (lb h^{-1})	92	79
Oil feed rate (kg h^{-1})	41.8	35.9
Oil feed rate (gmol s^{-1})	0.055	0.047
Steam feed rate (lb h^{-1})	117	102
Steam feed rate (kg h^{-1})	53.2	46
Feed temp. of oil and steam (°K)	900	900
Product temperature T_2 (°K)	973	983
Heat in C_{15} fed (kJ $gmol^{-1}$)	− 428.4	− 428.4
Heat in C_{15} fed (kW)	− 23.56	− 20.13
Heat in paraffins at T_2 (kW)	− 16.25	− 14.65
Heat in olefins at T_2 (kW)	− 1.47	1.20
Heat in butadiene (kW)	0.0078	0
Heat in products (kW)	− 17.72	− 13.45
Heat of reaction (kW)	5.845	6.685
Steam superheat 73 °K (kW)	2.393	2.070
Total heat load (kW)	8.238	8.755
Viscosity of reactants μ (mg m^{-1} s^{-1})	33	33
Recirculation ratio c	5	6.5
Mass recirculating M (g s^{-1})	132	148
Pipe diamater D (mm)	117.5	117.5
Reynolds no. $4M/\pi D\mu$	43327	48579
Thermal conductivity (Wm^{-1} °K^{-1})	0.0865	0.0865
Oval length (m)	3.96	3.96
$Q_c/(T_w - T)$ (kW °K^{-1})	0.122	0.135
Temperatures: (°K)		(Predicted)
Inside wall T_2	1023	1032
Outside wall	1026	1035
Furnace refractory	1098	1110
Furnace gas	1200	1214
Furnace gas reported		1473

7 — CONCLUSIONS

The mathematical model of the Jetube predicts its performance adequately. For steam cracking the Jetube yields ethylene, methane and hydrogen in high concentration in the C_4 gaseous product, however 1/c of the feed passes only once around the reactor and this leaves a significant amount of the feed stock uncracked (33.71 % in Table 3). For other multiple reaction systems where the order is not the same for all reactions, the residence time distribution of a PFR with recycle could be used to maximise the yield of a desired product.

SYMBOLS USED

A — Cross sectional area of Jetube
A — Feedstock in equation 1
(A) — Mole fraction of A
A_1 — Cross sectional area of feed nozzle

B — Constant in equation 17
c — Recirculation ratio = mass flow in reactor/mass feedrate
C_A — Molar concentration of reactant A
D — Inner diameter of reactor
D_4 — Fractional yield of butadiene from 1 mole pendadecane
(D_4) — Mole fraction butadiene in reactants
F — Overall radiation interchange factor
ΔH_N — Heat of formation of paraffin C_nH_{2n+2}
$\Delta H_N'$ — Heat of formation of olefin C_nH_{2n}
$\Delta H_4''$ — Heat of formation of butadiene
k_n — Rate constant for cracking paraffin C_nH_{2n+2}
k_n' — Rate constant for cracking olefin C_nH_{2n}
k_2'' — Rate constant for ethylene polymerisation
k_4'' — Rate constant for butadiene cracking
K — Thermal conductivity of reactants
KSF — Kinetic severity function; equation 7
L — Length of Jetube oval
MCH — Fractional yield of methyl cyclohexane
M — Mean molecular weight of reactants in Jetube
M_1 — Mean molecular weight of feedstock and steam
M_2 — Mean molecular weight of products
n — Carbon number of reacting hydrocarbon
N — Carbon number of specific product
N_A — Moles of reactant A in the reactants
N_T — Total moles per mole pentadecane fed
p — Positive integer in equation 3
P — Jetube pressure
P_n — Fractional yield of paraffin C_nH_{2n+2} from 1 mole of pentadecane
(P_n) — Mole fraction of paraffin C_nH_{2n+2} in reactants
Q_c — Convective heat transfer rate
Q_r — Radiative heat transfer rate
r_A — Rate of formation of A
R — Universal gas constant
Re — Reynolds' number
R_c — Fractional yield of residual carbon from 1 mole of pentadecane
R_h — Fractional yield of residual hydrogen from 1 mole of pentadecane
s — Molar ratio of steam to pentadecane
S — Number of velocity heads lost
t — Time
T — Absolute temperature in reactor
T_1 — Absolute temperature of feed mixture
T_2 — Absolute temperature of products
T_w — Absolute temperature of inside reactor wall
U_n — Fractional yield of olefin C_nH_{2n} from 1 mole of pentadecane
(U_n) — Mole fraction of olefin C_nH_{2n} in reactants
v — Average volumetric flow rate in reactor
v_1 — Volumetric flow rate of feed mixture
v_2 — Volumetric flow rate of products
v_m — Volume of 1 kmol of gas in the reactor = 8311 T/P m^3
V — Volume of Jetube
X — Fraction of feed reacted
X_p — Fraction of product which has been p times around the Jetube

GREEK LETTERS

μ — Dynamic viscosity
ρ — Density
τ — Mean residence time = V/v_2

REFERENCES

[1] EDMONDSON, P. D., «Twin Jetube Oil Gasifier», Memo to Incandescent Heat Co. Ltd., Birmingham (England), 7th July, 1959.
[2] DENT, F. J., *Gas World*, **161**, *275 (1965)*.
[3] KOWSZUN, J., Report No. ER-26 MR-67, Esso Research Ltd., Abingdon (Berkshire, England), 1967.
[4] PETTITT, C. G., U. S. Pat. 3,527, 586, 1970.
[5] LEVENSPIEL, O., «Chemical Reaction Engineering», Wiley International Edition, New York, 1966.
[6] BÉER, J. M. and LEE, K. B., Tenth Int. Symp. Comb., The Combustion Institute, U. S. A., 1965.
[7] FRANCIS, W. E., *Trans. Inst. Gas Engrs.*, **101**, *483 (1956)*.
[8] FREY, F. E. and HEPP, H. J., *Ind. Eng. Chem.*, **25**, *441 (1933)*.
[9] RICE, F. O. *et al.*, *J. Chem. Soc.*, **53**, *1959 (1931)*.
— RICE, F. O. *et al.*, *J. Am. Chem. Soc.*, **54**, *3529 (1932)*.
— RICE, F. O. *et al.*, *J. Am. Chem. Soc.*, **55**, *3035 and 4245 (1933)*.
— RICE, F. O. *et al.*, *J. Am. Chem. Soc.*, **56**, *284 (1934)*.
— RICE, F. O. *et al.*, *J. Am. Chem. Soc.*, **65**, *590 (1943)*.
[10] ZDONIK, S. B., GREEN, E. J. and HALLEE, L. P., *Oil Gas J.*, **64**, 28 Nov., 5 Dex., 19 Dec. *(1966)*.
— ZDONIK, S. B., GREEN, E. J. and HALLEE, L. P., *Oil Gas J.*, **65**, 2 Jan., 26 June, 10 July, 24 July, 7 Aug., 21 Aug., 11 Sept., 16 Oct. *(1967)*.
— ZDONIK, S. B., GREEN, E. J. and HALLEE, L. P., *Oil Gas J.*, **66**, 19 Feb., 11 Mar., 8 Apr., 27 May *(1968)*.
— ZDONIK, S. B., GREEN, E. J. and HALLEE, L. P., *Oil Gas J.*, **67**, 12 May, 26 May, 24 Nov. *(1969)*.

— ZDONIK, S. B., GREEN, E. J. and HALLEE, L. P., *Oil Gas J.*, **68**, 27 Apr., 11 May *(1970)*.
Available as a booklet from Stone and Webster Eng. Ltd., London (England).

[11] TOWELL, G. D. and MARTIN, J. J., *A. I. Ch. E. (Am. Inst. Chem. Engrs.) J.*, **7**, *693 (1961)*.

[12] PALMER, H. B. and HIRT, T. J., *J. Phys. Chem.*, **67**, *709 (1963)*.

[13] INGOLD, K. U. and STUBBS, F. J., *J. Chem. Soc.*, *1749 (1951)*.

[14] KINNEY, R. E. and CROWLEY, D. J., *Ind. Eng. Chem.*, **46**, *258 (1954)*.

[15] MOLERA, M. J. and STUBBS, F. J., *J. Chem. Soc.*, *381 (1952)*.

[16] TOWELL, G. D. and MARTIN, J. J., *A. I. Ch. E. (Am. Inst. Chem. Engrs.) J.*, **7**, *693 (1961)*.

[17] HURD, C. D., *Ind. Eng. Chem.*, **26**, *50 (1934)*.

[18] PAUSHKIN, Ya. M. and VISHNYAKOVA, T. P., «The Production of Olefin — Containing and Fuel Gases», Pergamon Press, London, 1964.

RESUMO

O Jetube é um reactor tubular de forma oval. Trocas de quantidade de movimento com a alimentação provocam a recirculação da massa reagente por c *vezes, digamos, em que* c *tem usualmente um valor entre 2 e 4. O Jetube é pois um reactor tipo êmbolo (PFR) com reciclagem, sendo o produto uma mistura de material de idades múltiplas p da razão* τ/c *em que* τ *é o tempo de residência médio. Operando a valores de* τ *e* c *adequados, o esquema de rendimento de reacções consecutivas ou paralelas pode ser ajustado. Por outro lado a recirculação por* c *vezes da massa processada melhora a transferência convectiva do calor das paredes Estudou-se extensivamente um reactor Jetube em reacções de «steam cracking», com gasóleo como alimentação. O tubo usado tinha 117,5 mm de diâmetro interno e 3,96 m de extensão sendo a capacidade do reactor de 0,044* m^3. *Avalia-se teoricamente o rendimento do Jetube nestas condições, estando o espectro de produtos previstos de acordo com os trabalhos experimentais.*

C. M. P. V. NUNES

P. J. GARNER

M. TOWHIDI

Department of Chemical Engineering
University of Birmingham — U. K.

PROCESS STUDIES CONCERNING THE AMMONOLYSIS OF 1,2-DICHLOROETHANE (1)

Almost all the production of 1,2-diaminoethane, in industry, is carried out through the ammonolysis of 1,2-dichloroethane but there are always other ethylene amines with higher molecular weight being formed. This is certainly due to further reactions, namely 1,2-diaminoethane formed reacting with 1,2-dichloroethane. Previous workers have shown that the temperature, the 1,2-diaminoethane : 1,2-dichloroethane molar ratio, the reaction time and, especially the presence of distilled water and strong acids can influence the composition of the products of this reaction. The reaction mechanism is complex; on theoretical grounds, it should involve nucleophilic substitutions. The results reported earlier and also the ones obtained during this work confirm the forecasts put forward through the concept of competing nucleophilic substitutions, which may lead to the prediction of other ways of obtaining a desired composition of the reaction product. This work also discusses the analysis of complex mixtures of ethylene amines, such as the reaction products of the reaction between 1,2-diaminoethane and 1,2-dichloroethane, by gas-liquid chromatography.

1 — INTRODUCTION

Almost all the production of 1,2-diaminoethane, in industry, is carried out through the ammonolysis of 1,2-dichloroethane. Ammonia is generally fed to the reactor either as a very concentrated aqueous solution (50-65 wt %) or as anhydrous NH_3, so that the reaction with EDC is carried out in a single phase, which avoids problems of mass transfer.

Although 1,2-diaminoethane is the main product obtained, there are always other ethylene amines (ethylene amines refer to a series of polyamines in which the molecule is made up of primary, secondary or tertiary amino groups connected through ethylene groups, thus forming linear, cyclic or branched structures) of higher molecular weight being formed. This is certainly due to further reactions, such as 1,2-diaminoethane formed previously reacting again with 1,2-dichloroethane.

Since the commercial demand for some of the ethylene amines may be greater than for others, a number of studies of the variables that can influence the composition of the reaction products, have been carried out.

In the present work, Triamines, Tetramines, Pentamines and Hexamines will refer to ethylene amines having three, four, five and six amino groups and including linear, cyclic and branched chained chemical structures.

---

(1) Presented at CHEMPOR' 75 held in Lisbon, 7-12 September 1975 at the Calouste Gulbenkian Foundation Center.

Papers presented at this International Chemical Engineering Conference can be purchased directly from Revista Portuguesa de Química (Instituto Superior Técnico, Lisboa 1, Portugal) at the following prices per volume sent by surface mail, postage included (in Portuguese Escudos):

Whole set	500
Transport processes	200
Reaction engineering	150
Environmental engineering	150
Management studies	150

This paper was presented at the Reaction engineering section

2 — GENERAL NOMENCLATURE

The following nomenclature is used throughout the text:

EDA $H_2NC_2H_4NH_2$
(1,2-diaminoethane)

EDC $Cl\,C_2H_4Cl$
(1,2-dichloroethane)

DETA $H_2N(C_2H_4NH)_2\,.\,H$

PIP

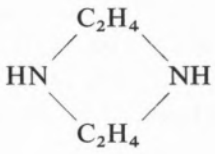

AEI

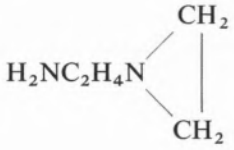

TETA $H_2N(C_2H_4NH)_3\,.\,H$

AAPIP

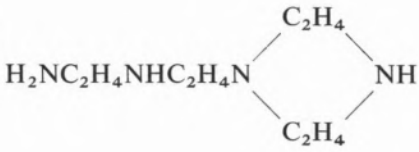

3 — METHODS OF INFLUENCING THE COMPOSITION OF THE PRODUCTS OF THE AMMONOLYSIS OF 1,2-DICHLOROETHANE (EDC)

During the last 15 years a great number of studies concerning the reaction of ammonolysis of EDC have been published. In this section is made a brief review of the ones especially concerned with methods to control the composition of the reaction products.

LESZEZYSKI *et al.* [1] studied the reaction of EDC with 50 % aqueous ammonia at an NH_3 : EDC molar ratio of 20 : 1. They found an optimum temperature in the range 0-100 °C with a reaction period of one hour and slow (60 r.p.m.) rate of mixing. Extensions of the reaction time to two hours and doubling the rate of mixing had little effect when carried out at the same temperature. The results indicate a 50-58 % conversion to EDA and the rest to higher ethylene amines.

Addition of excess ammonium chloride (equivalent to the saturation of the ammonia solution and greater) to the reactants, was found to increase the EDA formation to 60-62 % at 80 °C and 75-80 % at 120 °C.

S. ROPUSZYNKI *et al.* [2] studied the composition of the product of the ammonolysis of EDC with NH_3 : EDC mole ratio varying from 10 : 1 to 2 : 1, reaction time from 0.5 to 2.0 hours and temperature from 80 °C to 160 °C. Maximum Triamine yields were reached at a mole ratio of 6 : 1 and maximum Tetramine yields at 4 : 1. Conversion of EDC was shown to increase rapidly with temperature and increase in mole ratio.

Table 1

NH_3: EDC molar ratio (1)	EDA	Tri-amines	Tetra-amines	Penta-amines	Hexa-amines
10:1	48.0	25.5	12.3	6.8	2.7
6:1	40.0	22.4	14.9	10.6	5.9
2:1	15.0	22.6	15.9	20.9	14.7

(1) Temperature = 120 °C.

TOWHIDI [3] carried out a comprehensive process study on the ammonolysis of EDC to determine the effects of ammonia concentration, temperature, NH_3 : EDC mole ratio, reaction time and mixing in the relative yield of the various ethylene amines. The main conclusions on this aspect may be summarized as follows:

(i) At mole ratios of 10 : 1 and 6 : 1 the yield of EDA increased greatly with temperature, whereas the yield of DETA increases only slightly.
In general lower temperatures favour the formation of the higher linear ethylene amines. An optimum yield of TEPA and PEHA is indicated in the region of 120 °C with a drastic reduction when the temperature is increased much beyond this value.

(ii) The NH_3 : EDC mole ratio was shown to be the most significant single factor in controlling the reaction products. The higher the NH_3 : EDC molar ratio the greater the rate of reaction and, as a result, of EDC conversion.
The compositions achieved with several molar ratios are presented in Table 1.

(iii) The reaction time affects conversion at a mole ratio of 2 : 1 where 120 minutes are normally required to achieve a reasonable degree of conversion. But, with NH_3 : EDC = 6 : 1 and t = 120 °C complete conversion is achieved in about 20 minutes. When conversion of EDC is complete little or no further change in the product distribution takes place. So, there is no interest in letting the reaction proceed beyond the «conversion point».

From the results referred to previously, a high NH_3 : EDC mole ratio such as 20 : 1, will ensure a high yield of EDA (58 wt %). This EDA weight percentage may be further increased to 75-80 % by the addition of excess ammonium chloride [1]. An increase in the market demand for EDA at the expense of higher ethylene amines might be satisfied by the use of a very high NH_3 : EDC mole ratio together with the addition of ammonium chloride.
W. M. HUTCHINSON *et al.* [4] studied ways of converting high molecular weight polyethylene polyamines into EDA: the pyrolysis of a mixture containing tetramines, pentamines and hexamines has been reported to yield as high as 24 % EDA. However, higher boiling fractions consisting mainly of cyclized amines are also formed.
As it is shown in Table 1 a low NH_3 : EDC molar ratio such as 2 : 1 does increases the proportion of the higher molecular weight ethylene amines. A decisive drawback, however, is that the use of NH_3 : EDC molar ratios smaller than 10 : 1 drastically reduces the reaction rate and the residence time in the reactor becomes uneconomical. So, in order to increase the relative percentage of the ethylene amines with a higher molecular weight while using at the same time mole ratios that ensure completion of the reaction in a reasonable time, recycling of EDA, DETA and TETA has been studied.
A Japanese patent [5] describes a process in which the ammonolysis of EDC is carried out under pressure in a multistep reaction, with the presence of EDA and/or DETA. The reactor is a series of three 2 litres autoclaves connected to a piston-flow tubular reactor. The NH_3 : EDC mole ratio was 15 : 1, the ammonia was an aqueous solution of 70 % NH_4OH w/w and the temperature 140 °C.
The claimed product compositions are shown in Table II.

Table 2

Adding to the reactor	EDA	Tri-amines	Tetra-amines	Penta & Hexaamines
0 moles EDA	49 %	24 %	3 %	7 %
0.2 moles EDA	31 %	29 %	18 %	10 %
0.5 moles EDA	0 %	40 %	27 %	15 %

It was also reported that the content of TETA in the product was raised to 38 % by using a NH_3:EDC mole ratio of 20 : 1 and feeding to the reactor 0.5 moles of EDA and 0.1 moles of DETA.
A patent presented by Jefferson Chemical Co. [6] describes the effect of recycling EDA, DETA and TETA in a tubular reactor giving special emphasis to the point at which the recycling product enters the reactor. This injection point should be at a

Table 3

Run Number	1	2	3	4	5
NH_3: EDC mole ratio	15:1	15:1	15:1	15:1	15:1
NH_3 concentration (wt %)	65	65	65	65	65
Recycle injection point	None	(1)	(1)	(1)	(2)
Recycle amine (lbs/lb EDC)					
EDA	—	0.551	—	—	—
DETA	—	—	0.198	—	0.078
TETA	—	—	—	0.014	—
Production rate (lbs/100 lbs EDC)					
EDA	24.1	− 6.2	24.4	25.1	27.2
Triamines	8.7	14.2	− 3.8	7.0	6.4
Tetraamines	5.7	12.7	9.9	0.1	6.2
Penta and Hexamines	4.9	11.0	8.4	10.2	6.8
Residue	2.8	3.7	4.6	3.7	4.2

(1) At point in reactor where 1 chloro-, 2 aminoethane concentration is at a maximum.

(2) At reactor inlet.

point in the reactor at which the concentration of 1 chloro-, 2 aminoethane (produced by the reaction of one molecule of ammonia with one molecule of EDC) is at a maximum.

The reactor used was a jacketed tube 2// in diameter and 237// long, equipped with feed pumps, a preheater, product cooler and pressure and temperature controllers. The piping allowed that EDC was pumped directly to the beginning of the reactor and 65 % aqueous ammonia was preheated to about 100 °C and mixed with EDC at the reactor inlet. Recycle amine could be fed to the reactor at the inlet or through a nozzle located about 65// from the inlet. This latter point was the point at which the concentration of 1-chloro, 2-aminoethane was believed to be at a maximum under the conditions employed in the runs. The reactor temperature was controlled in the range of 90 °C to 100 °C and a reactor pressure of 700 p.s.i.g. was maintained.

The results obtained are given in Table 3.

The negative numbers in Table 3 indicate that the amount of that product recovered was less than the amount fed as recycle, indicating overall consumption of the product. Thus it would be possible in an industrial operation to recycle lower ethylene amines that were in oversupply, to extinction.

4 — FACTORS THAT INFLUENCE THE COMPOSITION OF THE PRODUCTS OF THE REACTION BETWEEN 1,2-DICHLOROETHANE AND 1,2-DIAMINOETHANE

The results of recycling EDA, DETA and TETA to the reactor where the ammonolysis of EDC is being promoted, as shown in Tables 2 and 3, only indicate the relative amount of Triamines, Tetraamines, Pentaamines, and Hexaamines produced and each of these contains a number of chemical compounds. In other words, the recycling both of EDA and DETA results in an increase in the complexity of the spectrum of products obtained mainly by increasing the relative proportion of the cyclic compounds [3].

Since EDA is more reactive with EDC than ammonia, the most direct way to study the recycle of EDA into the reaction of ammonolysis of EDC, is to study the reaction of EDA with EDC itself.

A study of the reaction of EDA with EDC published in 1969 [7] identified four chemical compounds as being produced: PIP, TETA, AAPIP and AEI. The branched-chain compound, tri-(2-aminoethyl)-amine, was not found in any products; this means that

Table 4

Run No.	EDA:EDC mole ratio	Reaction time (mins.)	Temp. (°C)	Yield, per cent			
				TETA	AAPIP	AEI	PIP
1	30:1	100	120	43.8	5.8	0	40.8
2	10:1	120	125	38.7	22.0	0	33.9
3	20:1	412	25	10.5	13.6	20.9	46.8
4	20:1	440	0	9.6	14.2	16.3	54.1
5	5:1	390	30	18.5	31.3	7.9	26.6
6 (1)	5:1	240	106	58.2	19.7	0	8.5
7 (1)	10:1	120	110	71.1	18.1	0	14.0
8 (2)	57:1	180	26	13.5	11.7	trace	49.0
9 (3)	20:1	60	123	50.8	15.9	0	37.2

(1) The EDA was diluted with an equal weight of water.

(2) The reaction mixture contained 6 wt % of HCl based on EDA + EDC, added as concentrated hydrochloric acid.

(3) The reaction mixture contained 3 moles of HCl per mole EDC, added as conc. hydrochloric acid.

there was no branched-chain structure formed. The composition of the reaction products was studied as a function of the EDA : EDC mole ratio, temperature and reaction time. The effects of the presence of water and/or HCl was also studied.

The presence of water and/or HCl in the reaction mixture improved the yields of TETA, and was said to accelerate the reaction. Suitable proportions are up to 20 % of water by weight (based on EDA) and up to 10 % of HCl, by weight (based on EDC). The latter is preferably added as ordinary aqueous hydrochloric acid of about 20-35 % concentration by weight. Pressure was not critical, normal atmospheric pressure is said to be suitable and convenient though temperatures of 120 °C were used.

The results are summarized in Table 4.

The piperazine is easily separated from TETA and AAPIP because of its low boiling point (145 °C at atm. press.). AEI is only reported to be produced when the temperature is very low (30 °C and

Table 5

Run No.	Temp. (°C)	Time (min.)	EDA:EDC mole ratio	base: EDC equivalent ratio	Base used	PIP	EDP	AAPIP	TETA	Hexa-amines
1	90-130	350	2:1	—	—	4	6	30	40	19
2	90-130	400	2:1	—	—	2	3	32	47	15
3	75	260	2:1	1:2.4	$(OH)_2Ca$	trace	trace	72	5	0
4	62	160	10:1	1:1	$(OH)_2Ca$	0	1	78	12	0
5	60-120	300	5:1	1:1	$(OH)_2Ca$	0	trace	88	2	5
6	50	450	10:1	1:1	$(OH)_2Ca$	trace	trace	90	9	0
7	58	410	10:1	—	—	trace	1	80	18	0
8	58	300	10:1	1:1	OHNa	trace	trace	98	trace	0
9	65	330	10:1	08:1	OHNa	trace	trace	84	15	0
10	60	320	5:1	1:1	OHNa	trace	trace	98	trace	0
11	67	420	10:1	2:1	OHNa	0	1	99	trace	0
12	70	480	10:1	1:1	OHNa	trace	1.5	65	33	0

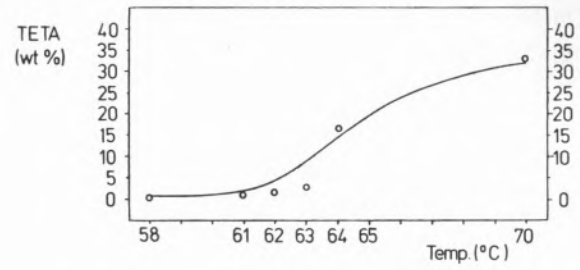

Fig. 1

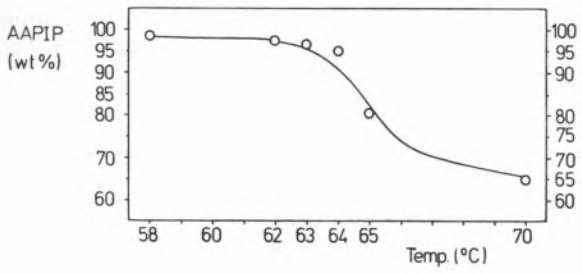

Fig. 2

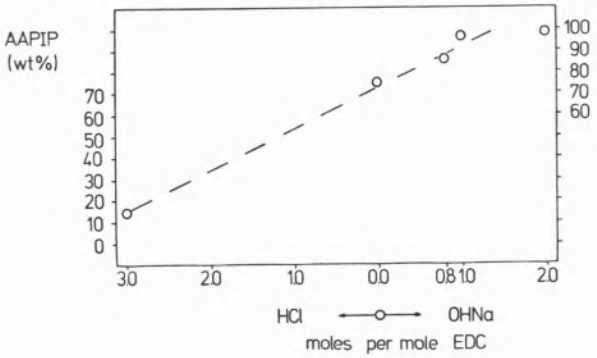

Fig. 3

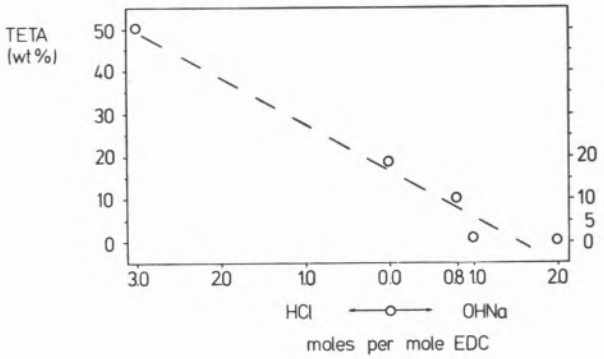

Fig. 4

below), and consequently the reaction times are very high, from 390 to 2,700 minutes. When this is produced it could be recycled in the process and be converted to TETA or AAPIP by further reaction with EDC.

For many applications a mixture of TETA and AAPIP is commercially acceptable and this can be obtained by distilling the lower boiling compounds. The residue consists essentially of TETA and AAPIP and is often used without further purification.

When EDC was substituted by 1,2-dibromoethane the rate of reaction was reduced substantially but the product composition was the same.

In the present work, the effects of adding a strong base and of varying the reaction temperature and EDA : EDC mole ratio were studied in a series of reaction whose main conditions are indicated in Table 5. All the reactions were carried out at atmospheric pressure.

The main compound promoted within the Tetramine group by the addition of a strong base is AAPIP. This compound is useful for many of the applications for which commercial TETA is employed. The results also indicate that high temperatures (100 °C) are essential if Hexamines are to be formed; an increase in temperature provokes a decrease in the yield percentage of TETA and an increase in the yield percentage of AAPIP as revealed in figs. 1 and 2.

Figs. 3 and 4 illustrate the effect of the addition of strong bases and of strong acids on the composition of the product of the reaction of EDA with EDC. It is clear that considerable changes in the type of polyethylene polyamines produced, can be affected by appropriate acid or base addition to the reaction mixture.

5 — DISCUSSION AND INTERPRETATION OF THE RESULTS

With a knowledge of the composition of the products of the reaction of EDA with EDC it is possible to postulate mechanisms for the step

reactions through which the overall transformation proceeds.

It is generally accepted that the amination of halogenated hydrocarbons is nucleophilic. The rate of the reaction of ammonolysis of EDC was shown to be strongly dependent upon the concentration of both reactants and nucleophilic substitutions on primary carbon atoms tend to proceed by a SN2 mechanism.

So, the most likely reaction mechanism that may be attributed to the first step of the reaction between EDA and EDC is a SN2 reaction.

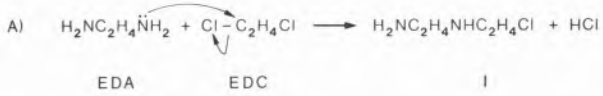

Once I has been produced, a second SN_2 type of reaction with EDA would lead to TETA:

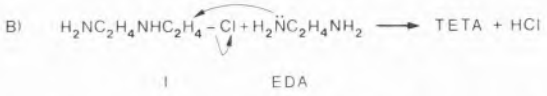

It is possible for I to undergo an internal SN reaction in which the nitrogen atom in the primary amine reacts with the halogenated carbon, forming a six-atoms ring. This mechanism is highly probable not only because these six-member rings are stable, but also because collision of a nitrogen on one end of a molecule with a halogenated carbon, five atoms removed is a very frequent occurrence (thus the formation of such rings have high entropies of activation).

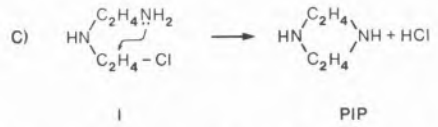

Once PIP has been formed the formation of AAPIP is probably due to the reaction between PIP and I again through nucleophilic substitution reaction, through which AAPIP is formed.

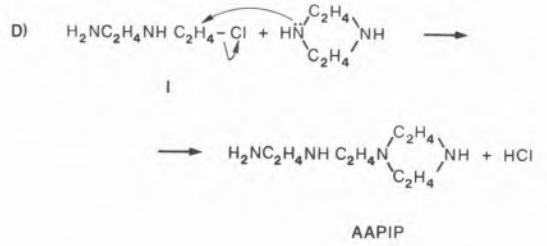

On the other hand the formation of AEI reported by COKER and HAM [7] when the temperature of the reaction was very low (between 0 °C and 30 °C) is probably due to an internal attack in I by the nearest nitrogen atom at the halogenated carbon, forming a three membered ring:

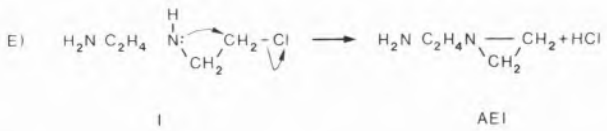

This three membered ring is very unstable and will react readily at higher temperatures to form TETA and AAPIP.

As the secondary amines in the piperazine ring are more basic than the primary amines, the former will tend to be preferentially neutralized by HCl. As *B*) and *D*) may be considered as competing reaction mechanisms this selective neutralization will enhance *B*) and thus favour the relative amount of TETA formed. Besides, PIP will be preferentially neutralized, will not react further and so the relative amount obtained at the end of the reaction will be increased.

When a strong base is added to the reaction it will neutralize the HCl generated by the reaction itself, and in so doing it will guarantee the natural nucleophilic superiority of the secondary amines in PIP in relation to the primary amines in EDA. This makes mechanism *D*) more likely than *B*) so that the relative amount of AAPIP should be increased as is found experimentally. PIP formed will preferentially react again to yield AAPIP and thus the percentage of PIP in the reaction products will decrease. These conclusions derived from a theoretical analysis of the proposed mechanism fit extremely well with the experimental data obtained before by Coker and Ham.

The experimental results also show that an increase in temperature favours the formation of linear TETA at the expense of the cyclic compound AAPIP under otherwise similar conditions. This may be explained by the fact that lower temperatures tend to favour internal «attack» while high temperatures by increasing the kinetic energy of the molecules tend to favour «collisions» between different molecules.

6 — METHODS FOR ANALYSIS OF ETHYLENE AMINES BY GAS LIQUID CHROMATOGRAPHY

At present the most successful way to analyze the ethylene amines is by Gas Liquid Chromatography (G. L. C.). However, till very recently, the analysis of the complex mixtures of any amines had remained a very neglected area. This was probably due to their high molecule weight, complex structure, and highly polar nature, that made them a very difficult group of compounds to separate in G. L. C.

The function of the solid support in a packed G. L. C. column is to provide a large surface area over which the liquid phase is spread in the form of a thin film. Ideally the support should be completely inert but most surfaces exhibit some type of chemical and adsorptive activity. When the support is not inert, interaction with the sample components will take place and depending upon the nature of the surface and type of sample, several characteristic properties are exhibited. Ordinarily the activity of the solid support is such that it does not seriously interfere with G. L. C. analysis but with polar type of compounds the activity can be so strong as to dominate and destroy any separation achieved by the stationary phase.

In their attempts at analysis of the lower aliphatic amines MARTIN and JONES [8] found severe tailing and poor resolution. They attributed this to the activity of the solid support and attempted to reduce this by washing the support repeatedly with acids and alkalis. SMITH and REDFORD [9] were the first to recognize that not only alkali treatment but its deposition on the support in relatively large quantities (2-10 % by weight) was an essential prerequisite in the G. L. C. analysis of ethylene amines.

This treatment allows the use of highly porous solid supports like Chromosorb P to be used, while attempts to use non-porous supports like glass beads were ineffective [10]. TOWHIDI [3] claims to have obtained very good results with AW-Celite, AW/DCMS and Chromosorb W, when they were impregnated with NaOH before application of the stationary phase, while BERGSTEDT and WIDMARK [11] claimed to be very successful when using Chromosorb W-HMDS alkalized with 10 % KOH in methanol.

The success or failure of a particular separation depends to a large extent on the choice of the stationary phase, rather than any other simple factor. Despite many attempts to rationalize the systems, the choice of liquid phase is still largely a matter of trial and error, and experience. However, a knowledge of the solvent-solutes interaction forces (hydrogen bonding, polarity etc.) is valuable in preliminary selection. In this case there was already some information from previous works.

TOWHIDI [3] found that Carbowax 20 M (polar) combined with caustic soda was capable of producing well resolved peaks with little or no tailing. Other products used like SE 30 and Triton × 305 gave very poor results.

BERGSTEDT and WIDMARK [11] examined the performance of three stationary phases all utilized in mixture with KOH: versamid 900, carbowax 20 M, and Apiezon L. The latter was found to be superior to the others, especially with regard to the later peaks of Pentaamines and Hexaamines. The presence of KOH was found necessary in order to avoid tailing.

In the present work two columns were used:

1) An all glass column, 0.2 cm i. d., packed with Diatomite CQ (from J J's Chromatography) 100-120 mesh treated with 3 % by weight of NaOH evaporated from a methanol solution; after this treatment 3 % versamid 940, from a solution in 50/50 chloroform/t-butanol, was added.

2) An all glass column 0.2 cm i.d., 265 cm long, packed with Diatomite C-AAW-HMDS (from J J's Chromatography) 60-80 mesh, treated with 6 % w/w NaOH dissolved in methanol; after this treatment a 25 % loading w/w (over the quantity of Diatomite) of Apiezon L, from a solution of Petroleum Spirit, 40-60 °C was added.

Both columns achieved a very good resolution of all the ethylene amines up to the pentaamines. The column 2 gave better results in analysing the Hexaamine peaks, although this was achieved with a much higher retention time.

ACKNOWLEDGEMENT

Clemente Pedro Nunes is deeply grateful to Instituto de Alta Cultura, Lisboa for granting a scholarship that made this work possible.

REFERENCES

[1] LESZEZYSKI, Z. *et al.*, *Przemysl Chem.*, **44**, *330 (1965)*.
[2] ROPUSZYNSKI, S. *et al.*, *Przemysl Chem.*, **47**, *542 (1968)*.
[3] TOWHIDI, M., «Ph. D. Thesis», University of Birmingham, 1971.
[4] HUTCHINSON, W. M. *et al.*, *J. Am. Chem. Soc.*, **67**, *1966 (1965)*.
[5] *Japanese Patent 12, 723 (1969)*, to Toyo Soda Manufg. Co. Ltd.
[6] *U. S. Patent 3,484,488 (1969)*, to Jefferson Chem. Co.
[7] *U. S. Patent 3,462,493 (1969)*, to Dow Chem. Co.
[8] MARTIN, A. J. P. *et al.*, *Biochem. J.*, **52**, *242 (1952)*.
[9] SMITH, E. D. *et al.*, *Rev. Chim. (Bucharest)*, **15**, *565 (1964)*.
[10] O'DONNEL, J. F. *et al.*, *Anal. Chem.*, **36**, *2097 (1964)*.
[11] BERGESTEDT, L. *et al.*, *Acta Chem. Scand.*, **24**, *2713 (1970)*.

RESUMO

A quase totalidade da produção industrial de 1,2-diaminoetano (EDA) é feita através da amonólise do 1,2-dicloroetano (EDC). A amónia é geralmente adicionada ao reactor quer em solução aquosa muito concentrada (50 a 65 % em peso) quer no estado de NH_3 anidro, de maneira que a reacção com EDC é realizada numa única fase, o que simplifica os problemas de transferência de massa. Embora o EDA seja o principal produto obtido, formam-se sempre outras etilenoaminas (série de grupos poliamino nos quais a molécula é formada por grupos amino primários, secundários ou terciários, ligados através de grupos etileno e formando, portanto, estruturas cíclicas ou ramificadas de maior peso molecular, devido certamente a reacções posteriores, nomeadamente a do EDA formado que reage com o EDC. O estudo da reacção do EDA com o EDC é, pois, de importância se se pretender atingir o mais alto rendimento em EDA. Trabalhos anteriores mostraram que a temperatura, a razão molar EDA : EDC, o tempo de reacção e, em especial, a presença de água destilada e ácidos fortes, podem influenciar a composição dos produtos da reacção.

O mecanismo da reacção é complexo podendo, contudo, prever-se por análise teórica, que envolva substituições nucleofílicas. Resultados anteriores e também os obtidos no presente trabalho confirmam as previsões feitas com base no conceito de competição entre as substituições nucleofílicas possíveis e que conduzem à aceitação de caminhos alternativos para a obtenção de determinada composição no produto da reacção. Discute-se também a análise de misturas complexas de etilenoaminas, tais como os produtos da reacção entre o EDA e o EDC, por cromatografia gás-líquido.

M. FARINHA PORTELA

Instituto Superior Técnico
Lisboa
Portugal

SIMULAÇÃO DA OXIDAÇÃO MODERADA E ISOMERIZAÇÃO CATALÍTICAS DO BUTENO-1 NUM REACTOR DE LEITO FIXO EM FUNÇÃO DO TEMPO DE CONTACTO (1)

Trabalhos anteriormente realizados permitiram a elaboração de um modelo mecanístico geral para a reacção do buteno-1, em presença de oxigénio, sobre catalisadores de molibdato de bismuto. Desse modelo foi possível derivar equações cinéticas, tanto para a oxidação a butadieno como para as isomerizações. Apresenta-se agora a simulação, em computador digital, da evolução do processo reaccional em causa, com base no modelo elaborado e em função do tempo de contacto, num reactor de leito fixo. Obtiveram-se curvas para a evolução da conversão do buteno-1 e das selectividades e rendimentos de butadieno, buteno-2 cis *e buteno-2* trans *as quais se ajustam satisfatoriamente a curvas experimentais obtidas para 350 e 393 °C, correspondentes a tempos de contacto máximos respectivamente de 5,5 e 1,6 segundos e conversões máximas respectivamente de 27 e 47 % em buteno-1. A discrepância entre a evolução simulada e a evolução observada é sensível a 350 °C, na zona dos maiores tempos de contacto investigados experimentalmente, mas é explicável.*

1 — INTRODUÇÃO

A reacção do buteno-1, em presença de oxigénio, sobre catalisadores de molibdato de bismuto é um processo complexo, em que avultam como principais as seguintes reacções:

1) $C_4H_8(1) + \frac{1}{2} O_2 \rightarrow C_4H_6 + H_2O$

2) $C_4H_8(1) \rightarrow C_4H_8(2\ cis)$

3) $C_4H_8(1) \rightarrow C_4H_8(2\ trans)$

4) $C_4H_8(1) + 6O_2 \rightarrow 4CO_2 + 4H_2O$

5) $C_4H_8(1) + 4O_2 \rightarrow 4CO + 4H_2O$

Tais reacções são francamente preponderantes sobre as que conduzem à formação de furano, formaldeído, acetaldeído, acroleína, crotonaldeído, acetona, metiletilcetona, metilvinilcetona, ácidos acético, propiónico, maleíco, acrílico, etc. A conversões não muito elevadas, as vias de oxidação moderada e isomerização (reacções 1 a 3) sobrelevam notoriamente em importância as vias de oxidação profunda (reacções 4 e 5).

Trabalhos anteriormente realizados [1-4], nomeadamente um estudo cinético, efectuado em condições de cinética inicial e corrente numa larga zona de pressões parciais dos intervenientes na reacção, em paralelo com estudos directos da acção dos reagentes e produtos sobre o catalisador, permitiram a elaboração de um modelo mecanístico geral, englobando as vias de oxidação moderada e isomerização.

---

(1) Presented at CHEMPOR' 75 held in Lisbon, 7-12 September 1975 at the Calouste Gulbenkian Foundation Center.
Papers presented at this International Chemical Engineering Conference can be purchased directly from Revista Portuguesa de Química (Instituto Superior Técnico, Lisboa 1, Portugal) at the following prices per volume sent by surface mail, postage included (in Portuguese Escudos):

Whole set	500
Transport processes	200
Reaction engineering	150
Environmental engineering	150
Management studies	150

This paper was presented at the Reaction engineering section.

Desse modelo foi possível derivar as equações cinéticas seguintes, tanto para a oxidação a butadieno, que é a reacção industrialmente interessante, como para as isomerizações (1-1) a (1-3).

$$r_{Bd} = \frac{1 + \dfrac{z_3(1+z_4)}{z_2P_{O_2} + P_{B_1}^2 + z_5P_{B_1}P_{O_2}^{1/2}P_{Bd}} P_{B_1}P_{O_2}^{1/2}P_{H_2O}}{\dfrac{z_2P_{O_2} + P_{B_1}^2 + z_5P_{B_1}P_{O_2}^{1/2}P_{Bd}}{z_1P_{B_1}P_{O_2}} + \dfrac{2z_3}{z_1}\dfrac{P_{H_2O}}{P_{O_2}^{1/2}}} \qquad (1\text{-}1)$$

$$r_{B_{2c}} = \frac{\dfrac{s_{B_{2co}}}{s_{Bdo}} + \dfrac{z_3\left(\dfrac{s_{B_{2co}}}{s_{Bdo}} + z'_4\right)}{z_2P_{O_2} + P_{B_1}^2 + z_5P_{B_1}P_{O_2}^{1/2}P_{Bd}} P_{B_1}P_{O_2}^{1/2}P_{H_2O}}{\dfrac{z_2P_{O_2} + P_{B_1}^2 + z_5P_{B_1}P_{O_2}^{1/2}P_{Bd}}{z_1P_{B_1}P_{O_2}} + \dfrac{2z_3}{z_1}\dfrac{P_{H_2O}}{P_{O_2}^{1/2}}} \qquad (1\text{-}2)$$

$$r_{B_{2t}} = \frac{\dfrac{s_{B_{2to}}}{s_{Bdo}} + \dfrac{z_3\left(\dfrac{s_{B_{2to}}}{s_{Bdo}} + z''_4\right)}{z_2P_{O_2} + P_{B_1}^2 + z_5P_{B_1}P_{O_2}^{1/2}P_{Bd}} P_{B_1}P_{O_2}^{1/2}P_{H_2O}}{\dfrac{z_2P_{O_2} + P_{B_1}^2 + z_5P_{B_1}P_{O_2}^{1/2}P_{Bd}}{z_1P_{B_1}P_{O_2}} + \dfrac{2z_3}{z_1}\dfrac{P_{H_2O}}{P_{O_2}^{1/2}}} \qquad (1\text{-}3)$$

$$r_{B_1} = \frac{\dfrac{1}{s_{Bdo}} + \dfrac{z_3\left(\dfrac{1}{s_{Bdo}} + z'''_4\right)}{z_2P_{O_2} + P_{B_1}^2 + z_5P_{B_1}P_{O_2}^{1/2}P_{Bd}} P_{B_1}P_{O_2}^{1/2}P_{H_2O}}{\dfrac{z_2P_{O_2} + P_{B_1}^2 + z_5P_{B_1}P_{O_2}^{1/2}P_{Bd}}{z_1P_{B_1}P_{O_2}} + \dfrac{2z_3}{z_1}\dfrac{P_{H_2O}}{P_{O_2}^{1/2}}} \qquad (1\text{-}4)$$

E quando as vias de oxidação profunda são desprezáveis em face das vias reaccionais atrás indicadas (reacções 1 a 3), a velocidade de reacção do buteno-1 pode ser expressa por (1-4).

Estas equações provaram ajustar-se bem aos dados experimentais [2, 3] na extensa gama de condições investigada.

No Quadro 1 agrupámos valores das constantes que intervêm naquelas equações para várias temperaturas. Os valores de z_1 e z_2 foram calculados aplicando o método dos quadrados mínimos a conjuntos de valores obtidos de experiências cinéticas em que a acção dos produtos da reacção era desprezável. Os valores de s_{Bdo}, $s_{B_{2co}}$ e $s_{B_{2to}}$ das selectividades iniciais de formação do butadieno, buteno-2 *cis* e buteno-2 *trans* — que se verificou serem independentes das pressões parciais dos reagentes, nas condições anteriormente mencionadas [4] — foram calculados como a média aritmética dos valores experimentais encontrados.

Quadro 1

Constantes das equações cinéticas

	300 °C	350 °C	393 °C	420 °C
z_1 moles butadieno/h g de cat.	$0{,}614 \times 10^{-4}$	$0{,}171 \times 10^{-2}$	$0{,}251 \times 10^{-1}$	0,107
z_2 atm.	$0{,}117 \times 10^{-1}$	$0{,}230 \times 10^{-1}$	0,150	0,343
z_3 atm.$^{-1/2}$	—	1,49	73,6	—
z_4 adimensional	—	1,18	1,72	—
z'_4 moles buteno-2 *cis*/mole butadieno	—	1,69	0,530	—
z''_4 moles buteno-2 *tr.*/mole butadieno	—	1,13	0,330	—
z'''_4 moles buteno-1/mole butadieno	—	3,94	2,60	—
z_5 atm.$^{-1/2}$	—	89	115	—
s_{Bdo} moles butadieno/mole buteno-1	0,596	0,703	0,787	0,839
$s_{B_{2co}}$ moles buteno-2 *cis*/mole buteno-1	0,216	0,167	0,119	0,088
$s_{B_{2to}}$ moles buteno-2 *tr.*/mole buteno-1	0,147	0,119	0,088	0,066

Para a determinação dos valores de z_3, z_4, z_4', z_4'' e z_4''' usou-se também o método dos quadrados mínimos aplicado a valores que provieram de experiências cinéticas conduzidas a pressões parciais de buteno-1 e oxigénio constantes. Nessas experiências fazia-se a introdução de água em quantidades variáveis na mistura reaccional antes da entrada no reactor, e trabalhava-se com tempos de contacto muito curtos, isto é, em condições diferenciais. O cálculo da constante z_5 foi realizado através da derivação gráfica de curvas experimentais dos rendimentos de butadieno em função do tempo de contacto.

2 — EQUAÇÕES DA EVOLUÇÃO DO SISTEMA COM O TEMPO DE CONTACTO

2.1 — *GENERALIDADES*

Dispomos das equações que regem cineticamente as principais vias reaccionais do sistema, e de todas as constantes cinéticas para as temperaturas de 350 e 393 °C. Esse facto sugeriu-nos tentar simular a evolução do sistema reaccional com o tempo de contacto num reactor de leito fixo, trabalhando isotermicamente, para composições de partida idênticas às usadas num estudo experimental da influência do tempo de contacto efectuado para aquelas temperaturas. Isso permite comparar as evoluções calculadas com as evoluções experimentais para as vias de oxidação moderada e de isomerização. E se o processo de cálculo da constante z_5 implica alguma dependência entre as evoluções calculada e experimental para o butadieno, o mesmo já não se verifica com os butenos-2.

Considerando que o comprimento do reactor é muito maior do que o respectivo diâmetro — como aconteceu nas experiências que realizámos — podemos considerar o perfil de velocidades de escoamento como recto e escrever

$$F dx = r_{B_1} dW \tag{2-1}$$

$$F dy = r_{Bd} dW \tag{2-2}$$

$$F dy_1 = r_{B_{2c}} dW \tag{2-3}$$

$$F dy_2 = r_{B_{2t}} dW \tag{2-4}$$

Este sistema de equações diferenciais pode ser posto sob a forma de

$$\frac{dy}{dx} = \frac{r_{Bd}}{r_{B_1}} \tag{2-5}$$

$$\frac{dy_1}{dx} = \frac{r_{B_{2c}}}{r_{B_1}} \tag{2-6}$$

$$\frac{dy_2}{dx} = \frac{r_{B_{2t}}}{r_{B_1}} \tag{2-7}$$

$$\frac{dx}{d\frac{W}{F}} = r_{B_1} \tag{2-8}$$

Se conseguirmos agora exprimir r_{B_1}, r_{Bd}/r_{B_1}, $r_{B_{2c}}/r_{B_1}$ e $r_{B_{2t}}/r_{B_1}$ em função da composição da mistura reaccional à entrada do leito catalítico, da conversão x e do rendimento de butadieno y, teremos o seguinte sistema de equações diferenciais:

$$\frac{dy}{dx} = \varphi_1(x, y) \tag{2-9}$$

$$\frac{dy_1}{dx} = \varphi_2(x, y) \tag{2-10}$$

$$\frac{dy_2}{dx} = \varphi_3(x, y) \tag{2-11}$$

$$\frac{dx}{d\frac{W}{F}} = \varphi_4(x, y) \tag{2-12}$$

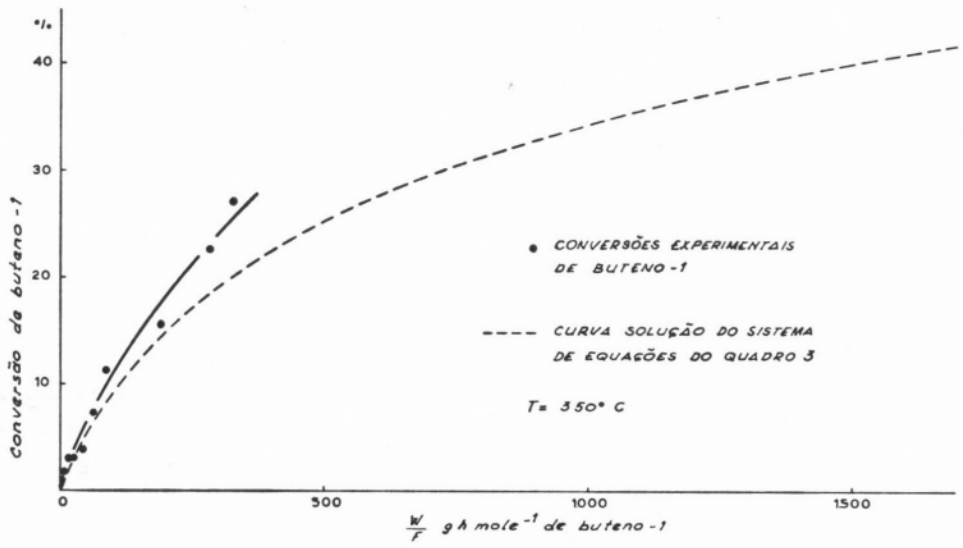

Fig. 1

que integrado dará

$$x = \psi_1\left(\frac{W}{F}\right) \qquad (2\text{-}13)$$

$$y = \psi_2\left(\frac{W}{F}\right) \qquad (2\text{-}14)$$

$$y_1 = \psi_3\left(\frac{W}{F}\right) \qquad (2\text{-}15)$$

$$y_2 = \psi_4\left(\frac{W}{F}\right) \qquad (2\text{-}16)$$

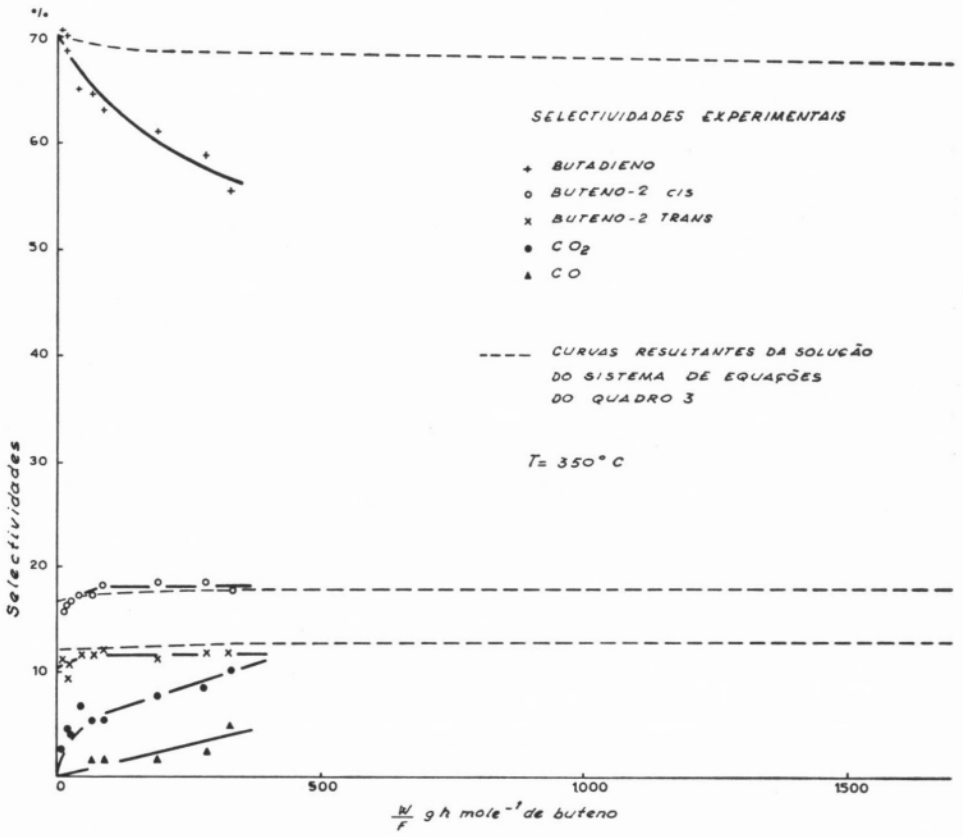

Fig. 2

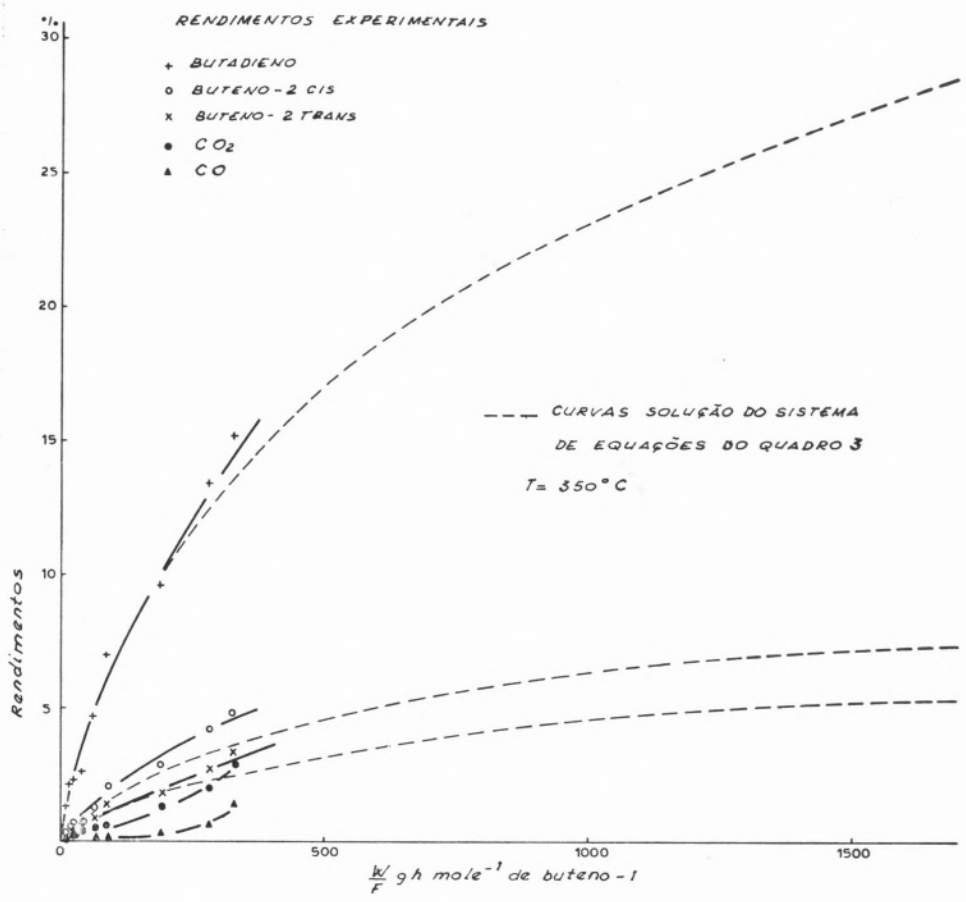

Fig. 3

As representações gráficas destas funções corresponderão às curvas experimentais das figs. 1, 3, 4 e 6, com as quais poderão ser comparadas. Por outro lado, a evolução das selectividades de formação dos produtos será dada pelas equações

$$s_{Bd} = \frac{y}{x} = \chi_1\left(\frac{W}{F}\right) \qquad (2\text{-}17)$$

$$s_{B_{2c}} = \frac{y_1}{x} = \chi_2\left(\frac{W}{F}\right) \qquad (2\text{-}18)$$

$$s_{B_{2t}} = \frac{y_2}{x} = \chi_3\left(\frac{W}{F}\right) \qquad (2\text{-}19)$$

e as curvas experimentais correspondentes a estas funções são as das figs. 2 e 5.

2.2 — *ESTABELECIMENTO DAS EQUAÇÕES*

Vamos tomar como composições da mistura reaccional à entrada do reactor as seguintes:

T = 350°C 17,9 % de buteno-1 e 17,8 % de oxigénio

T = 393°C 17,8 % de buteno-1 e 17,7 % de oxigénio

Considera-se a pressão total dentro do reactor igual a 12 cm de Hg e a perda de carga desprezável. A diferença para 100 % nas composições é constituída por azoto, que é inerte nas condições da reacção. Estas condições foram as usadas no estudo experimental já referido e que nos servirá de termo de comparação.

Tendo em conta a elevada percentagem de azoto usada e admitindo fraca relevância para as vias de oxidação profunda, chegamos às seguintes

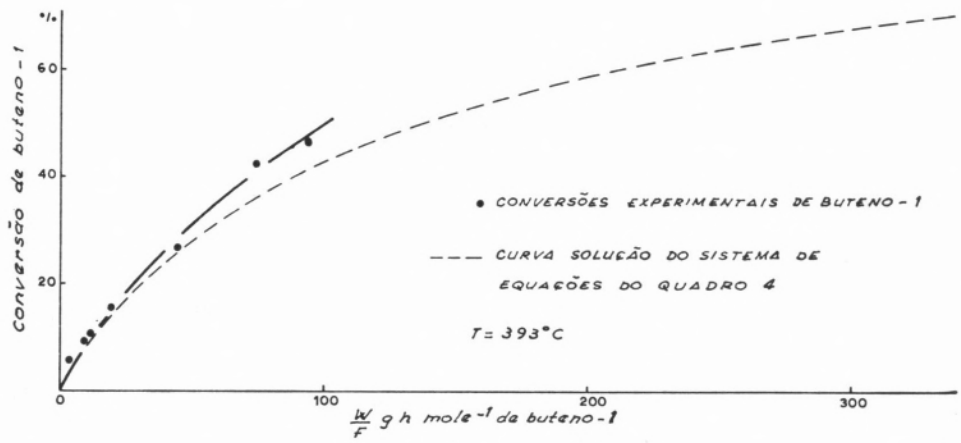

Fig. 4

expressões para as pressões parciais dos intervenientes na reacção

$$P_{B_1} = \frac{(1 - x)P}{n_1 + n_2 + 1} \qquad (2\text{-}20)$$

$$P_{O_2} = \frac{\left(n_1 - \frac{y + 12y_3 + 8y_4}{2}\right)P}{n_1 + n_2 + 1} \qquad (2\text{-}21)$$

$$P_{H_2O} = \frac{(y + 4y_3 + 4y_4)P}{n_1 + n_2 + 1} \qquad (2\text{-}22)$$

$$P_{Bd} = \frac{yP}{n_1 + n_2 + 1} \qquad (2\text{-}23)$$

Os termos relativos aos rendimentos de CO_2 (y_3) e CO (y_4) tiveram de ser mantidos nas expressões acima principalmente por causa da forte influência

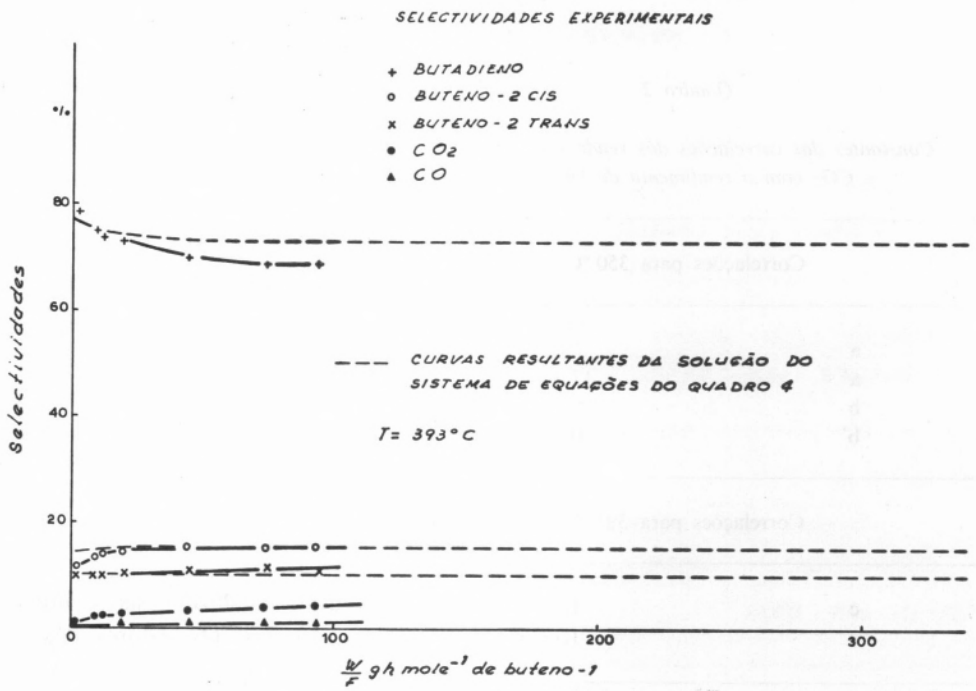

Fig. 5

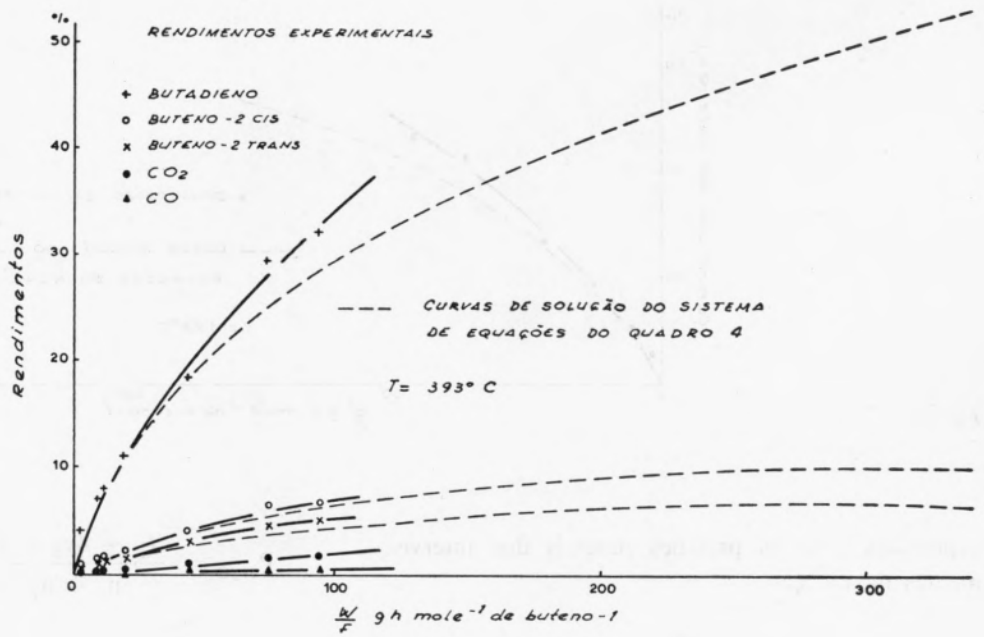

Fig. 6

da água sobre a evolução do sistema na zona de baixas concentrações deste produto [2, 3]. Cada molécula de CO ou CO_2 formada dá lugar ao aparecimento simultâneo de uma molécula de água.

Para tentarmos resolver o problema que propusemos temos de procurar exprimir os termos $12y_3 + 8y_4$ e $4y_3 + 4y_4$, em que intervêm os rendimentos de formação de CO e CO_2, em função de x e y. Importa notar que para as condições escolhidas a sensibilidade das velocidades de reacção a variações de P_{O_2} é pequena. Por outro lado, aquelas grandezas são muito sensíveis a variações de P_{H_2O}, para pequenos valores desta variável, mas deixam de o ser para valores altos [2, 3]. Por isso as correlações entre $12y_3 + 8y_4$ e $4y_3 + 4y_4$ de uma parte, e x e y da outra, que têm de intervir, basta que sejam particularmente rigorosas para valores pequenos da pressão parcial da água.

Lançou-se mão para o efeito das seguintes correlações empíricas, derivadas dos valores encontrados no estudo experimental [3]:

$$T = 350°C \qquad 4y_3 + 4y_4 = ay^2 + b \tag{2-24}$$

$$12y_3 + 8y_4 = a'y^2 + b' \tag{2-25}$$

$$T = 393°C \qquad y + 4y_3 + 4y_4 = cy \tag{2-26}$$

$$y + 12y_3 + 8y_4 = c'y \tag{2-27}$$

que satisfazem as condições base acima mencionadas. Os valores das constantes a, a′, b, b′, c e c′ podem ver-se no Quadro 2. Nessas circuns-

Quadro 2

Constantes das correlações dos rendimentos de CO e CO_2 com o rendimento de butadieno

Correlações para 350 °C	
a	6,61
a′	17,9
b	0,00154
b′	0,00664
Correlações para 393 °C	
c	1,27
c′	1,77

tâncias as expressões (2-20) a (2-23) tomam a seguinte forma:

Para 350 °C

$$P_{B_1} = \frac{1 - x}{4{,}81} \text{ atm.} \qquad (2\text{-}28)$$

$$P_{O_2} = \frac{0{,}991 - 8{,}95y^2 - 0{,}5y}{4{,}81} \text{ atm.} \qquad (2\text{-}29)$$

$$P_{H_2O} = \frac{6{,}61y^2 + y}{4{,}81} \text{ atm.} \qquad (2\text{-}30)$$

$$P_{Bd} = \frac{y}{4{,}81} \text{ atm.} \qquad (2\text{-}31)$$

Para 393 °C

$$P_{B_1} = \frac{1 - x}{4{,}84} \text{ atm.} \qquad (2\text{-}32)$$

$$P_{O_2} = \frac{0{,}994 - 0{,}883y}{4{,}84} \text{ atm.} \qquad (2\text{-}33)$$

$$P_{H_2O} = \frac{1{,}27y}{4{,}84} \text{ atm.} \qquad (2\text{-}34)$$

$$P_{Bd} = \frac{y}{4{,}84} \text{ atm.} \qquad (2\text{-}35)$$

Agora podemos nas equações (2-5) a (2-8) substituir r_{B_1}, r_{Bd}, $r_{B_{2c}}$ e $r_{B_{2t}}$ pelas suas expressões (1-1)

Quadro 3

Equações da evolução do sistema reaccional com o tempo de contacto

T = 350 °C *P = 12 cm de Hg*

Composição inicial da mistura reaccional: 17,9 % de buteno-1 e 17,8 % de oxigénio

$$\frac{dy}{dx} = \frac{0{,}00333 + 0{,}0304(1-x)^2 - 0{,}00168y - 0{,}0301y^2 + (1-x)y(1{,}28 + 0{,}297y)(0{,}991 - 0{,}5y - 8{,}95y^2)^{1/2}}{0{,}00474 + 0{,}0432(1-x)^2 - 0{,}00239y - 0{,}0428y^2 + (1-x)y(1{,}86 + 0{,}732y)(0{,}991 - 0{,}5y - 8{,}95y^2)^{1/2}}$$

$$\frac{dy_1}{dx} = \frac{0{,}000791 + 0{,}00722(1-x)^2 - 0{,}000399y - 0{,}00715y^2 + (1-x)y(0{,}333 + 0{,}263y)(0{,}991 - 0{,}5y - 8{,}95y^2)^{1/2}}{0{,}00474 + 0{,}0432(1-x)^2 - 0{,}00239y - 0{,}0428y^2 + (1-x)y(1{,}86 + 0{,}732y)(0{,}991 - 0{,}5y - 8{,}95y^2)^{1/2}}$$

$$\frac{dy_2}{dx} = \frac{0{,}000564 + 0{,}00514(1-x)^2 - 0{,}000285y - 0{,}00509y^2 + (1-x)y(0{,}236 + 0{,}177y)(0{,}991 - 0{,}5y - 8{,}95y^2)^{1/2}}{0{,}00474 + 0{,}0432(1-x)^2 - 0{,}00239y - 0{,}0428y^2 + (1-x)y(1{,}86 + 0{,}732y)(0{,}991 - 0{,}5y - 8{,}95y^2)^{1/2}}$$

$$\frac{dx}{d\frac{W}{F}} = \frac{1{,}42 + \dfrac{0{,}157(1-x)y(1 + 6{,}61y)(0{,}991 - 0{,}5y - 8{,}95y^2)}{0{,}00474 + 0{,}0432(1-x)^2 - 0{,}00239y - 0{,}0428y^2 + 1{,}75(1-x)y(0{,}991 - 0{,}5y - 8{,}95y^2)^{1/2}}}{\dfrac{0{,}00474 + 0{,}0432(1-x)^2 - 0{,}00239y - 0{,}0428y^2 + 1{,}75(1-x)y(0{,}991 - 0{,}5y - 8{,}95y^2)^{1/2}}{0{,}0000739(1-x)(0{,}991 - 0{,}5y - 8{,}95y^2)} + \dfrac{795y(1 + 6{,}61y)}{(0{,}991 - 0{,}5y - 8{,}95y^2)^{1/2}}}$$

Quadro 4

Equações da evolução do sistema reaccional com o tempo de contacto

T = 393 °C *P = 12 cm de Hg*

Composição inicial da mistura reaccional: 17,8 % de buteno-1 e 17,7 % de oxigénio

$$\frac{dy}{dx} = \frac{0{,}0242 + 0{,}0336(1-x)^2 - 0{,}0215y + 5{,}64(1-x)y(0{,}994 - 0{,}883y)^{1/2}}{0{,}0308 + 0{,}0427(1-x)^2 - 0{,}0274y + 7{,}76(1-x)y(0{,}994 - 0{,}883y)^{1/2}}$$

$$\frac{dy_1}{dx} = \frac{0{,}00367 + 0{,}00508(1-x)^2 - 0{,}00326y + 1{,}24(1-x)y(0{,}994 - 0{,}883y)^{1/2}}{0{,}0308 + 0{,}0427(1-x)^2 - 0{,}0274y + 7{,}76(1-x)y(0{,}994 - 0{,}883y)^{1/2}}$$

$$\frac{dy_2}{dx} = \frac{0{,}00271 + 0{,}00376(1-x)^2 - 0{,}00241y + 0{,}828(1-x)y(0{,}994 - 0{,}883y)^{1/2}}{0{,}0308 + 0{,}0427(1-x)^2 - 0{,}0274y + 7{,}76(1-x)y(0{,}994 - 0{,}883y)^{1/2}}$$

$$\frac{dx}{d\frac{W}{F}} = \frac{1{,}27 + \dfrac{7{,}02(1-x)y(0{,}994 - 0{,}883y)^{1/2}}{0{,}0308 + 0{,}0427(1-x)^2 - 0{,}0274y + 2{,}23(1-x)y(0{,}994 - 0{,}883y)^{1/2}}}{\dfrac{0{,}0308 + 0{,}0427(1-x)^2 - 0{,}0274y + 2{,}23(1-x)y(0{,}994 - 0{,}883y)^{1/2}}{0{,}00107(1-x)(0{,}994 - 0{,}883y)} + \dfrac{3390y}{(0{,}994 - 0{,}883y)^{1/2}}}$$

a (1-4) e fazer depois intervir, conforme a temperatura, os conjuntos de expressões (2-28) a (2-35). Teremos sistemas de 4 equações diferenciais, que integrados darão soluções do tipo (2-13) a (2-16). Os sistemas a que chegámos foram dispostos nos Quadros 3 e 4.

3 — RESULTADOS DA SIMULAÇÃO E COMPARAÇÃO COM A EVOLUÇÃO EXPERIMENTAL

Integrámos numericamente os sistemas de equações diferenciais acima referidos pelo método de Runge-Kutta de quarta ordem [5]. O intervalo de integração usado foi de 1 % de conversão para 350 °C e 0,5 % para 393 °C. As evoluções calculadas podem ser vistas nos Quadros 5 e 6 e foram representadas graficamente nas figs. 1 a 6 para efeitos de comparação com as curvas experimentais.

A 350 °C, a comparação entre as evoluções experimental e simulada da conversão de buteno-1 revela que as ordenadas da curva de simulação são inferiores às correspondentes da curva experimental, e que o desvio absoluto aumenta com com o tempo de contacto. Mas para o valor máximo desta variável usado nas determinações experimentais (5,5 segundos), o desvio relativo é apenas de 23 %. Além disso, a não concordância das duas curvas é explicável. A curva calculada foi obtida considerando-se que era desprezável a oxidação profunda. Ora as figs. 2 ou 3 evidenciam que, com os maiores tempos de contacto que usámos, a oxidação a CO e CO_2 começa a ser relevante. Para a mesma temperatura, o ajustamento das curvas experimental e calculada do rendimento de butadieno é bastante bom, o que não é até certo ponto de surpreender dado o modo como foi efectuado o cálculo da constante z_5. Mas a concordância entre os dois referidos tipos de curvas, no caso dos rendimentos de buteno-2 *cis* e buteno-2 *trans*, que está isenta das dependências que se verificam para o butadieno, parece-nos bastante razoável e encorajante. Nas evoluções das selectividades nota-se apenas discrepância apreciável no

caso do butadieno, que é interpretável, pelo facto já apontado, de as nossas equações não considerarem a oxidação profunda a CO e CO_2. E sabe-se, além disso, que estes últimos produtos se formam também do butadieno [6].

O acordo entre a evolução simulada e a experimental é muito melhor a 393 °C, embora experimentalmente se tenham atingido conversões maiores. Mas, como se trabalhou com tempos de contacto substancialmente menores (o máximo foi de 1,6 segundos), isso parece ter dado lugar a menor relevância das vias de oxidação profunda. Por esse facto, a evolução experimental desenrolou-se por forma mais coincidente com as condições admitidas para a evolução simulada e daí a boa concordância evidenciada.

4 — CONCLUSÕES

Os acordos verificados nesta simulação sugerem uma via mais precisa para o cálculo da constante z_5 do que o processo a partir da derivação gráfica da curva do rendimento de butadieno, que é obviamente grosseiro. Bastará arbitrar valores para a constante z_5, realizar para cada um desses valores

Quadro 5

Evolução calculada do sistema reaccional com o tempo de contacto

T = 350 °C *P = 12 cm de Hg*

Composição inicial da mistura reaccional: 17,9 % de buteno-1 e 17,8 % de oxigénio

Tempo de contacto $\frac{W}{F}$ g h mole^{-1} de buteno-1	Conversão de buteno-1 x %	Rendimentos			Selectividades		
		Butadieno y %	Buteno-2 c y_1 %	Buteno-2 t y_2 %	Butadieno y/x %	Buteno-2 c y_1/x %	Buteno-2 t y_2/x %
11,5	2	1,40	0,339	0,241	70,0	17,0	12,1
37,1	5	3,50	0,859	0,610	69,5	17,2	12,2
60,0	7	4,85	1,21	0,860	69,3	17,3	12,3
103	10	7,00	1,75	1,24	69,1	17,5	12,4
138	12	8,27	2,10	1,49	68,9	17,5	12,4
200	15	10,3	2,65	1,88	68,7	17,7	12,5
248	17	11,7	3,01	2,13	68,7	17,7	12,6
331	20	13,7	3,56	2,52	68,5	17,8	12,6
394	22	15,0	3,93	2,78	68,4	17,9	12,7
502	25	17,1	4,49	3,18	68,2	18,0	12,7
584	27	18,4	4,87	3,44	68,1	18,0	12,7
725	30	20,4	5,43	3,84	68,0	18,1	12,8
833	32	21,7	5,81	4,11	67,9	18,2	12,8
1020	35	23,7	6,38	4,51	67,7	18,2	12,9
1170	37	25,0	6,76	4,78	67,7	18,3	12,9
1450	40	27,0	7,33	5,18	67,5	18,3	13,0
1690	42	28,3	7,72	5,45	67,5	18,4	13,0
2410	45	30,3	8,29	5,85	67,3	18,4	13,0

Quadro 6

Evolução calculada do sistema reaccional com o tempo de contacto

T = 393 °C *P = 12 cm de Hg*

Composição inicial da mistura reaccional: 17,8 % de buteno-1 e 17,7 % de oxigénio

Tempo de contacto $\frac{W}{F}$ g h mole^{-1} de buteno-1	Conversão de buteno-1 x %	Rendimentos			Selectividades		
		Butadieno y %	Buteno-2 c y_1 %	Buteno-2 t y_2 %	Butadieno y/x %	Buteno-2 c y_1/x %	Buteno-2 t y_2/x %
3,64	5	3,75	0,716	0,496	75,0	14,3	9,92
9,56	10	7,43	1,48	1,02	74,3	14,8	10,2
17,9	15	11,1	2,26	1,54	73,9	15,1	10,3
28,8	20	14,7	3,05	2,07	73,7	15,2	10,3
42,4	25	18,4	3,83	2,60	73,6	15,3	10,4
58,7	30	22,0	4,62	3,12	73,4	15,4	10,4
78,0	35	25,7	5,41	3,65	73,3	15,5	10,4
100	40	29,3	6,20	4,18	73,3	15,5	10,5
126	45	33,0	6,99	4,71	73,2	15,5	10,5
154	50	36,6	7,78	5,25	73,2	15,6	10,5
187	55	40,2	8,58	5,78	73,2	15,6	10,5
223	60	43,9	9,37	6,31	73,1	15,6	10,5
263	65	47,5	10,2	6,84	73,1	15,6	10,5
308	70	51,2	11,0	7,37	73,1	15,6	10,5
357	75	54,8	11,7	7,90	73,0	15,7	10,5
412	80	58,4	12,5	8,43	73,0	15,7	10,5
472	85	62,1	13,3	8,96	73,0	15,7	10,5
541	90	65,7	14,1	9,49	73,0	15,7	10,6
620	95	69,4	14,9	10,0	73,0	15,7	10,6
732	99,5	72,7	15,6	10,5	73,0	15,7	10,5

a integração do sistema de equações diferenciais (2-9) a (2-12) e determinar a soma dos quadrados dos desvios entre os rendimentos experimentais e calculados do butadieno e butenos-2. O valor de z_5 para o qual essa soma for mínima será o melhor valor desta constante.

Por outro lado, as concordâncias encontradas também constituem um argumento adicional a favor da validez das equações cinéticas nas quais a simulação se baseou e, consequentemente, do modelo mecanístico a partir do qual tais equações foram derivadas.

SIMBOLOGIA

F — caudal de buteno-1, moles/h

n_1 — moles de O_2 por mole de buteno-1 à entrada do leito catalítico

n_2 — moles de N_2 por mole de buteno-1 à entrada do leito catalítico

P — pressão total, atm.

P_{B_1} — pressão parcial de buteno-1, atm.

P_{Bd} — pressão parcial de butadieno, atm.

P_{H_2O} — pressão parcial da água, atm.

P_{O_2} — pressão parcial de oxigénio, atm.

r_{B_1} — velocidade de reacção do buteno-1, moles h^{-1} g^{-1} de catalisador

$r_{B_{2c}}$ — velocidade de formação do buteno-2 *cis*, moles h^{-1} g^{-1} de catalisador

$r_{B_{2t}}$ — velocidade de formação do buteno-2 *trans*, moles h^{-1} g^{-1} de catalisador

r_{Bd} — velocidade de formação do butadieno, moles h^{-1} g^{-1} de catalisador

$s_{B_{2c}}$ — selectividade de formação do buteno-2 *cis*

$s_{B_{2t}}$ — selectividade de formação do buteno-2 *trans*

s_{Bd} — selectividade de formação do butadieno

$s_{B_{2co}}$ — selectividade inicial de formação do buteno-2 *cis*

$s_{B_{2to}}$ — selectividade inicial de formação do buteno-2 *trans*

s_{Bdo} — selectividade inicial de formação do butadieno

x — conversão de buteno-1

y — rendimento de butadieno

y_1 — rendimento de buteno-2 *cis*

y_2 — rendimento de buteno-2 *trans*

y_3 — rendimento de CO_2

y_4 — rendimento de CO

W — peso de catalisador, g

z — constante cinética (ver Quadro 1)

BIBLIOGRAFIA

[1] BOUTRY, P., MONTARNAL, R. e PORTELA, M. F., *Bull. Soc. Chim. France*, **1**, *23 (1969)*.

[2] PORTELA, M. F., «Tese de Doutoramento», Lisboa, 1971.

[3] PORTELA, M. F., «A Isomerização e a Oxidação Catalíticas do Buteno-1 sobre Óxidos de Bismuto-Molibdénio», Lisboa, 1973.

[4] PORTELA, M. F., PIRES, M. J. R. e RIBEIRO, F. R. Comunicação ao IV Simpósio Iberoamericano de Catálise, México, 1974.

[5] LAPIDUS, L., «Digital Computation for Chemical Engineers», McGraw-Hill, New York, 1962.

[6] MAL'YAN, A. N., BAKSHI, Yu. M. e GEL'BSHTEIN, A. I., *Kinetika i Kataliz* (Tradução inglesa), **9**, *1266 (1968)*.

ABSTRACT

Reaction of 1-butene at atmospheric pressure, in presence of oxygen, on bismuth-molybdenum-oxide catalysts in a fixed bed reactor is simulated as a function of contact time. Such simulation was based on the kinetic expressions for the formation of butadiene, cis-*2-butene and* trans-*2-butene, which were developed from a detailed mechanism for the catalytic process, established in earlier studies of the author, when it is allowable to disregard deep oxidation.*

The calculated curves for conversion, selectivities and yields match the available experimental data over the referred three main reaction paths, or the deviations are understandable. This gives additional support to the model used for simulation.

D. H. ALLEN

Department of Chemical Engineering
University of Nottingham
U. K.

THE ANALYSIS OF FINANCIAL UNCERTAINTY AND RISK IN A PROJECT[1]

Information used in the economic evaluation of a project is based on estimates and forecasts and is therefore uncertain. A realistic evaluation should take account of these uncertainties so that the consequential financial risks can be properly faced in making project decisions. This paper discusses problems in assessing the effects of uncertainty and describes the use of the computer-based technique known as risk analysis by which the logical consequences of subjective assessments of uncertainty can be explored. Recognition of the existence of uncertainty requires an explicit policy towards its risks and possible bases for such policies are considered.

1 — INTRODUCTION

The economic evaluation of a project assesses its potential profitability in terms of an appropriate measure such as net present value (NPV) or discounted cash flow (DCF) return, sometimes known as the internal rate of return (IRR). The numerical value of a profitability measure is a function of the predicted yearly cash flows for the project, and these in turn depend on estimates and forecasts of all the contributing expenditures and incomes and on their timings. All forecasts are uncertain to a greater or lesser extent and associated with these uncertainties is risk, the risk that the project will not achieve the expected financial results. Investment and project planning decisions under conditions of uncertainty and risk require the use of judgement in some form, but this does not mean taking decisions arbitrarily. Good judgement involves the identification, consideration and weighing of the relevant factors, including uncertainties and risks. These may be taken into account in reaching decisions in a rational way by expressing subjective assessments of uncertainties in quantitative terms and then following an explicit strategy or policy towards the corresponding risks.

2 — SENSITIVITY ANALYSIS

Sensitivity analysis involves investigating the effect on a project as a whole of changes in individual contributing estimates. For example, for a particular project a 10 per cent increase in capital cost might be found to reduce the project's DCF return by

---

(1) Presented at CHEMPOR' 75 held in Lisbon, 7-12 September 1975 at the Calouste Gulbenkian Foundation Center.
Papers presented at this International Chemical Engineering Conference can be purchased directly from Revista Portuguesa de Química (Instituto Superior Técnico, Lisboa 1, Portugal) at the following prices per volume sent by surface mail, postage included (in Portuguese Escudos):

Whole set	500
Transport processes	200
Reaction engineering	150
Environmental engineering	150
Management studies	150

This paper was presented at the Management studies section.

5 per cent p.a., whereas a shortfall of 10 per cent in the subsequent annual income generated might reduce the DCF return by 15 per cent p.a. Sensitivity analysis identifies those estimates in which variations, i.e, uncertainty, have significant effects on the project's financial well-being. It therefore shows where accurate estimates are more vital and also where they are not so important.

Although sensitivity analysis is very useful in demonstrating the effects of variations, it only looks at half the problem. It takes no account of the relative likelihood, or probability, of different variations occuring. For a full risk analysis we need to include not only the effects of variations in estimates, but also the chances that they will occur.

3 — 'BLANKET' ASSESSMENT OF RISK

A somewhat crude method of allowing for risk in the financial evaluation of a project is to vary the 'cut-off' level of the project's financial index (DCF return or NPV) according to an overall general assessment of the risks involved in the project. Thus for a project which is entirely predictable and risk-free, a DCF return greater than, say, 15 per cent p.a. (if this is the cost of capital) might be acceptable; for a moderately risky project a DCF return greater than, say, 25 per cent p.a. would be necessary, while for a high-risk, speculative project a DCF return of, say, 50 per cent p.a. would be required before deciding to go ahead. In terms of NPV, the corresponding situations would be a positive NPV when discounting at 15, 25 and 50 per cent p.a. respectively.

The reasoning behind this is that as the risk that the target DCF return will not be achieved increases, the target itself should be increased. Another way of looking at it is that risky projects which succeed financially should, in the long run, pay for those that fail. The assessment of risk is a general one for the project as a whole and is not explicitly related to specific contributing factors.

A closely related method of risk assessment at this same level involves the subjective assessment of a project's 'probability of sucess'. The financial index for the project is then multiplied by the probability of success to discount it for risk, and the resulting return is considered to see whether it would be acceptable for an equivalent risk-free project. For the examples mentioned above the equivalent probabilities of success would be 1.0, 0.6 and 0.3 respectively so that the DCF returns of 15, 25 and 50 per cent p.a. would all be reduced to 15 per cent p.a. Some methods use several probabilities of success multiplied together, e.g. a probability of initial engineering success and then, given this, the probability of subsequent commercial success.

The limitation of these 'blanket' methods of assessing and allowing for risk is that they do not go back to the sources of uncertainty, i.e. the original estimates and forecasts. Hence it is very difficult to defend or justify these subjective hunches as to the level of risk or the probability of success.

4 — SUBJECTIVE PROBABILITIES

At this point the subjective nature of any measure of project uncertainty should be emphasized. No two projects are exactly alike. Even apparently similar projects differ in time or in location and are therefore influenced to different extents by economic, social or other environmental factors. The experience gained with one project in this respect cannot be used directly to assess what is going to happen to another project, although of course it is still very relevant and useful information.

Subjective probabilities are commonly used as a way of quantifying uncertainty. It is important to realise that they are merely a way of expressing personal feelings about uncertainty and have no objective reality. Objective probabilities can be demonstrated and tested. For example, the probability that a tossed coin will come down heads can be found by repeating the event a large number of times, or the probability that a person will live to a stated age can be found by analysis of population life records, as is done by life assurance companies. There is no similar basis for probabilities about the future of a project, since there are not enough similar projects to reach a satisfactory conclusion, and anyway each project is different in some ways from previous ones. These subjective probabilities cannot be proved right or wrong — they depend

on the estimator's knowledge of the situation and his relevant past experience. Note that once the situation occurs, past assessment of its probability is irrelevant. For example, if it is estimated that there is an 80 per cent chance of the capital investment for a project exceeding £x, when the time arrives it either does or does not exceed £x and the probability is then meaningless.

The advantage of using subjective probabilities as means of expressing opinions about uncertain situations is not that the numbers have any objective reality (which they do not), but that they enable the consequences of these opinions to be explored in a logical and rational way. Thus given that there is an 80 per cent chance of capital investment exceeding £x, the effect on DCF return or other aspects of the project can be evaluated and an appropriate decision taken. However, putting numbers on uncertainties in the form of probabilities in no way alters their subjective origin in being based on experience, intuition, or mere hunch.

A better way of expressing uncertainty and consequent risk than giving a project a probability of success is to relate project uncertainty to its origins in the uncertainty in individual contributing estimates and forecasts. The outcome of a project may be discrete alternatives depending on an 'either/or' situation, or it may vary continuously with variations in contributing factors.

5 — DISCRETE ALTERNATIVE OUTCOMES AND PROJECT EXPECTATION

The general process of decision-making involves identifying alternative courses of action, establishing the possible outcomes of each action, evaluating the economic desirability of these outcomes, and then assessing them in some way to select the best course of action to take. To illustrate this, consider a simplified situation where the decision is whether or not to go ahead with an investment project in a new production plant. Note that any decision involves at least two possible courses of action, where one is always to do nothing, or to continue as at present. In the simplest case, with no uncertainty, each action leads to only one possible outcome. Suppose in this example the course of action to go ahead with the project would lead to a profitable venture which over its life would have a net present value of £500,000. If the project does not go ahead the capital would instead remain invested in the City with a corresponding NPV of £150,000. The decision situation is summarised in the payoff table (Table 1).

Table 1

Payoff table, no uncertainty

	Action on project	
	Yes	No
NPV, £1,000	500	150

With no uncertainty the decision is straightforward, and assuming the economic objective is to maximise NPV, the positive action to go ahead would be selected. Uncertainty in the outcome of a project decision can be introduced by supposing that there may be competitive activity in selling the product from the plant. If there is no competition the project will achieve the previous anticipated NPV, but if competition does occur, the adverse effect on sales and price will reduce the NPV to a £100,000 loss, as shown in Table 2 where the units are again £1000's NPV. The negative decision on the project is of course not affected.

Whether there is competition or not is called a 'state of the environment' or a 'state of nature'. It is something over which those involved in the decision have no direct control. The decision is no longer straightforward, since it can be seen that

Table 2

Payoff table, alternative outcomes

State of environment	Action on project	
	Yes	No
Competition	— 100	150
No competition	500	150

if there is competition the project should not go ahead, whereas without competition it should.

The next step is to consider the relative chances or subjective probabilities of the alternatives in the uncertain situation. Supposing we feel that the odds against competition are 3 to 1, i.e. the probability of competition is 0.25 and of no competition is 0.75 (the probabilities of all possible alternatives must add up to one). The payoff table can now be written as in Table 3.

The so-called expectations of each course of action are calculated as the weighted average of the possible outcomes, each weighted according to its subjective probability. The expectations of alternative actions are then compared to select the best, in this case the positive action to go ahead.

Table 3

Payoff table with expectations

State	Probability	Action on project	
		Yes	No
Competition	0.25 (A)	− 100 (Y)	150 (Y)
No competition	0.75 (B)	500 (Z)	150 (Z)
Expectation = (A.Y) + (B.Z)		350	150

If the assessment of the probabilities is different, e.g. the reverse for competition and no competition, this would affect the relative standing of the alternatives actions:

$$E\ (yes) = (0.75 \times -100) + (0.25 \times 500) = 50$$
$$E\ (no) = (0.75 \times 150) + (0.25 \times 150) = 150$$

The 'No' alternative is thus the better in this situation. Thus the use of expectation is a way of systematically allowing for uncertainty in evaluating a project and selecting a course of action.

In practice instead of deciding on values for probabilities and then evaluating the corresponding action it is sometimes easier to start at the other end and find the critical values of the probabilities which change the action selected. It is then only necessary to judge whether the probabilities are greater or less than these critical values instead of fixing their values exactly.

In the example, let P = critical probability of there being competition. Then:

$$(P \times -100) + (1 - P)\ 500 = 150$$
$$\therefore \quad -100P + 500 - 500P = 150$$
$$\therefore \quad P = 0.583$$

If the probability of competition is deemed to be greater than 0.583 the 'No' alternative is the better; if it is less than 0.583 the 'Yes' alternative is appropriate.

6 — ATTITUDES TOWARDS UNCERTAINTY AND POLICIES TOWARDS RISK

Information on uncertainty can be treated in several different ways in reaching a decision. For example, it can be ignored altogether. If in Table 2 the state of 'no competition' is considered to be more likely than competition, then the course of action is selected on the basis of the consequences of 'no competition' alone and the consequences of 'competition' are ignored. This method of only taking account of the most likely situation and ignoring other possible ones is in effect what is done when single-valued estimates are used. It does of course take no account of any risk that the most likely may not in fact occur.

At the other extreme, risk may be the dominant factor in selecting an appropriate action. Suppose a project would absorb a major part of a company's resources, and that if it failed the economic consequences for the company would be disastrous, e.g. it would become bankrupt. Then an appropriate policy might well be to avoid the potentially worst situation at all costs. This is equivalent to selecting the course of action which minimises the maximum loss which could be sustained, even though it may only be a remote possibility. Thus in the example, the application of this 'minimax loss' policy leads to the selection of the negative action since this avoids the possibility of a £100,000 loss should there be competition. This policy of playing safe is always carried out at the expense of the chance of achieving a much better gain — in

avoiding the chance of a £100,000 loss it also gives up the chance of achieving £500,000 should there be no competition and settles for a definite £150,000 whatever happens.

The use of expectation combines the two aspects of an uncertain situation, namely the alternatives and their subjective probabilities, into a single figure. It represents the policy of taking an acceptable calculated risk if the expectation value is attractive. In the event of course the expectation value is not the NPV actually achieved. In Table 3 if the project goes ahead, the NPV will be either — £100,000 or £500,000 but not the £350,000 expectation value. Note that an expectation value of DCF return cannot be obtained by multiplying possible DCF returns by their probabilities and adding since, unlike NPV's, DCF returns are not additive and cannot be averaged.

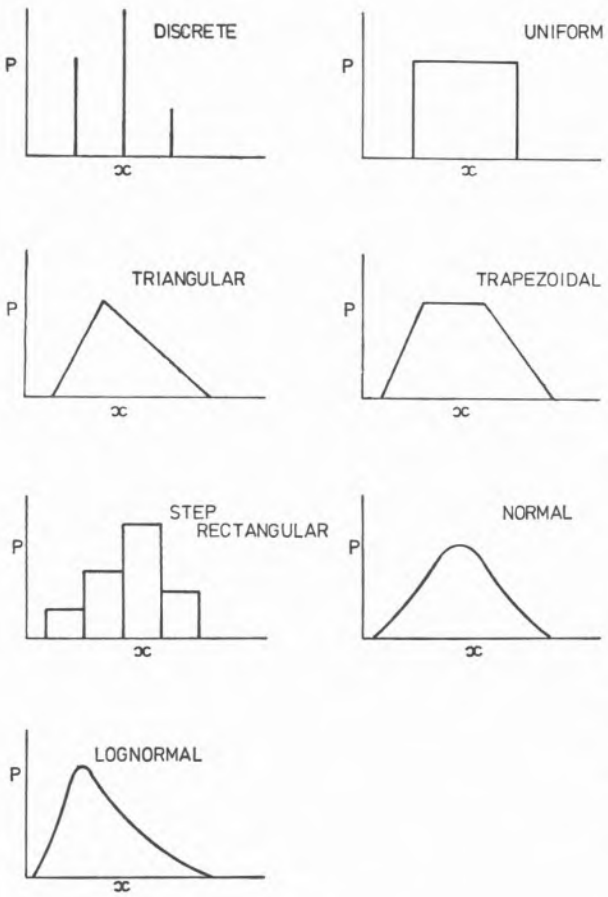

Fig. 1
Some types of probability distributions P of a variable x

7 — UTILITY FUNCTIONS

The use of expectation with maximum permissible loss as a constraint on potential disaster generally works fairly well. In some situations however it may not adequately take account of the fact that in practice the subjective value of money appears to vary with the amount in question compared with the total available. For example, an additional £100 to a man with £1000 is subjectively of more value to him (his incremental 'satisfaction' is greater) than £100 to a man with £10,000. Similarly the impact of a given gain (or loss) to a company depends on its existing financial state.

By evaluating an individual's or an organisation's response to hypothetical risk situations (e.g. gambles) involving different magnitudes of money it is possible to construct a corresponding 'utility function' of money. The use of this utility function in calculating expectations would lead to evaluations more consistent with the individual's or company's situation. The real problem is obtaining the utility function in the first place.

8 — SUBJECTIVE PROBABILITY DISTRIBUTIONS

Uncertainty in an estimate or forecast can best be represented by a probability distribution which expresses subjectively the relative chances that the variable estimated will turn out to have various different values. Although it may be convenient to express a distribution in terms of mathematical functions, e.g. as a normal distribution, we are not limited to these and according to our opinion of the situation a distribution may be of any arbitrary shape. Some common shapes describing different types of uncertainty are shown in fig. 1. Whereas for discrete alternatives the sum of the probabilities of all possible alternatives must be one, for continuous distributions (i.e. the limiting case) the area under the distribution expresses the total probability of one. The probability of the variable having a value in any particular range is the ratio of the area enclosed by that range to the total area under the distribution.

In making estimates in terms of subjective probability distributions one should first consider whether it

is appropriate to use a standard type of distribution or whether some other arbitrary shape better describes the situation. Instead of estimating directly in terms of probabilities it is often more convenient to use an arbitrary measure such as 'relative chances'. For example, the most likely value could be given ten chances and other values their appropriate number of chances relative to this. It is then an easy matter to convert these to probabilities as the ratio of the number of chances to the total sum of chances.

As will be seen in describing the use of distributions in project evaluation and risk analysis, smooth distributions are usually considered as approximating to step-type distributions or histograms. The smaller the range of each step the better is the approximation. The purpose of this is to facilitate handling of the data by computer.

9 — THE PROBLEM OF HANDLING STOCHASTIC DATA IN THE ECONOMIC EVALUATION OF A PROJECT

Data expressed in terms of probability distributions is known as stochastic data. Where elements contributing to project cash flow are expressed in this way then they early cash flows themselves and the project's financial index (NPV or DCF return) will also be stochastic. The uncertainty in individual estimates, i.e. their probability distributions, will of course all contribute to the nature of the probability distribution for the project index. We therefore need a method of combining input distributions according to the cash flow rules for a particular project to obtain as output the resulting project index distribution.

If all the input distributions can be expressed analytically as mathematical curves then in theory it is possible to calculate the equation for the combined output distribution. In practice however the mathematics become rather involved for any but the very simplest of cases unless sweeping assumptions are made which in practice may be difficult to justify. The problem could be approached numerically by representing the input distributions as histograms and then calculating the project index value for each possible combination with its resulting probability, and summing these to obtain the output distribution. The number of possible combinations, however, rises astronomically with the number of input distributions and number of steps considered in each, and again the method is not practical for any but the simplest of cases.

There is another type of approach which is not subject to the same difficulties or assumptions. It is known as Monte Carlo simulation and is a technique of much wider application than just the combination of probability distributions, since it can be used to analyse the behaviour of stochastic systems under different conditions. However, only its use in project evaluation and risk analysis are described here.

10 — MONTE CARLO SIMULATION APPLIED TO PROJECT EVALUATION

Monte Carlo simulation takes its name from its association with chance or uncertain situations, in particular gambling ones, and its use of random numbers to simulate their consequences. In a project evaluation subject to stochastic cash flow data there are many, in many cases an infinite number, of possible 'futures' for the project. A project future is defined as one particular pattern of cash flow over its life and hence a particular value of the project index. Where we are dealing with *independent* stochastic inputs one particular project future can be obtained by selecting any value from the distribution of each stochastic input and using them to calculate the corresponding project cash flows and project index. Selecting a different value for any input will lead to a new possible project future.

The basic idea of the technique is to carry out a large number of project evaluations with different input data selected from their specified distributions in any combination. However, this is done in such a way that the *frequency* with which any value is selected corresponds to its probability in the distribution. Thus if one value in an estimate is thought to be twice as likely as another, it is selected twice as many times as the other. After a large number of evaluations has been carried out the result is a corresponding list of values for the project

index. The same value for the project index could of course be derived from different combinations of selected values of input estimates. The large number of values of the project index obtained are split into ranges, e.g. of 1 per cent p.a. DCF return, and analysed for the frequency with which they occur. The frequency histogram obtained then corresponds to the probability distribution of the project index based on the input distributions of the initial data.

This method depends on being able to select different values from a probability distribution with frequencies corresponding to their probabilities. This is done with the aid of random numbers. A sequence of random numbers has no predictable pattern and satisfies various statistical tests of randomness. However, by weighting them in an appropriate way they can be used to represent the effect of any probability distribution.

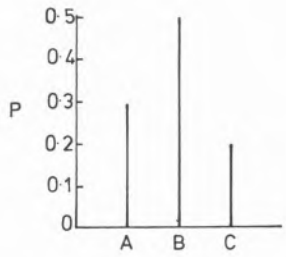

Fig. 2
Discrete probabilities of A, B + C

To illustrate how this can be done, consider the discrete distribution in fig. 2 in which the probabilities of A, B and C are 0.3, 0.5 and 0.2 respectively. A simple random number generator is a properly balanced spinning disc. If its circumference is divided into 10 parts, each labelled with a number from 1 to 10, and it is spun beside a fixed marker then a random number can be selected by noting the number nearest the marker when it comes to rest, as shown in fig. 3. The random numbers on the disc are next grouped to represent the probabilities of A, B and C as in fig. 4. Thus numbers 1-3 are allocated to A (i.e. three-tenths), 4-8 to B (five-tenths) and 9-10 to C (two-tenths). Now when the disc is spun, although the numbers are still selected randomly, A, B and C are selected with frequencies corresponding to their probabilities.

Since a Monte Carlo simulation involves repeating a large number of project evaluations it is advantageous to program it on a computer. A computer is also able to generate the required random numbers.

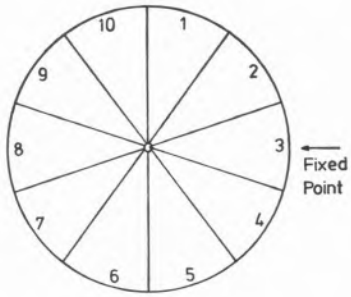

Fig. 3
Spinning disc generator for ten random numbers

Strictly speaking they are 'pseudo' random numbers since they are generated by a type of calculation which can be repeated to reproduce the same sequence of random numbers. Nevertheless they still meet the statistical tests of randomness. The sequence is initiated by inputing a 'random initiating' number. The same initiator always produces the same sequence whereas a different value for the initiator produces a different sequence.

To selected values from a distribution a computer program matches random numbers against the cumulative form of the distribution. The cumulative discrete distribution corresponding to fig. 2 is shown in fig. 5 along with the matched random numbers. By analogy with the disc method, it can be seen that this also results in A, B and

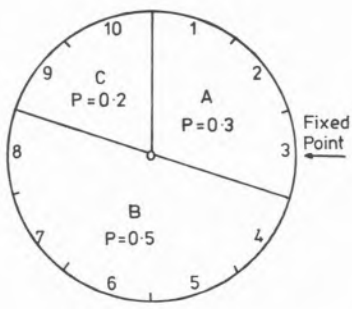

Fig. 4
Allocation of random numbers to Select A, B and C

C being selected with frequencies corresponding to their probabilities.

The complete Monte Carlo simulation procedure applied to project evaluation is summarised in

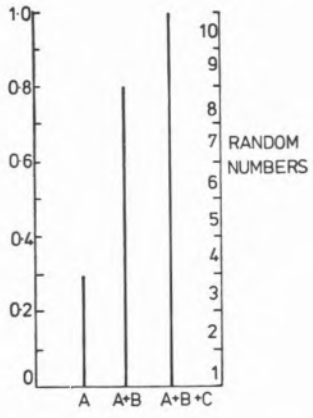

Fig. 5
Matching random numbers against cumulative distribution

fig. 6. For each iteration, i.e. pass through the evaluation corresponding to one potential project future, a random number is selected for each stochastic input and is matched with it to select a particular value. These selected values along with other data are used to calculate a value for the project index which is stored. As this is repeated more and more times the relative frequencies with which particular values are selected from distributions approach more and more closely to their probabilities. When sufficient iterations have been performed the stored values for the resulting project index are analysed and transformed into a frequency histogram.

Although the number of iterations necessary to achieve a desired level of accuracy can be estimated mathematically with various assumptions, it is easier to test it on the computer, especially since the only drawback of more iterations than is strictly necessary is use of computer time. The output histogram can be tested in two ways to see if it is stable or 'robust'. If sufficient iterations have been performed it should be insensitive to a change in the number of iterations and also insensitive to a change in the sequence of random numbers used (i.e. changing the random initiator).

As the number or range of input distributions is increased a larger number of iterations is of course required to reach this robust state.

Since different random numbers are used to select from each stochastic input this infers that the value selected from one distribution is completely independent of the values selected from other distributions. Where this is not the case, it is best to combine interdependent data into a combined distribution for use as input. For example, estimates of sales volume and selling price may not be independent of each other, in which case they should be combined into an estimate of sales income with a corresponding distribution. In cases where different estimates will be similarly affected by a chance event, e.g. future government policy, the same random number should be used in an iteration for these estimates instead of different ones.

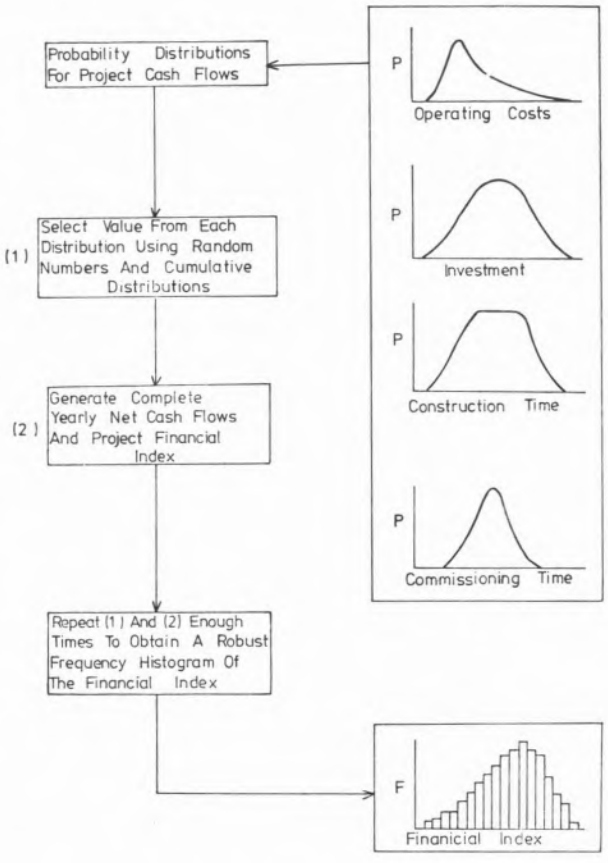

Fig. 6
Risk analysis procedure using Monte Carlo simulation